Department of Civil Engineering and Mechanics

The University of South Florida

Durability of CFRP Pretensioned Piles in Marine Environment

Volume II

Rajan Sen, Satya Sukumar and Jose Rosas

Department of Civil Engineering and Mechanics

August 1995

A Report on a Research Project Sponsored by the

Florida Department of Transportation in cooperation with

the U.S. Department of Transportation

Contract C-4478

Tampa, Florida

Technical Report Documentation Page

1. Report No.	2. Government Accession No.	3. Recipient's Catalog No.
0510642		2104-183-LO

4. Title and Subtitle

Durability of AFRP Pretensioned Piles in a Marine Environment, Vol I
Durability of CFRP Pretensioned Piles in a Marine Environment, Vol II

5. Report Date
August, 1995

6. Performing Organization Code
CEM/FDOT/183-LO

8. Performing Organization Report No.
CEM/ST/95/1

7. Author's
R. Sen, J. Rosas and S. Sukumar (Vol I)
R. Sen, S. Sukumar and J. Rosas (Vol II)

9. Performing Organization Name and Address

Department of Civil Engineering and Mechanics
University of South Florida
4202 East Fowler Avenue
Tampa, FL 33620-5350

10. Work Unit No. (TRAIS)

11. Contract or Grant No.
C-4478

13. Type of Report and Period Covered
Interim Final Report
August 1992 - March 1995

12. Sponsoring Agency Name and Address

Florida Department of Transportation
Structural Research Center
2007 East Dirac Drive
Tallahassee, FL 32310 Attention: Dr. Mohsen Shahawy

14. Sponsoring Agency Code

15. Supplementory Notes

Prepared in cooperation with the Federal Highway Administration

16. Abstract

This report provides experimental results from an investigation to assess the long term durability of aramid fiber reinforced plastic (AFRP) and carbon fiber reinforced plastic (CFRP) pretensioned elements used as piles driven in Florida's tidal waters. A total of 66 identical beams - 33 aramid and 33 carbon - were cast in a single pour. The beams each 114 mm x 150 mm x 2.44 m were pretensioned using two AFRP or CFRP rods at an eccentricity of 50 mm. They were designed to fail due to rupture of the AFRP or CFRP rod.

Three identical series of tests are being conducted on each material. These are outdoor exposure, wet/dry cycles in salt water simulating tide change (durability) and a combination of wet/dry cycles and hot/cold cycles to simulate the effect of temperature range (bond). The testing is near complete excepting for the final series of tests from each of the three studies. These will be delayed as long as possible to allow maximum time of exposure.

Preliminary findings indicate that AFRP pretensioned elements may be vulnerable to thermal cycling in a marine environment. The CFRP pretensioned elements performed satisfactorily in this environment. However, some loss in strength was detected in the CFRP pretensioned specimens exposed to wet/dry cycles simulating tidal waters after 24 months.

17. Key Words	18. Distribution Statement
AFRP, CFRP, pretensioned, durability, temperature, concrete, salt, exposure, outdoor, bond	No restrictions. This document is available to the public through the National Technical Information Service, Springfield, VA 22161

19. Security Classif.(of this report)	20. Security Classif. (of this page)	21. No. of Pages	22. Price
Unclassified	Unclassified	Vol 1 - 147 pp. Vol 2 - 124 pp.	

Form DOT F 1700.7 (8-72)

TABLE OF CONTENTS

LIST OF TABLES

LIST OF FIGURES

LIST OF PLATES

1. INTRODUCTION

1.1 Introduction

This is the second volume of an interim report presenting the preliminary findings from an on-going investigation on the durability of carbon fiber reinforced plastic (CFRP) pretensioned elements in a marine environment. The study, funded by the Florida and US Department of Transportation since August 1992, is expected to be completed in 1996.

1.2 Background

Florida's long coastline and sub-tropical climate have led to the rapid deterioration of reinforced or prestressed concrete substructures exposed to a marine environment. The resulting concrete spall is usually repaired by patching but this needs to be repeated as often as every two years, e.g. for the Long Key Bridges, Monroe County, Florida, Sagues, 1994. In rare instances, an impressed current cathodic protection system is installed but its implementation for substructures in a marine environment is far more complex than in bridge superstructures since fluctuations in concrete resistivity (due to tide change) cause large variations in current distribution that have to be controlled.

The high costs associated with the maintenance and repair of substructures in a

marine environment have prompted highway authorities to explore radical alternatives such as the use of fiber reinforced plastics (FRPs) that offer the prospect of lower life cycle costs. Although the potential of fiber reinforced plastics for prestressing applications was recognized more than 40 years ago, Crepps 1951, it is only since the 1980's that there has been a worldwide resurgence of interest in their application, e.g. Iyer & Sen 1991. FRPs have the desirable properties of high tensile strength, low modulus and corrosion resistance that make it particularly attractive for prestressing applications. They are, however, by no means inexpensive.

The price of FRPs ranges from 2.5-166 times that of steel (on a weight basis), Nojiri 1992. The lower range corresponds to glass and the upper range to carbon. However, since the quantity of steel used is relatively small, the incremental cost in using the more expensive FRP material will not be as great. Moreover, in Florida higher initial material costs will be partially offset by the lower cost of using smaller sized piles and its associated lower transportation and driving costs (current Florida Department of Transportation specifications require piles located in salt or brackish water containing chlorides exceeding 0.2% to be at least 60 em x 60 cm irrespective of load).

As relatively little was known regarding the suitability of FRP material for pretensioning substructures, a comprehensive 26 month program of research was initiated at the University of South Florida, Tampa in 1989, Sen *et* al 1992, Sen *et* al 1993a,b. Fiberglass was selected for the investigation because it was the least expensive.

Following completion of this study in 1992, a new investigation was initiated to

plastics pretensioned beams that is the subject of this thesis.

1.3 Objectives of Study

The primary aim of the study was to establish whether carbon fiber reinforced plastics could be used to replace steel in pretensioned piles driven in Florida's aggressive environment. Since previous research had indicated adequate material resistance to alkaline solutions, the focus of the research was on their durability as pretensioned piles exposed to wet/dry cycles in salt water.

The aim of the investigation can be summarized as:

1. To assess the durability of CFRP pretensioned elements exposed to wet/dry cycles in salt water.
2. To examine whether the long term bond between the CFRP element and concrete was adversely affected by diurnal and seasonal temperature change.
3. To determine whether outdoor exposure had any detrimental effect on the service and ultimate response of CFRP pretensioned elements.

To meet the objectives of the study, full sized CFRP pretensioned beams were designed to fail by rupture of the CFRP prestressing rods. By comparing the failure of exposed specimens with unexposed control specimens, the effect of exposure could be understood in the context of changes in service and ultimate performance.

In addition to the larger specimens tested, other durability studies were also initiated using smaller specimens. These include pullout and moisture absorption studies. In these

tests, the smaller specimens were subjected to the same environment as the larger specimens. The aim was to determine whether simpler tests could be devised to assess durability. The results from these studies will be part of the final report to be submitted next year.

1.4 Organization of Report

Information on materials used in these studies is summarized in Chapter 2. The fabrication and preparation of specimens for testing is discussed in Chapter 3. The results of field tests to determine transfer length and subsequent efforts to reconcile the test data with predictions from finite element analyses are presented in Chapter 4. To accelerate degradation, all specimens were pre-cracked. The analysis of the pre-cracking load to determine the effective prestress is presented in Chapter 5.

A description of the test set-up and instrumentation used for all the ultimate load tests is presented in Chapter 6. The three studies relating to outdoor exposure, durability and bond are described in Chapters 7-9 respectively. The principal conclusions are summarized in Chapter 10.

2. MATERIAL PROPERTIES

2.1 Introduction

This chapter provides essential data on carbon fiber reinforced plastic (CFRP) rods used in the study. The properties of fibers and the rods are presented in Section 2.2. Those of the CFRP spirals appear in Section 2.3. The mix design for the concrete is summarized in Section 2.4.

2.2 CFRP Properties

2.2.1 New Prestressing Materials

Advances in composite materials over the past several decades have led to the development of several high strength, light weight fiber reinforced plastics, FRP. Although these composites are more expensive than prestressing steel (see Table 1), life cycle costs may be significantly lower, Dolan 1990.

Of the commercially available fibers three, glass, carbon and aramid fibers, have the necessary combination of strength and stiffness suitable for prestressing, Rostasy 1988. Resins or polymers form the continuous matrix to which these fibers are bonded. The most

commonly used resins are polyesters, vinylesters and epoxies.

Table 1. Relative Cost of Non-Metallic Prestressing Materials Compared to Steel

Fiber reinforcement	Carbon	Aramid	Glass
Fiber fraction, % wt	72	67	80
Materials cost ratio on a weight basis	16 - 20	10 -15	6
Materials cost ratio on a strength basis	4 - 5	2 - 3	3
Materials cost ratio on a stiffness basis	5 - 6	5 - 8	7

2.2.2 Carbon Fiber Reinforced Plastic

Carbon fibers were first used in Edison's incandescent electric lamps. Many fibers, referred to as precursors later, can be converted into carbon fibers provided they carbonize rather than melt under heat.

The majority of carbon fibers commercially available use polyacrylonitrile (PAN) precursors since it yields superior material properties. Pitch precursors from coal tar, asphalt yield lower cost, lower strength fibers used for reinforcing plain concrete in cladding type applications.

The CFRP rod supplied by AKZO is made from FORTAFIL 3(C) continuous carbon fibers obtained from PAN precursors made in the United States. FORTAFIL 3(C) continuous carbon fiber is a high strength, standard modulus fiber supplied as 50,000 filament continuous

tow, suited for use in processes such as filament winding, pultrusion, or prepregging which require the efficient use of large quantities of carbon fiber. The fiber surface is treated to improve the fiber to resin interfacial bond strength.

Table 2 gives the properties of FORTAFIL carbon fibers. The resin properties were not available from the manufacturer. The properties of the CFRP/epoxy rods as reported by the manufacturers are summarized in Table 3.

Table 2. Properties of FORTAFIL Carbon Fiber

Typical Fiber Properties	U.S. units	SI units
Tensile Strength	550 ksi	3800 MPa
Tensile Modulus	33 Msi	227 GPa
Ultimate Elongation	1.7 %	1.7 %
Density	0.065 lb/in^3	1.8 g/cm^3
Cross-Sectional Area	6.7x10^{-8} in^2	4.3x10^{-5} mm^2
Filament Diameter	0.30x10^{-3} in	7.3 μm
Axial Thermal Expansion	-0.18x10^6/°F	-0.1x10^{-6}/°C

2.3 CFRP Spirals

CFRP spirals were made using Fortafil 50K with an effective cross-section of 2.2 mm^2. The tensile strength was about 7 kN (Bottcher, 1992). The spirals were 15 cm long with a diameter of approximately 2.5 cm.

Table 3. Short Term Properties of CFRP Rods, Waal 1992

Property	CFRP
Carbon fiber rod diameter with grit, mm smooth, mm	6.15 5.80
Fiber volume, %	53.2
Breaking Load, kN	43
Elastic Modulus, GPa	121
Failure Strain, %	1.5
Jacking Force, (% of ultimate)	60
Expansion coefficient transverse, x 10^{-6} /°C (Gerritse 1993) longitudinal, x 10^{-6} /°C (Gerritse 1993)	 25 0

2.4 Concrete Properties

The concrete used was normal weight concrete from Type I cement. The sodium oxide equivalent of the cement was under 0.6% indicating a low alkali cement in accordance with ASTM C150 designation.

The concrete was supplied by Florida Rock Industries, Inc. of Tampa. The mix proportions per cubic meter are shown in Table 4.

The minimum design strength for the mix was 34.5 MPa. The actual strength obtained at the time of initial testing averaged at 62.8 MPa, which is about 82 % more than the design strength.

Table 4. Concrete Properties

Ingredients	Weight/m^3
Florida Mining & Material Corp. Type I Cement, kg	475
Florida Rock Industries, Inc. # 89 stone, kg	920
Florida Rock Industries, Inc. Silica sand, kg	798
Water, kg	168
Air entrainment, %	1.0
Daracam 100, oz.	2.0
Concrete unit weight, kg	2361
Water/cement ratio, by weight	0.35
Slump, cm	13
Compressive strength @ transfer, MPa	51.4

3. FABRICATION OF CFRP BEAMS

3.1 Introduction.

This chapter describes the fabrication of the carbon fiber reinforced plastic pretensioned beams used for investigating long term performance. Because all beams were cast in a single pour, many technical problems had to be overcome. This is also discussed in a recently published paper, Sen et al 1994.

Section 3.2 presents the design of the specimens. Section 3.3 describes the construction of the forms and addresses some of the measures taken to iron out difficulties faced during their mass production. Details of the actual fabrication and concreting are included in Section 3.4.

3.2 Beam Design

The beams used in this study were designed to fail by rupture of the CFRP rods. The cross-section was 114 mm x 150 mm and the CFRP rods had an eccentricity of 50 mm. The length was 2.44 m to match the size of available plywood sheeting. The assumed concrete strength was 41.4 MPa and the CFRP properties are those summarized in Table 3. The design calculations are included in Sukumar 1995.

.

Under these assumptions, the beams failed under two point loading at a load of 20.2 kN. The calculated ultimate shear capacity, based on the simplified ACI equation, was 13.2 kN that exceeded the failure load. In view of this, no shear reinforcement was needed. Figure 1 shows the design beam cross-section.

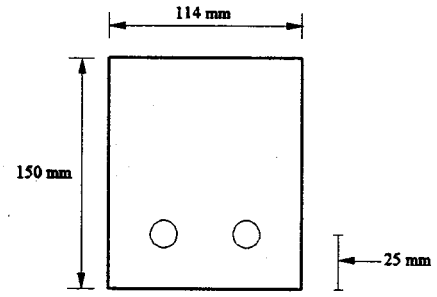

Figure 1. Cross-section

3.3 Formwork

In this investigation, degradation over time is linked to changes in ultimate capacity. Therefore, to conduct the three exposure studies, a minimum of twenty eight carbon fiber reinforced plastic pretensioned beam specimens were needed. However, a total of thirty three CFRP pretensioned beams were fabricated to provide spares. The 114 mm x 150 mm x 2.44 m beams were fabricated in a 122 m long prestressing bed normally used for producing 250 mm square steel pretensioned piles.

To fabricate so many specimens, a novel approach was used. A 122 m prestressing bed used for commercially producing steel pretensioned piles was modified to allow

pretensioning of all the carbon fiber reinforced plastic specimens *in* a *single pour.* The cross-sections of the CFRP specimens is shown in Figure 1.

3.3.1 Adaptation of Prestressing Bed

The beams were fabricated at Henderson's Prestress, Tarpon Springs, FL since they had several 122 m prestressing beds that were suitable. More importantly, their facility had been used earlier in the successful fabrication of the world's first fiberglass pretensioned piles, Sen et al 1993c. The use of this facility additionally provided the benefit of experienced personnel and equipment needed for the placement, curing and removal of specimens. A 250 mm x 250 nun pile bed was used for the fabrication of the CFRP specimens.

It was evident that drop-in forms would be needed to cast the much smaller beam specimens. Other changes were also necessitated because of the design and relative age of the prestressing beds. Frequent tensioning of steel strands had resulted in burrs to the strand holes in the stressing headers at both the dead and live ends that could potentially damage the highly anisotropic CFRP rods. Furthermore, the prestressing jack used for stressing steel strands was unsuitable in view of the relatively small jacking forces needed for the CFRP specimens (see Table 3). Finally, since the entire 122 m bed was not used to make the thirty three carbon specimens (33 x 2.44 m = 80.5 m plus spacers), measures had to be taken to eliminate danger to personnel or specimens during release of the prestressing force. Some of these concerns are addressed later.

3.3.2 Assembling Formwork

A prototype form was constructed to ensure that the openings for the CFRP rods aligned with the openings in the stressing headers and to check that the concrete cover was correct. This was carefully dismantled into its constituent parts a bottom board, two side boards, two end pieces and appropriate spacers. These were then used as templates for production of the remaining forms.

All component pieces for the thirty three beams cast were cut, labeled and partially pre-assembled at USF. At the prestress yard, each form piece was unloaded, assembled and positioned in the prestress bed. The final assembling procedure, consisting of attaching two side boards to a bottom board, was performed with the use of a pneumatic stapler and nail gun. These forms were then placed end to end at the "dead end" in the prestress bed. This methodology permitted the complete assembly of each form and minimized the damage potential of the formwork until the appropriate time to properly secure them in their final positions.

Following placement of the forms, spacers and end pieces were fastened and the forms moved to their final position. As a further strand alignment check a string was threaded through the header plate and each form for the length of the pile bed. Minor adjustments were made and the formwork was secured in place with wooden spacers and braces. The form interiors were then sprayed with two applications of form oil to facilitate stripping. The positioning of the forms allowed for a 24.4 m and 6.1 m space at the live

Plate 1. Installation of Formwork

Plate 2. Prestressing Bed with All Thirty Three Forms

and dead ends of the prestressing bed, respectively. Plates 1 and 2 show the formwork assembly and the thirty three assembled forms, respectively.

3.3.3 Transfer Assembly

As noted earlier, burrs to the strand openings made it inadvisable to chuck the CFRP rods directly to the stressing headers. Instead, transfer assemblies were used to attach each CFRP rod to its steel counterpart. The CFRP rods were chucked at one end of the transfer assembly using custom designed chucks with plastic inserts that were provided by HBG shown in Plate 3. A 13 mm steel strand was chucked to the other end of the transfer assembly. The free end of the steel strand was then continued and chucked at the stressing headers. This arrangement was similar to that used earlier in the fabrication of fiberglass piles excepting that the transfer assemblies were based on a design provided by HBG that used a thick walled pipe.

3.3.4 Safety Measures

Two preventive measures were incorporated into the fabrication process to countermand the effects of the stresses induced upon release of the prestressing force. First, supplementary specimens were cast between each transfer assembly and the first and last specimens at either end of the pile bed. These mock beams acted as buffers to minimize and prevent the transfer assembly from hitting the actual test members upon

release. Second, short pile sections were placed across the top of the pile bed directly over the transfer assemblies. This confined the physical movement of the assemblies.

3.4 Fabrication

Following installation of formwork, CFRP rods were threaded through each of the specimen forms. During this operation care was exercised to ensure that the sand coating on the rods was not scraped off and there was no direct contact with the previously applied form oil. The CFRP tails were chucked and placed in the transfer assembly as mentioned earlier. Additionally, 150 mm length CFRP spirals were provided at each end of each beam, Plate 4.

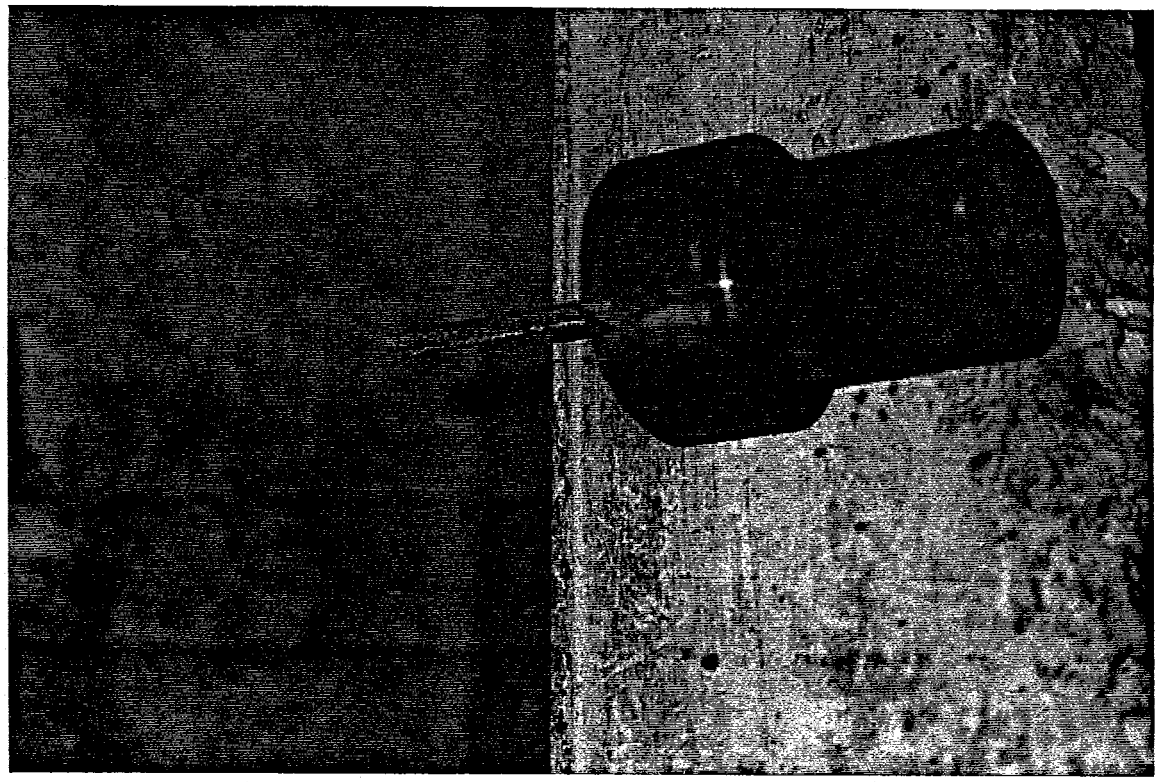

Plate 3. Chuck with Plastic Inserts

Plate 4. Spirals Used Around the CFRP Rods

3.4.1 Stressing

Each steel strand was individually tensioned to the target jacking force (Table 3) by a 20 ton capacity, 10 in. (250 mm) stroke special PSI PT twin cylinder hydraulic stressing jack driven by an electric motor. No problems were experienced unlike AFRP, Rosas 1995.

3.4.2 Concreting

Concrete was poured and consolidated approximately two hours following the completion of the prestressing operation. This procedure was performed by a crew from

Henderson Prestress in a similar manner utilized in commercial production. One important difference mandated was that the CFRP rods did not come into direct contact with the head of the vibrator. The surface of the concrete was screeded, trowel finished and covered with plastic sheeting to retain the moisture.

3.4.3 Release

The specimens were continually cured until the concrete compressive strength reached 41.4 MPa, Plate 5. This occurred after eight days when the CFRP rods were cut with an electric grinding wheel (Plate 6).

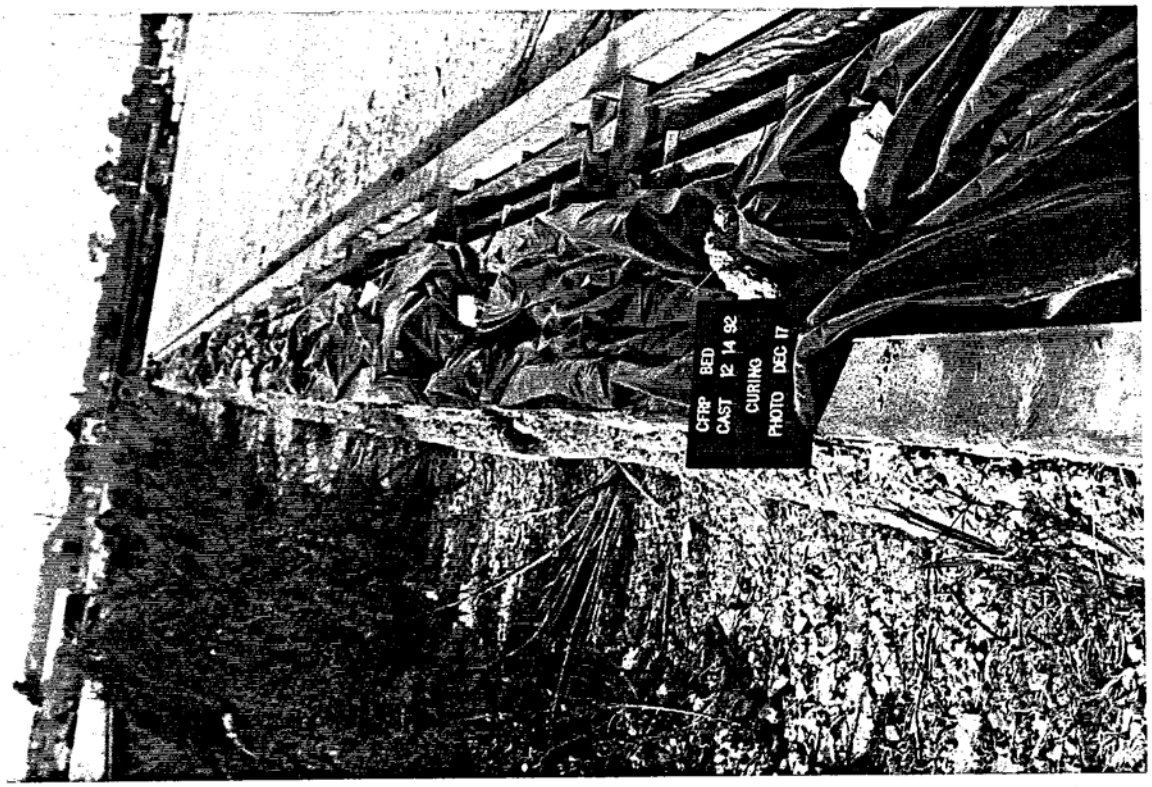

Plate 5. Curing of the CFRP Beams

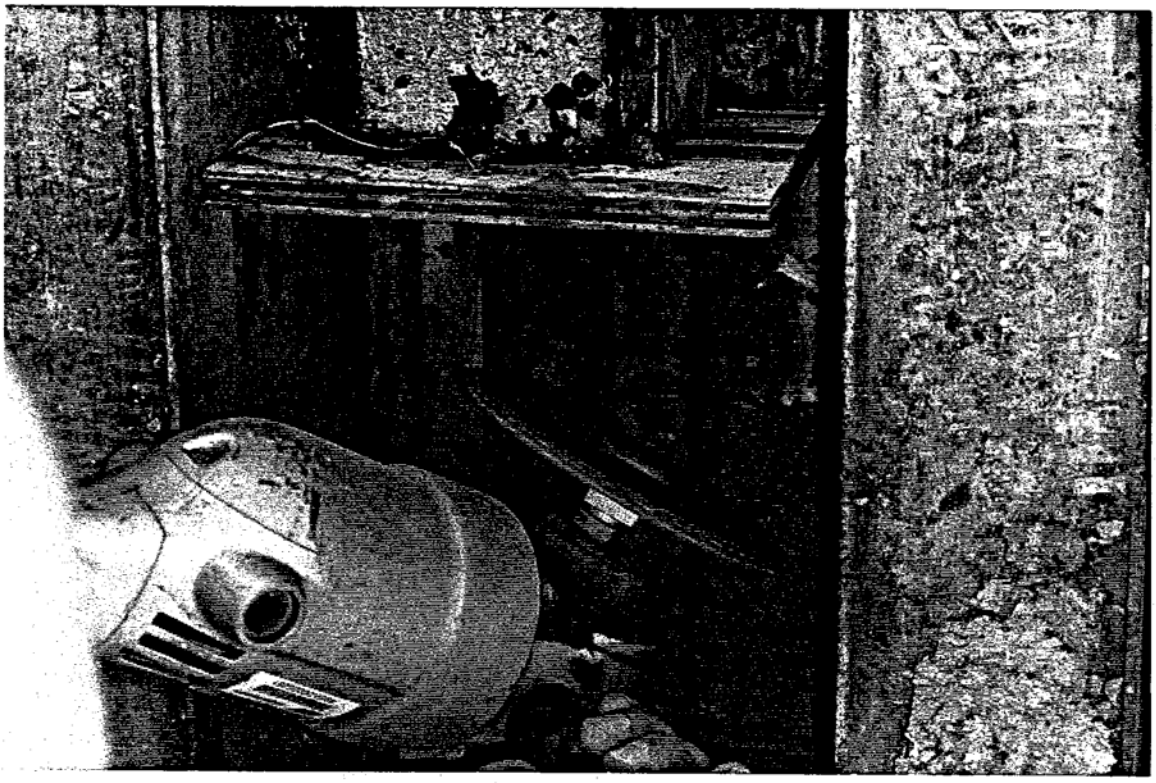

Plate 6. Releasing the Prestressing Force in CFRP Beam

3.4.4 Removal

The beams were removed from the bed using specially fabricated hooks that were placed at each end. They were then transported to the USF campus where the long term exposure testing was to be conducted.

4. TRANSFER LENGTH

4.1 Introduction

In pretensioned beams, when the external jacking force is released the prestressing tendons attempt to return to their normal unstressed position. This motion is resisted by the bond developed between the concrete and the prestressing strand and it is this bond that transfers the prestressing force to the concrete. This transfer occurs near the end of the specimen over a distance referred to as the *transfer length.*

To determine the transfer length in CFRP prestressed concrete beams, five of the thirty three specimens cast were instrumented while still in the prestressing bed. Load cells were used to monitor the prestressing force at both live and dead ends and a computerized data acquisition system recorded the strain variation at release.

The experimental program is briefly outlined in Section 4.2. The test results are summarized in Section 4.3. The details of finite element analyses carried out to determine transfer length and comparisons of predictions with test results are described in Section 4.4.

4.2 Experimental Program

The logistics involved in outdoor experimentation limited the number of beams that

could be instrumented. The two most important constraints were the number of strain gage channels available in the data acquisition system and the length of wiring needed. Based on these considerations, only five of the thirty three specimens cast were instrumented.

The basic strategy was to instrument two specimens, CA-1, CA-33, closest to the live and dead ends respectively. Since load cells were mounted at both these ends, these specimens enabled the accuracy of the measurements to be assessed and also provided an index of the instantaneous elastic shortening losses.

The three remaining specimens selected, CA-16, CA- 17and CA-18 were located near the middle of the bed where more uniform conditions were expected. More importantly, their proximity to the data acquisition system minimized the length of wiring needed.

4.2.1 Instrumentation

To capture the strain variation, five gages were affixed to the concrete at each end spaced 5 cm. apart. This meant that strains were measured at 2.5 cm., 7.5 cm., 12.5 cm., 17.5 cm. and 22.5 cm. In addition, two further gages were placed symmetrically 119.4 cm. from each end. The arrangement of these gages is shown schematically in Figure 2.

The location of the gages on the top surface of the selected beams was carefully marked and the surface ground to a smooth finish. The gages were positioned as carefully as possible given that this operation was carried outdoors. A more complete description of the installation procedure is given in Section 6.3. A total of sixty gages were attached. The most difficult task was in tracking the individual wires from the strain gages so that they

correctly hooked up to the data acquisition system.

As mentioned already, the applied prestressing force was monitored with load cells located at both the live and dead ends of the prestressing bed. AP-3500 Strain Indicator Box was used in conjunction with SB-10 Switch and Balance Units, both supplied by the Measurement Group, for this purpose.

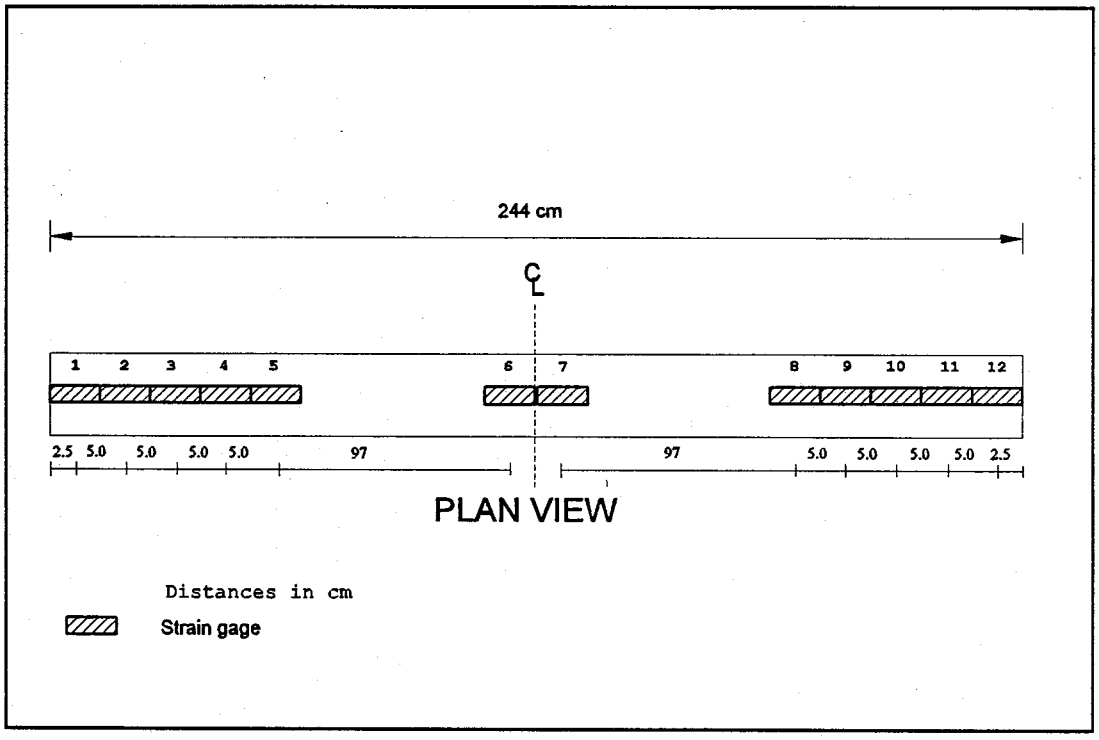

Figure 2. Typical Gage Locations

In order to record the strain gage readings, a SYSTEM 4000 data acquisition system was used. This was housed inside a vehicle belonging to the USF College of Engineering that was stationed near the middle of the prestressing bed (see Plate 7). A portable generator provided electricity.

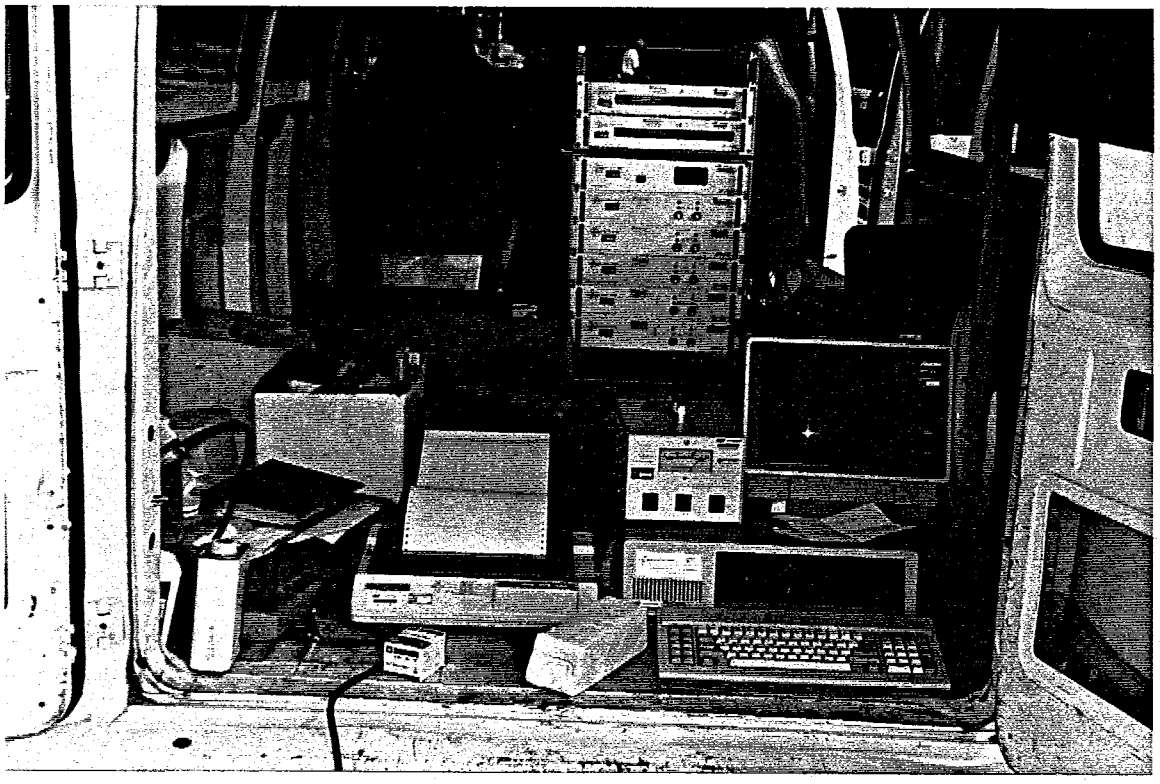

Plate 7. Data Acquisition System Used at Prestressing Yard

4.2.2 Test Set Up and Release

Load cell readings were taken just prior to release and all strain gage readings initialized. The prestressing force was released by cutting the two CFPP rods at each end of the beams starting from the live end (beam CA-1). Plates 8 and 9 illustrate the release operation.

As each rod was cut, strain readings were automatically recorded using the computerized data acquisition system. This operation was repeated until the prestressing force had been released in all 33 beams. The results reported correspond to strain magnitudes taken at this time.

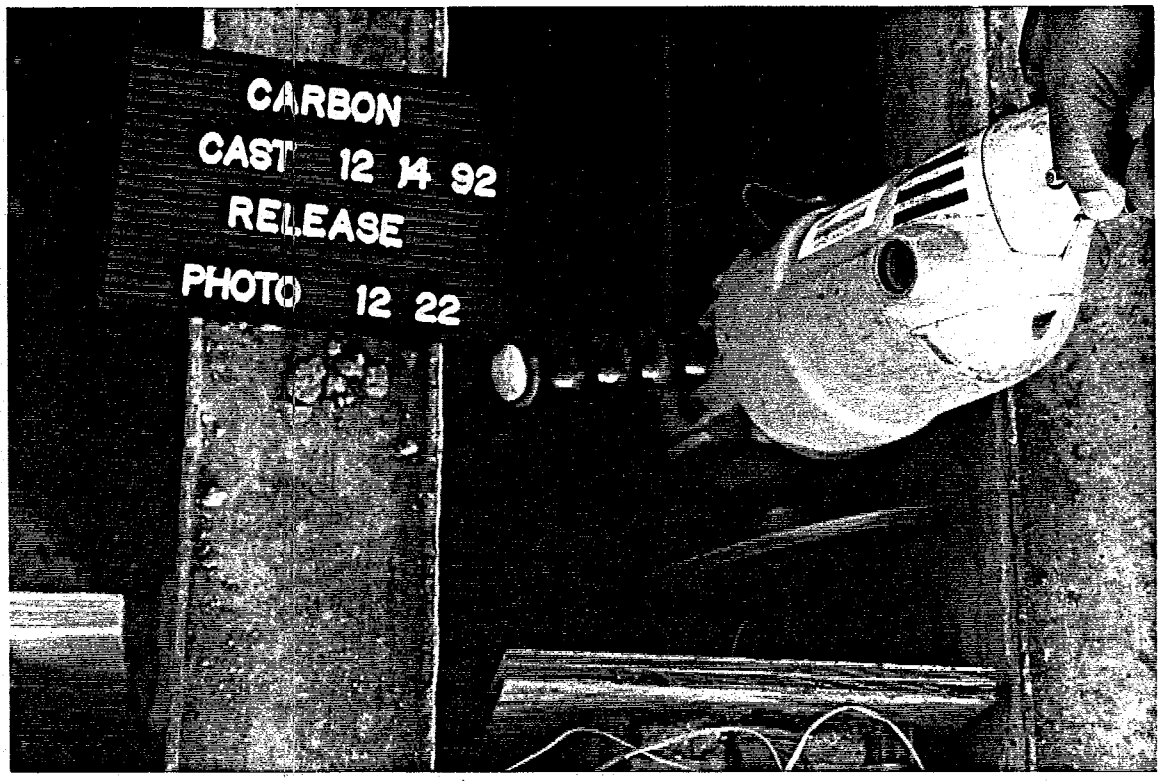

Plate 8. Release of Prestressing Force

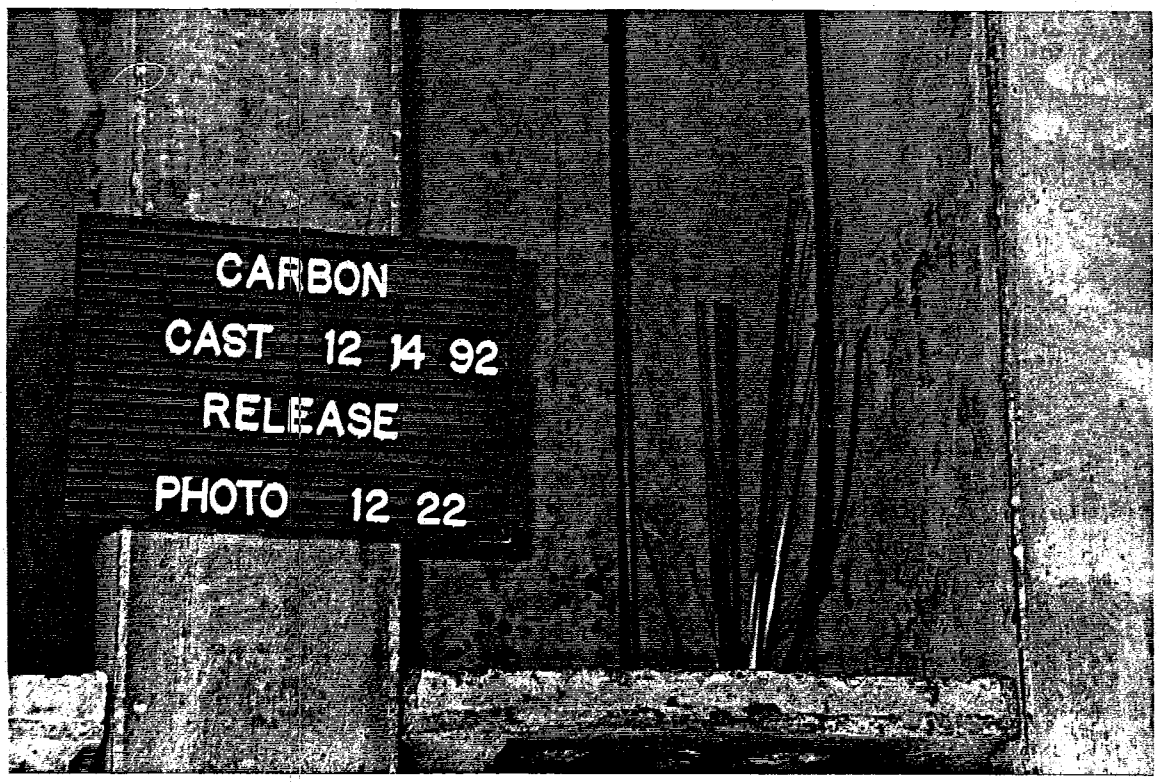

Plate 9. CFRP After Release

4.3 Test Results and Discussion

4.3.1 Field Test Results

Figure 3 shows the identifiers for the load cells used for monitoring the prestressing force. Table 5 summarizes the load cell readings just prior to release.

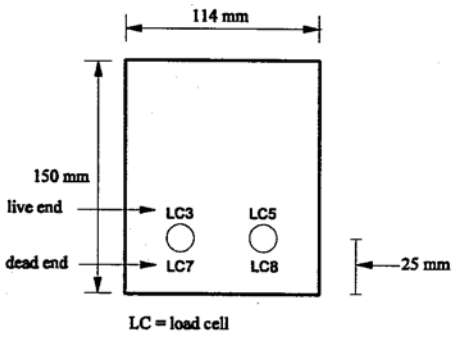

Figure 3. Load Cell Identifiers

Table 5. Summary of Prestressing Force at Release

Location	Load cell	Prestressing force at release (kN)	Average prestressing force (kN)	% of ultimate tensile force
Live end	LC3 LC5	21.8 25.1	23.5	55%
Dead end	LC7 LC8	20.2 20.4	20.3	47%

The target jacking force was 60% of the reported ultimate tensile force of 43 kN. Inspection of Table 5 shows that there is some difference between the forces measured at the live and dead ends of the CFRP rods. The average prestressing force, 51%, indicates larger than expected short term losses.

Since the gages were attached to the top surface of the beams, the concrete strain should reach a terminal value approximately given by Eq. 1.

$$\frac{P}{AE} - \frac{Pe}{SE} + \frac{M}{SE}$$

In Eq. 1, P is the prestressing force, M the bending moment due to self weight, A the crosssectional area of the beam, S its section modulus and E the Young's Modulus for concrete. Using P as 43.8 kN (Table 5), A as 174.2 cm^2, S as 442.5 cm^3 and E as 30.7 GPa (the concrete strength was measured as 51.4 MPa) based on Nilson's equation for high strength concrete, the strain value comes out as 81 ge in tension near the ends where self weight bending moments are minimal. At mid-span, the bending moment is at its highest and induces a compressive strain of 22με, making the total strain 59με in tension.

The results summarizing recorded concrete strains are presented in Table 6 (tension positive). Plots of the strain variation along the length of the beam for each of the five instrumented beams are shown in Figures 4-8. A comparative plot of all the results appears in Figure 9.

Inspection of Figures 4-9 shows that although the strain variation is more or less symmetrical, it does not agree with the expected distribution shown in Figure 10 determined from Eq. 1. Moreover, the recorded maximum strain of 44ge (see Table 6) is lower than the theoretical value of 81 με.

Because the strain variation was similar for all the five beams tested, and in five other AFRP specimens tested on the same day, Rosas 1995, instrumentation error was ruled out. Instead, it was hypothesized that when the prestressing force was released, the upward movement of the beams was impeded by frictional type forces that developed between the

wood forms and concrete. Normal forces required for the frictional force to develop were due in part to bending about the weak axis caused by the unsymmetric placement of the prestressing rods in the beam and their unequal magnitude. Consequently, finite element analyses were carried out to determine the theoretical transfer length and also to establish the kind of frictional force that would lead to the type of strain variation shown in Figures 4-9. Table 6. Summary of Concrete Strains at Release

Strain gage	concrete strain (με)				
	Beam CA-1	Beam CA-16	Beam CA-17	Beam CA-18	beam CA-33
1	5	0	12	-15	-6
2	32	35	40	44	17
3	39	38	36	41	5
4	32	28	23	31	-7
5	15	16	13	19	-23
6	-31	-73	-66	-62	-52
7	-71	-76	12	-61	22
8	9	8	31	14	0
9	28	17	43	27	11
10	40	35	42	37	24
11	34	35	-12	36	-
12	9	2	-15	1	5

4.4. Finite Element Analyses

Two finite element analyses were carried out using ANSYS Revision 5.0 from

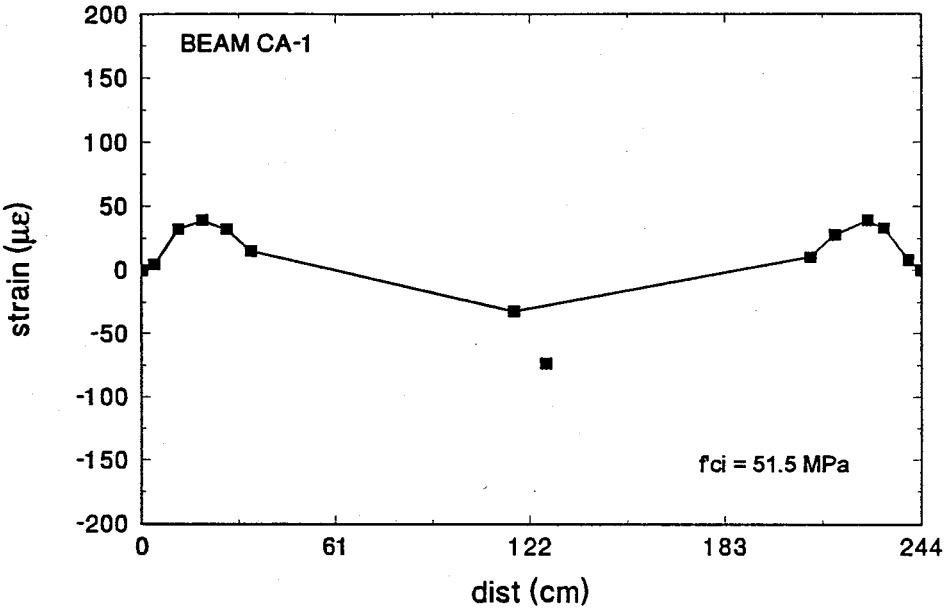

Figure 4. Field Results for Beam CA-1

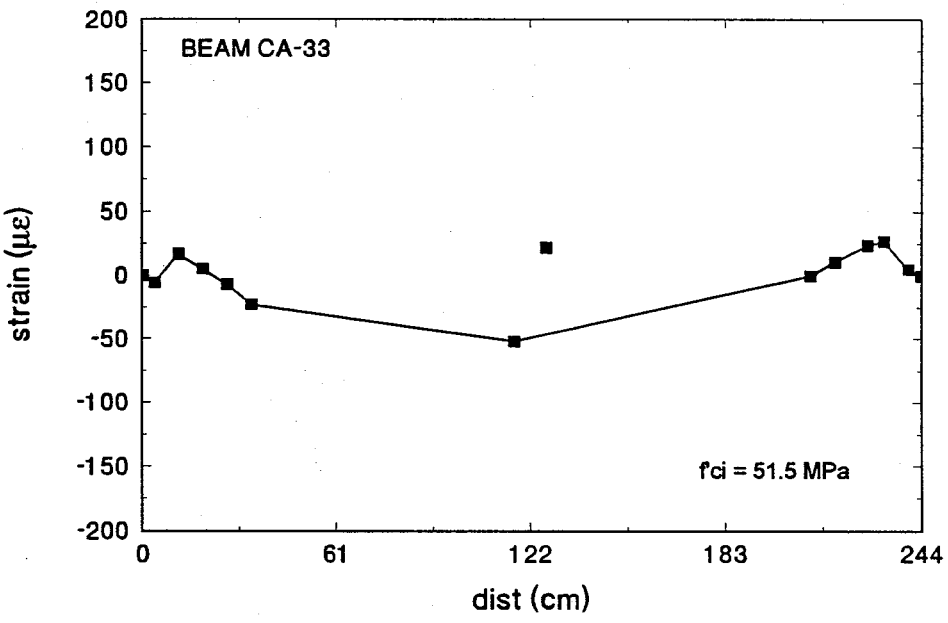

Figure 5. Field Results for Beam CA-33

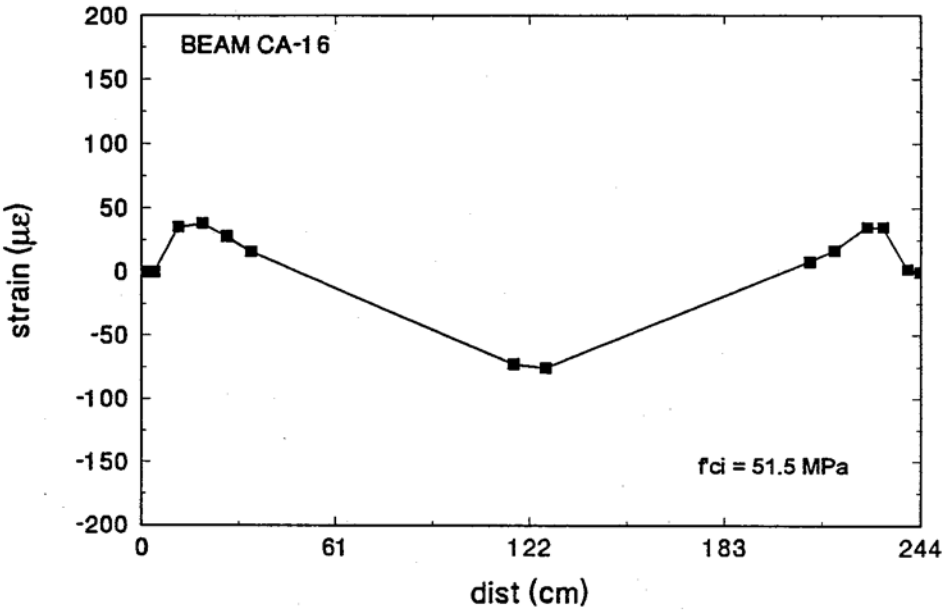

Figure 6. Field Results for Beam CA-16

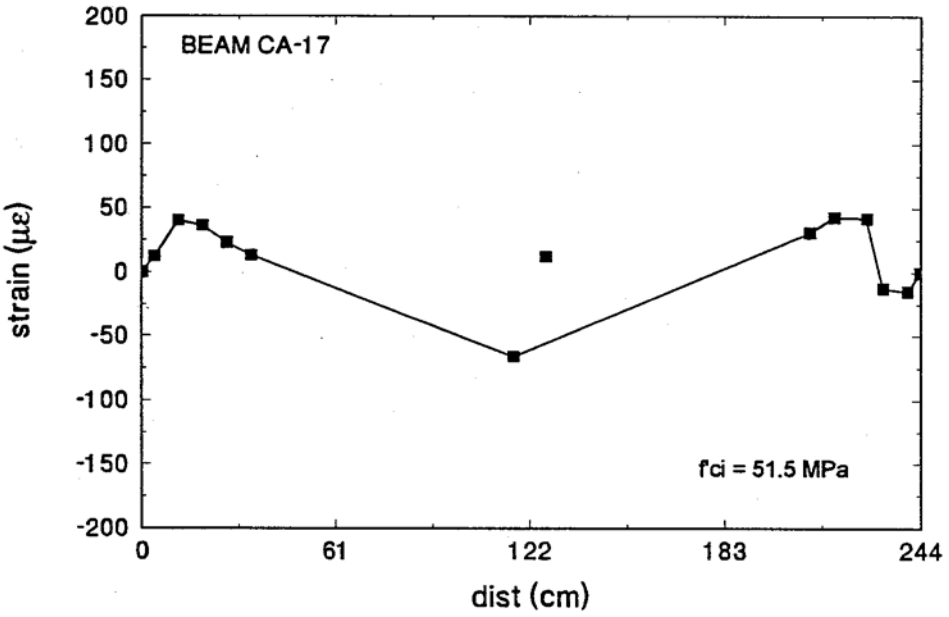

Figure 7. Field Results for Beam CA-17

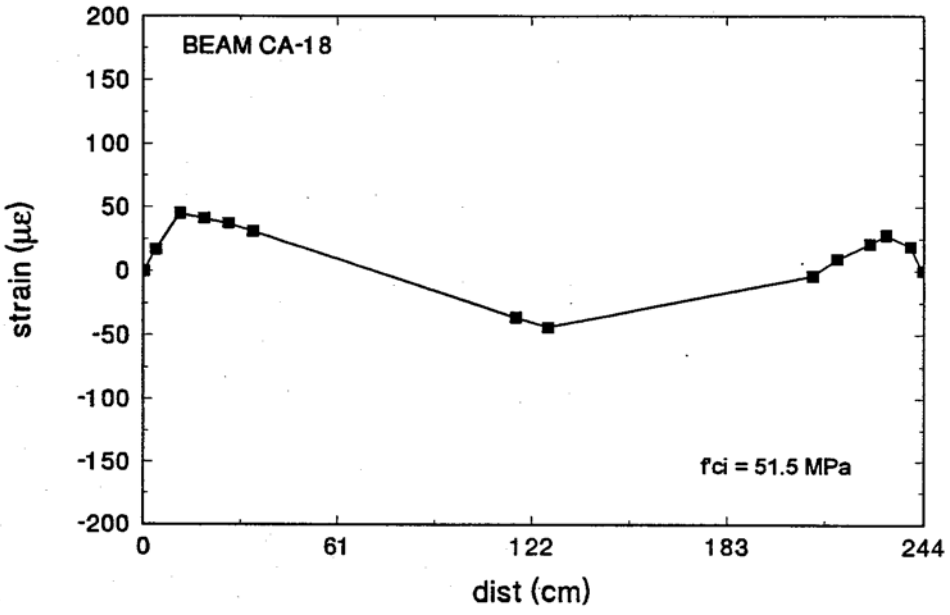

Figure 8. Field Results for Beam CA-18

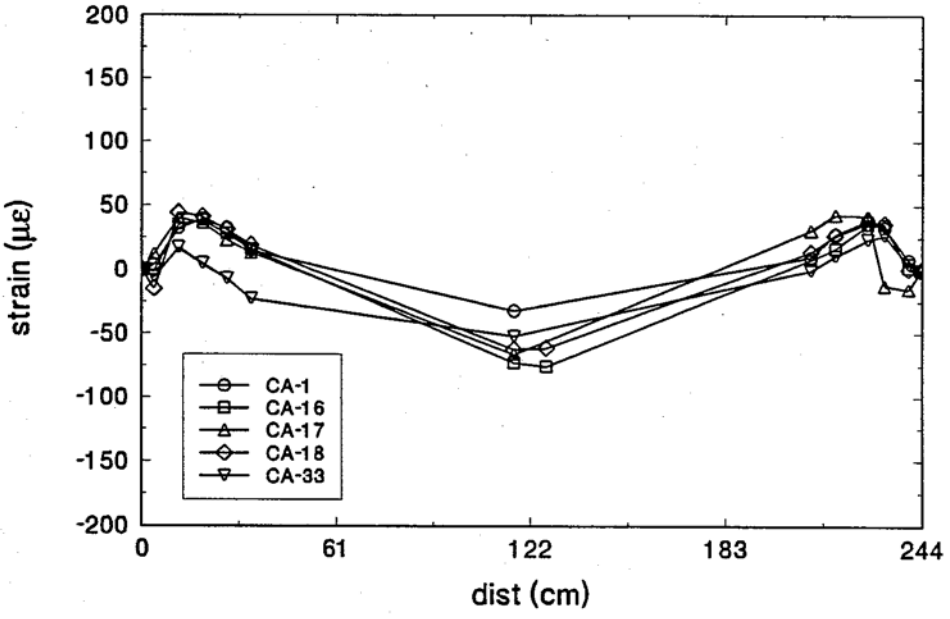

Figure 9. Field Results for All the Beams Instrumented

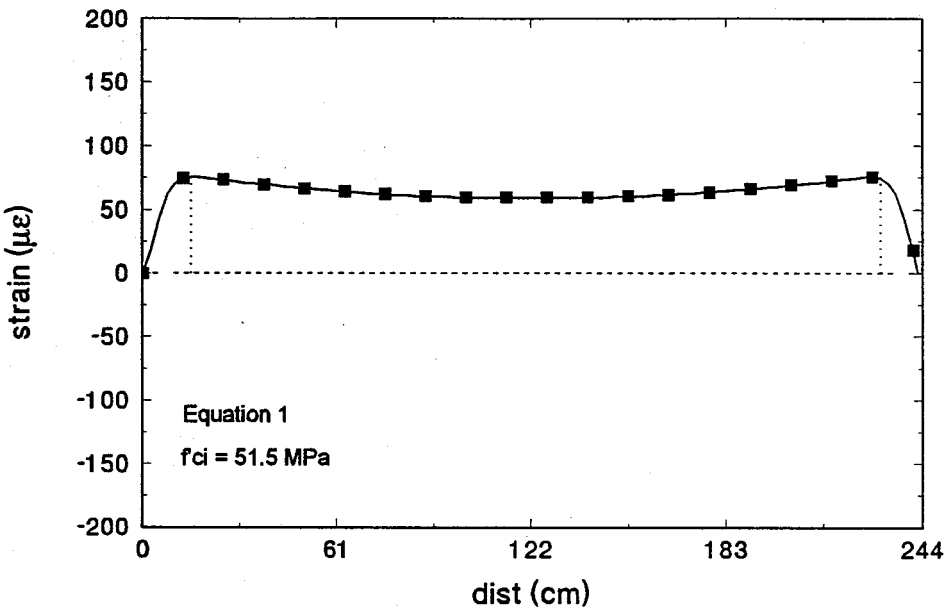

Figure 10. Expected Results

Swanson Analysis Systems Inc, Houston, Pennsylvania. The first used a model with the prestressing rods located symmetrically with respect to the centerline whereas the second model took into account their actual position. Figure 11 and Table 7 summarize the measured distances of the rods from the sides of the specimens tested.

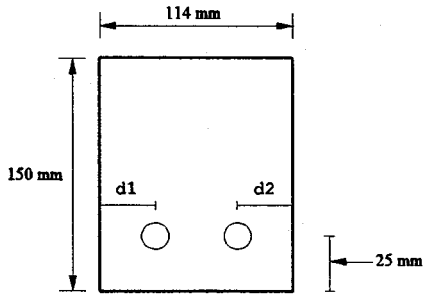

Figure 11. Edge Distances

Table 7. Summary of Strands Locations

Beam	d1 (mm)	d2 (mm)
CA-1	27.0	35.0
CA-16	29.0	34.0
CA-17	35.0	29.0
CA-18	27.0	34.0
CA-33	34.0	31.0

The beams were modeled using SOLID95 type elements. These are 3-D structural elements defined by twenty nodes, eight at each face and four intermediate nodes. Each node had three degrees of freedom - translations in the "x", "y" and "z" directions.

The cross-section was discretized for the two analyses as shown in Figure 12a (for the symmetric case) and Figure 12b (for the unsymmetric case). For the former case, symmetry allowed the problem size to be greatly reduced. Because the results for transfer length were found to be insensitive to the exact location of the CFRP rod, only one representative mesh was used (see Table 7) for all five beams.

The discretization along the length (see Figure 12c) was the same for the two analyses. Since the prestressing force was assumed to be unchanged over the length of the specimen it was only necessary to model half the length. To obtain agreement with the theoretical transfer strain (see Eq. 1), a very fine discretization was needed. A total of 48 elements each 2.5 cm long were used to model half the length. Because of the discretization of the cross-section this meant that six layers of 48 elements were provided along the length

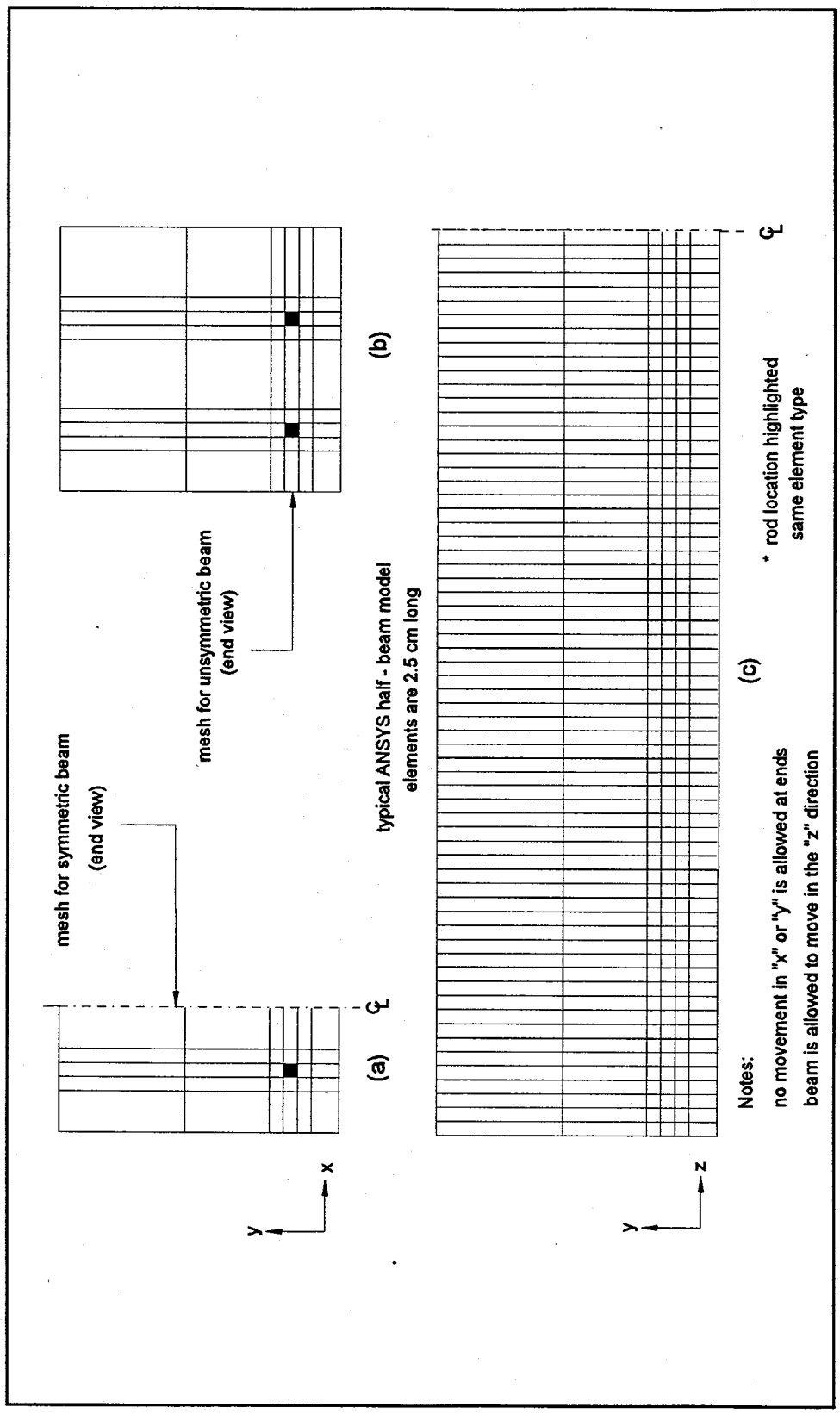

Figures 12 a,b & c. ANSYS Model

(see Figure 12c). Their height varied as shown in Figure 12a,b. A total of 2,592 elements and 12,817 nodes were used in the discretization. In the cross-section, 193 nodes were present.

Since prestress forces are transferred to the concrete by the *Hoyer* effect, the Poisson's ratio of the two materials is an important variable. For concrete, a value of 0.2 given in the AASHTO specifications was used. For CFRP, the values were different in the axial and radial directions. In the axial direction, the CFRP value of 0.28 was used. In the radial directions, the resin value of 0.35 was used.

The elastic modulus of concrete was determined using Nilson's equations corresponding to a concrete strength of 51.5 MPa. This gave a value of 30.7 GPa. For CFRP, the calculated modulus of 109 GPa was used in the longitudinal direction. In the transverse direction, the resin modulus of 4 GPa was assumed.

To determine the theoretical transfer length ideal conditions were assumed. Thus, the beam was free to move longitudinally because of elastic shortening (z) and upward (y) because of eccentricity of the prestressing force. However, the ends were assumed to be simply supported and restrained to prevent out of plane movement (x direction).

The prestressing load was equally distributed among each of the corners of the element(s) representing CFRP (see darkened element(s) in Figures 12a,b). Details of the loads, material properties and boundary conditions as input may be found in Sukumar, 1995.

The results from the finite element analyses for the two meshes were identical and are shown in Figures 13 (without self weight) and Figure 14 (including self weight). The transfer

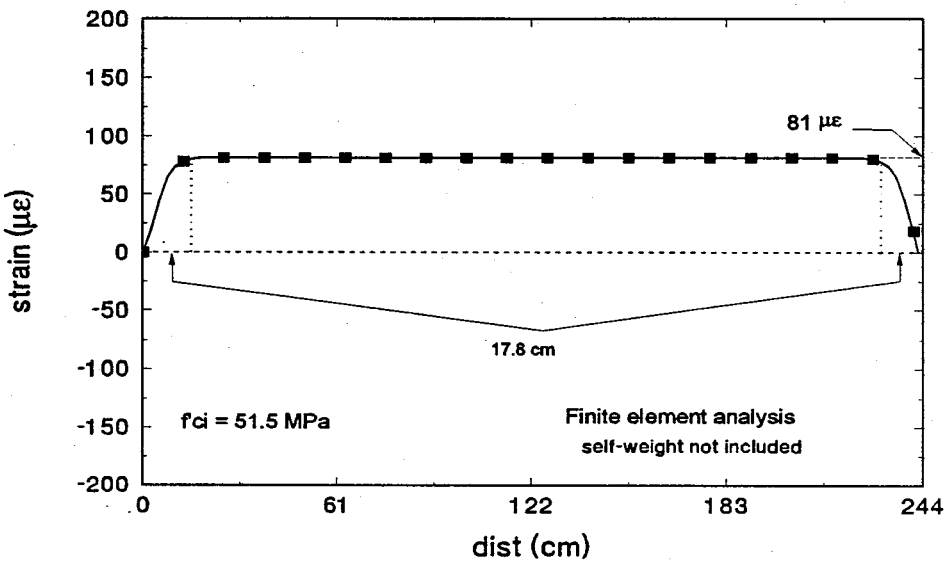

Figure 13. Finite Element Analysis Results

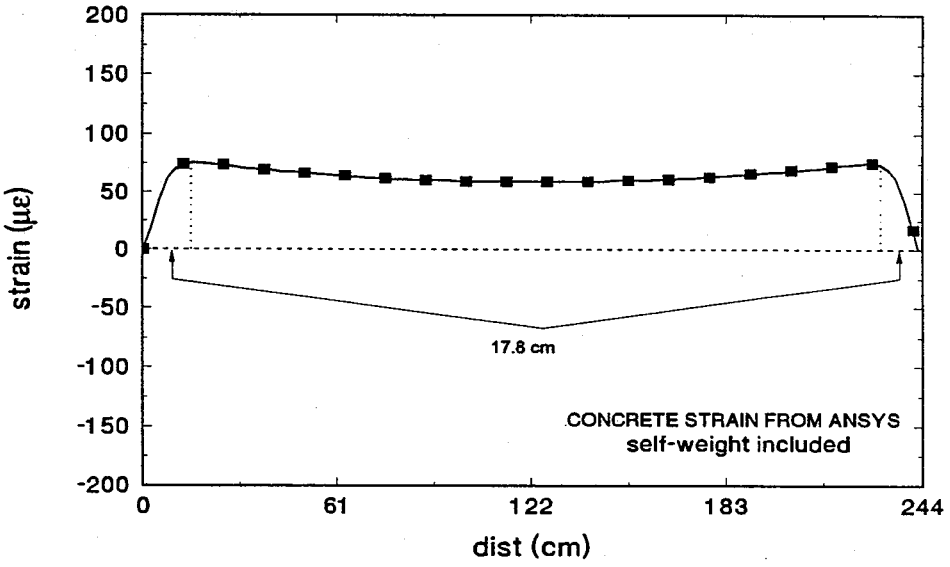

Figure 14. Finite Element Analysis Results Including Self-Weight

length predicted is about 17.8 cm as indicated in these figures. The concrete strain corresponding to transfer of 81με is identical to that obtained from Eq. 1 neglecting self-weight. This suggests that the finite element discretization was satisfactory.

4.4.1 Friction Forces

As noted earlier, the discrepancy between the field results (Figures 4-9) and expected results (Figure 10) was attributed to possible friction forces that impeded the upward movement of the beam at transfer. In view of this, finite element analyses were carried out.

Because the frictional forces were believed to be caused by bending about the weak axis, only movement of the surface pressing against the wood, i.e. in tension, was restricted, The face moving away from the formwork, i.e. the compression face, was unaffected. Moreover, only apart of the tension face actually in contact with the form would be subjected to frictional forces.

Based on the above considerations, the frictional force was assumed to have a parabolic distribution that extended from quarter point to quarter point. This is consistent with the upward movement which is greater in the middle and smaller near the ends. This force was additionally assumed to act on only one face as shown in Figure 15.

Trial and error was used to obtain correlation between test results and predictions from ANSYS. Since the frictional force was not identical in each beam, the magnitude of this force varied from beam to beam. Table 8 summarizes the forces used in the analysis. These

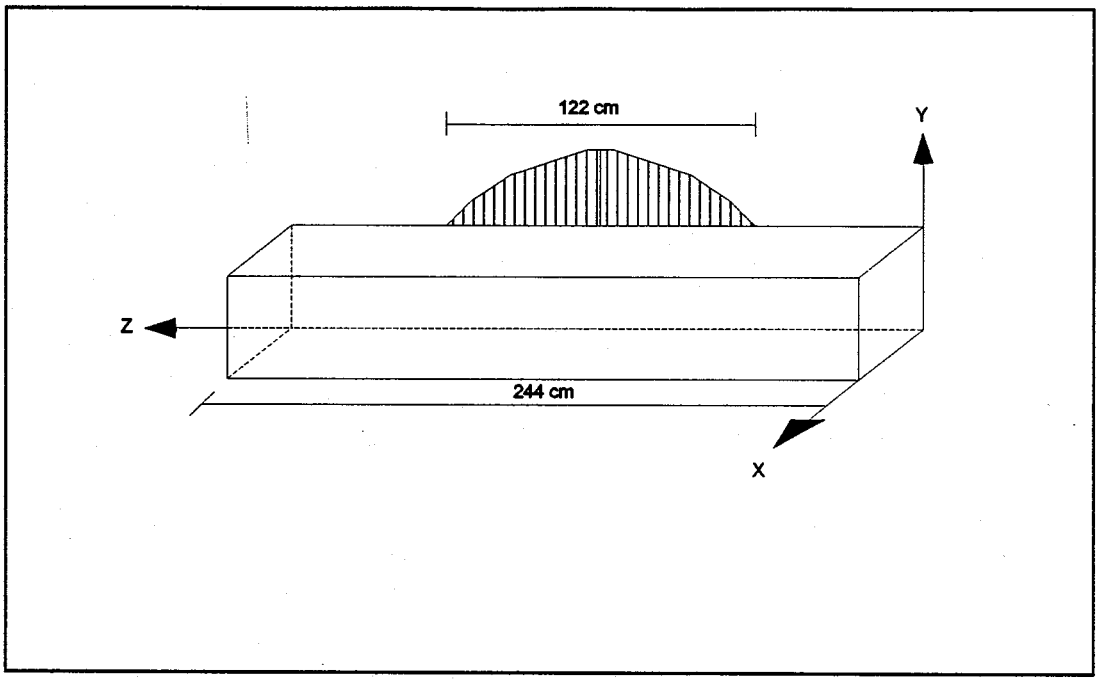

Figure 15. Schematic of Frictional Forces Distribution

Table 8. Friction Forces Used in ANSYS

Beam	Friction Force (kN)	Friction coefficient*
CA-1	2.3	4.0
CA-16	2.6	6.4
CA-17	2.6	5.3
CA-18	3.2	4.6
CA-33	2.4	10.7

range from 2.3 kN to 3.2 kN. Using a very simplified model, this suggests a large friction coefficient, Sukumar 1995.

Figures 16-20 compare the predictions from finite element analysis incorporating frictional forces and test results. The overall agreement is close and appears to confirm the validity of the hypothesis.

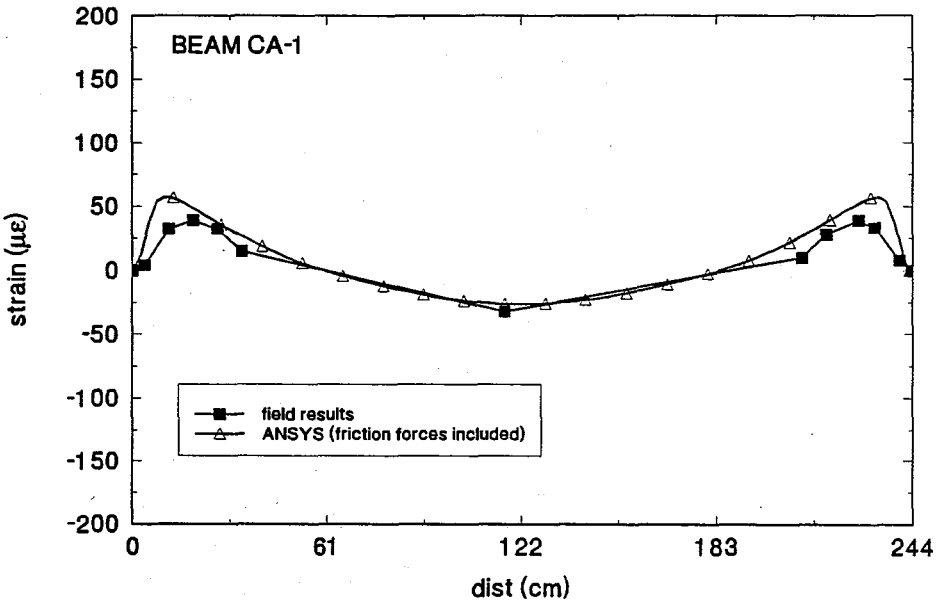

Figure 16. Comparative Results for Beam CA-1

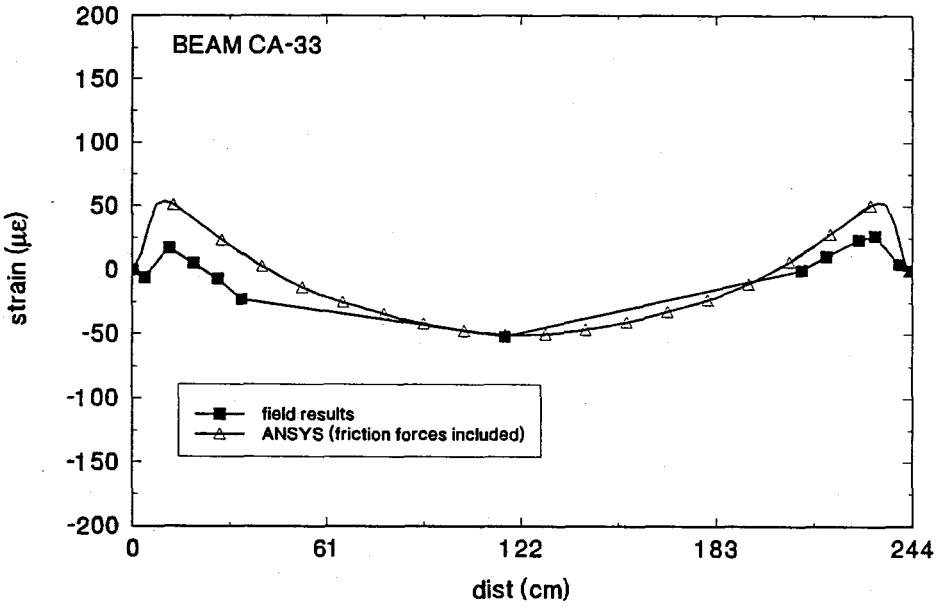

Figure 17. Comparative Results for Beam CA-33

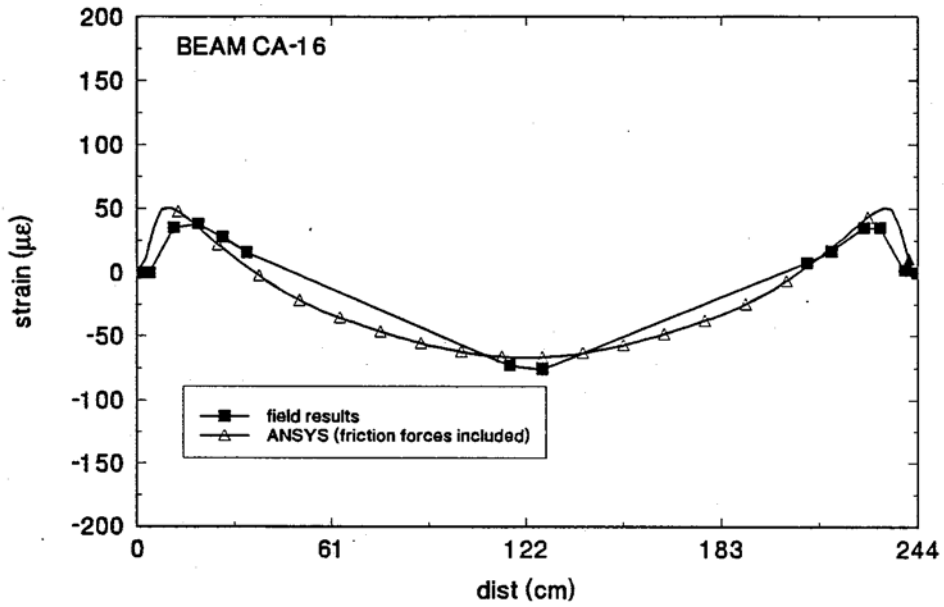

Figure 18. Comparative Results for Beam CA-16

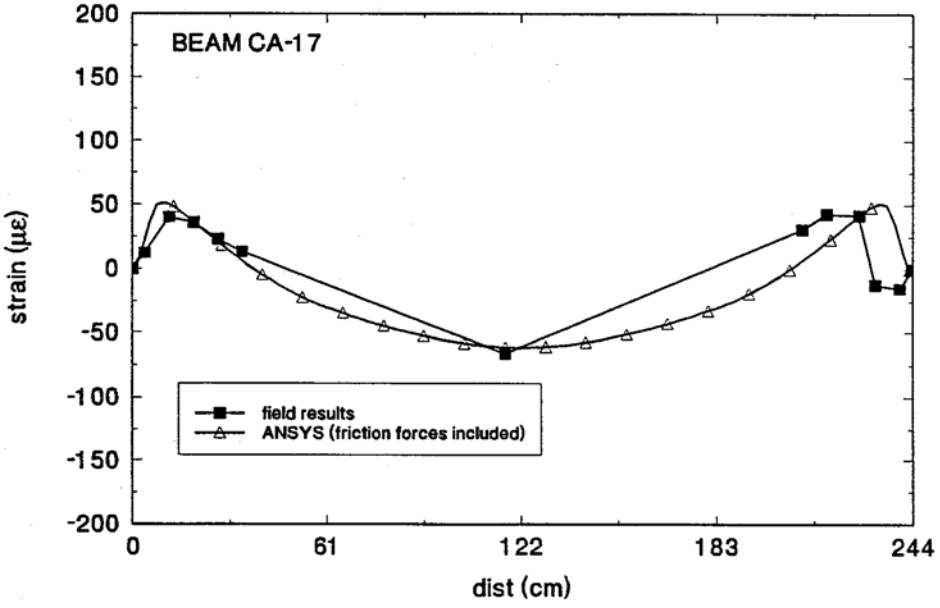

Figure 19. Comparative Results for Beam CA-17

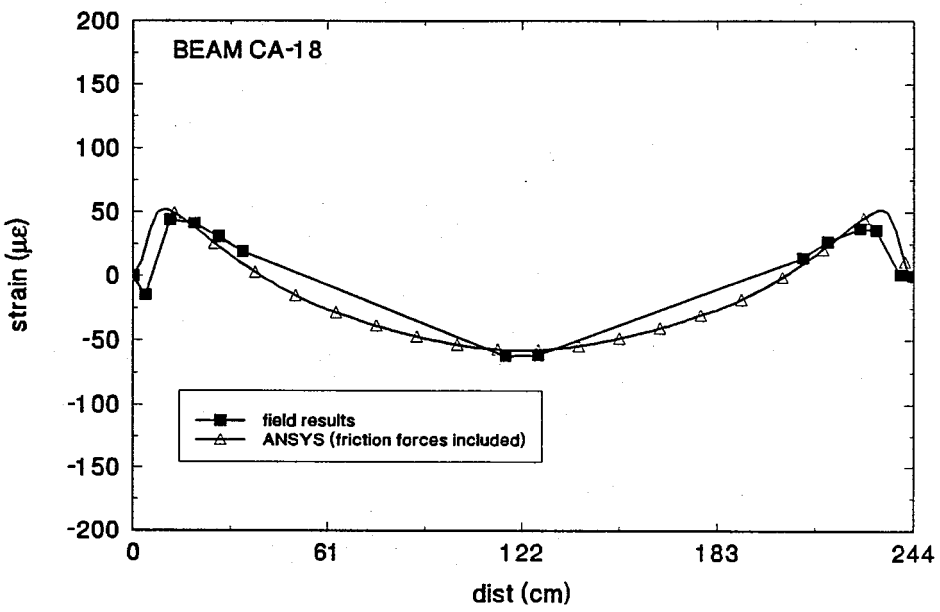

Figure 20. Comparative Results for Beam CA-18

5. EFFECTIVE PRESTRESS

5.1 Introduction

This chapter analyses pre-cracking load results to determine the effective prestress. The beams cast on December 14, 1992 were pre-cracked three weeks later on January 6, 1993. Since three beams CA 1, CA 10 and CA 20 were damaged during removal from the bed, only thirty beams were pre-cracked. Section 5.2 gives the setup for the precracking. The calculation of the effective prestress is summarized in Section 5.3.

5.2 Test Procedure

The beams were pre-cracked at the prestressing yard where the beams were poured. Since no cylinders were tested during pre-cracking, the concrete strength was extrapolated from the concrete strengths at transfer and the initial controls tests carried in February 1993, Mehta & Monteiro 1993. This indicated that the concrete strength would be approximately 92% of the 28 day strength giving a strength of 58 MPa.

The outdoor test set-up used is shown in Figure 21. The beams were placed upside down (span of 2.29 m) in a temporary metal frame so that the bottom surface, i.e. the pre-compressed tension zone was exposed. This meant that any crack could be immediately

detected. A hydraulic jack was used to apply a point load at mid-span. The magnitude of the applied load was determined using a proving ring, Plate 10.

The load at which the first crack was detected was recorded. This is the cracking load, P_{cr}, for the beam. Since the purpose of the cracking was to simulate damage during pile driving, the load was somewhat increased to allow more cracking to occur. A summary of the beam dimensions, cracking loads and the number of cracks obtained is presented in Table 9.

5.3 Effective Prestress

Procedures for calculating the effective prestress are well known and described in texts, e.g. Nilson 1986 . However, since the beams were tested upside down in our case, dead load led to compressive stresses rather than tensile stresses as are customary.

To calculate the effective prestress, the modulus of rupture value for concrete, i.e. the maximum allowable tensile stress in bending, must be known. The modulus of rupture for ordinary strength concrete is given by ACI 318-89 as $7.5\sqrt{f'_c}$. For high strength concrete, the modulus of rupture is higher and ranges from 7.5 to $12\sqrt{f'_c}$. In view of this, four separate values were investigated: these were $7.5\sqrt{f'_c}$, $2.3(f'_c)^{2/3}$ Shah & Ahmad 1985, $11.7\sqrt{f'_c}$ and $12\sqrt{f'_c}$, Carrasquillo *et al* 1981.

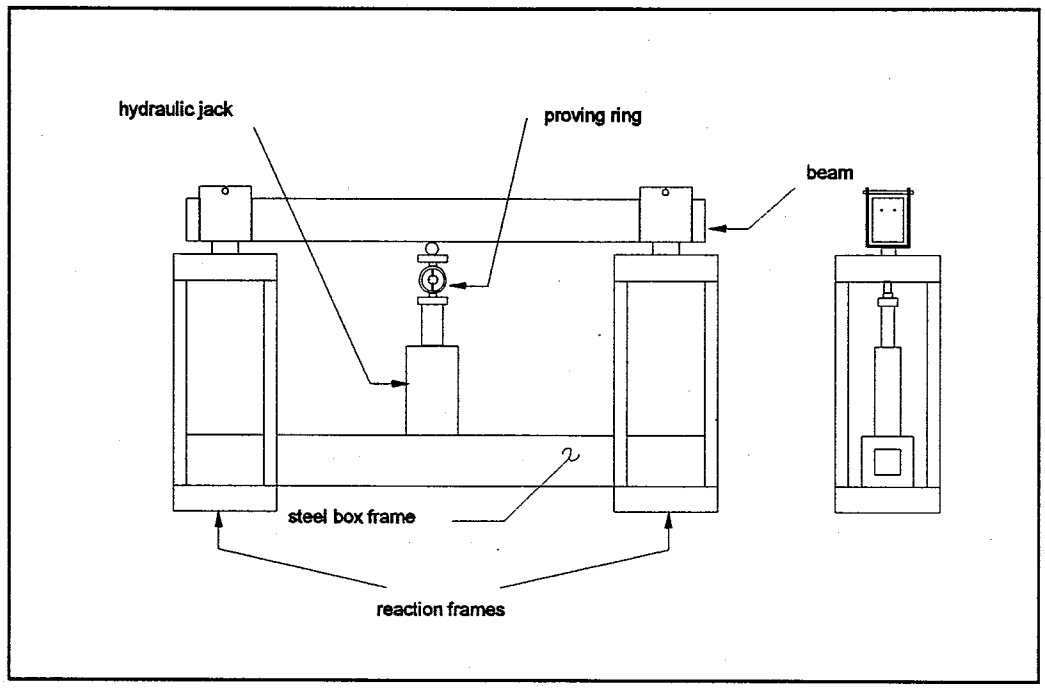

Figure 21. Schematic of the Test Set Up

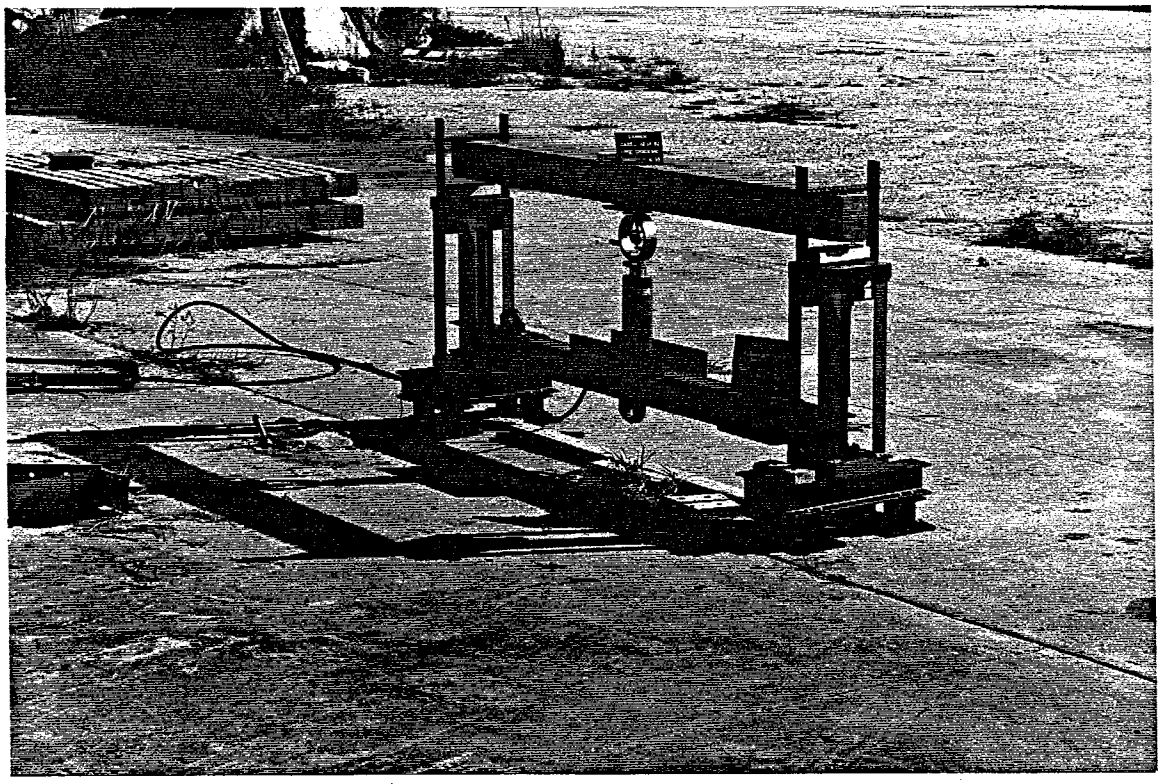

Plate 10. Pre-cracking Test Set Up

Table 9. Cracking Loads for Carbon Beams

Beam #	Width (cm)	Depth (cm)	Eccentricity (cm)	P_{cr} (kN)	# of Cracks
CA - 2	11.4	14.7	5.3	10.1	5
CA - 3	11.4	15.6	5.3	13.4	4
CA - 4	11.4	14.7	5.3	10.2	4
CA - 5	11.4	14.9	4.6	11.8	5
CA - 6	11.4	15.1	4.6	11.6	5
CA - 7	11.4	15.2	4.6	11.7	4
CA - 8	11.4	15.1	5.3	13.2	4
CA - 9	11.3	15.4	5.3	12.5	4
CA - 11	11.1	14.7	4.6	12.5	4
CA - 12	11.3	15.1	4.6	12.2	3
CA - 13	11.3	15.4	5.3	12.4	2
CA - 14	10.9	15.2	3.6	11.6	3
CA - 15	11.3	15.2	4.6	11.5	3
CA - 16	11.3	15.7	4.6	9.9	5
CA - 17	11.3	15.4	5.3	11.6	4
CA - 18	11.3	15.6	5.3	12.6	3
CA - 19	11.1	15.4	5.3	12.5	4
CA - 21	11.3	15.4	5.3	11.7	5
CA - 22	11.3	15.2	4.6	11.6	3
CA - 23	10.9	14.9	3.6	9.6	5
CA - 24	11.6	15.4	4.6	9.8	4
CA - 25	11.6	15.2	5.3	10.5	4
CA - 26	11.5	15.4	4.6	12.7	3
CA - 27	11.6	15.2	4.6	11.4	4
CA - 28	11.1	15.4	3.6	10.2	6
CA - 29	11.2	15.2	5.3	12.2	3
CA - 30	11.6	15.1	4.6	11.9	3
CA - 31	11.4	15.4	4.6	11.6	3
CA - 32	11.4	15.2	4.6	10.1	5
CA - 33	11.4	15.2	3.6	11.4	4

The effective prestress, P_e, was determined from Eq.

$$\frac{Pe}{A} + \frac{P_e e}{S} - \frac{P_{cr} L}{4S} + \frac{wL^2}{8S} = -f_r \qquad (2)$$

where P_{cr} is the pre-cracking load, w the unit weight of concrete, e is the eccentricity of the fibers, L is the length of the beam, S the section modulus of the beam, A the area of cross-section and f_r the modulus of rupture. Note the positive contribution of the dead load stresses in Eq. 2 due to the configuration of the beams in the testing.

Table 10 gives the effective prestress for each beam obtained using all four equations. Inspection of Table 10 shows that the lower the modulus of rupture value, the higher the calculated effective prestress. Since the jacking force (monitored through load cells at both the dead and live ends) was 0.6 x 2 x 43 = 51.6 kN, values above this magnitude indicated the use of an inappropriate modulus of rupture value.

Calculated means and standard deviations for the beams pre-cracked are summarized in Table 11. The mean values for all 30 beams range from 44.3 kN to 64.9 kN. Also provided in the same table are the calculated means, standard deviations excluding the highest and lowest values, the 95 percentile value, i.e. the effective prestress exceeded by 95% of all the beams tested, and the effective prestress expressed as a percentage of the ultimate capacity of the two CFRP rods, i.e. 86 kN.

Since different beams were used in the three long term studies, Table 12 summarizes the average calculated effective prestress for the beams in each of the studies.

Table 10. Effective Prestress for Carbon Beams

Beam #	P_e[1] (kN)	P_e[2] (kN)	P_e[3] (kN)	P_e[4] (kN)
CA - 2	50.5	35.9	34.8	31.3
CA - 3	70.9	55.0	53.9	50.1
CA - 4	51.4	36.8	35.7	32.3
CA - 5	65.2	49.6	48.6	44.9
CA - 6	62.5	46.6	45.6	41.8
CA - 7	62.6	46.5	45.4	41.5
CA - 8	72.7	57.7	56.6	53.0
CA - 9	65.9	50.4	49.3	45.7
CA - 11	72.5	57.7	56.5	53.1
CA - 12	68.6	52.9	51.8	48.1
CA - 13	65.0	49.5	48.4	44.8
CA - 14	65.7	49.6	48.5	44.7
CA - 15	61.1	45.2	44.1	40.4
CA - 16	46.6	29.9	28.7	24.7
CA - 17	58.7	43.3	42.1	38.4
CA - 18	66.0	50.3	49.1	45.4
CA - 19	66.3	51.1	49.9	46.3
CA - 21	59.4	43.9	42.8	39.1
CA - 22	62.0	46.2	45.1	41.3
CA - 23	51.3	35.7	34.6	30.9
CA - 24	46.4	29.8	28.6	24.6
CA - 25	50.6	34.9	33.9	30.1
CA - 26	69.0	52.6	51.4	47.5
CA - 27	60.3	44.0	42.9	39.0
CA - 28	53.7	37.1	35.9	31.9
CA - 29	64.2	49.1	48.0	44.4
CA - 30	64.9	48.9	47.7	43.9
CA - 31	60.8	44.5	43.3	39.5
CA - 32	55.2	37.6	36.3	32.1
CA - 33	63.5	46.6	45.4	41.5

[1] - $7.5\sqrt{f'_c}$ $\quad f'_c = 58$ MPa (8400 psi)

[2] - $11.7\sqrt{f'_c}$

[3] - $12\sqrt{f'_c}$

[4] - $2.3\ (f'_c)^{2/3}$

Table 11. Summary of Results

	# of beams	$7.5f'_c{}^{.5}$	$11.7f'_c{}^{.5}$	$12f'_c{}^{.5}$	$10.3f'_c{}^{(.5)1}$
Mean (X) (kN)	30	64.9	49.2	48.0	44.3
	28 [3]	61.3	45.4	44.3	40.6
	26 [4]	61.4	45.7	44.4	40.7
Std Deviation (σ) (kN)	30	7.3	7.4	7.4	7.5
	28	6.2	6.7	6.7	6.8
	26	5.8	5.8	5.8	5.8
% of P_{ult}	30	75.5	57.1	55.8	51.5
	28	71.2	52.8	51.5	47.2
	26	71.4	53.0	51.7	47.3
95 percentile[2]	30	73.1	57.6	56.5	52.8
	28	71.5	56.5	55.4	51.7
	26	71.0	55.1	53.9	50.2

1 Using $f_r = 2.3(f'_c)^{2/3}$
2 $X - 1.65\sigma$
3 excluding the highest and lowest values
4 excluding two highest and lowest values

Table 12. Average Effective Prestress for Each Study

Mean (kN)	Avg of beams	$7.5f'_c{}^{.5}$	$11.7f'_c{}^{.5}$	$12f'_c{}^{.5}$	$10.3f'_c{}^{(.5)1}$
Outdoor study	9	58.6	43.0	41.9	38.3
Durability study	10	67.8	46.7	45.6	41.7
Bond study	12	58.9	44.9	43.8	40.1

It may be seen that the effective prestress is lowest in the beams selected for the outdoor study and highest for those selected for the durability study.

5.4 Recommendations

The initial prestress determined from the transfer length was estimated as 51% of the ultimate force (Table 5). Since the beams were pre-cracked only two weeks later, the effective prestress should also be around this value. Based on this, the modulus of rupture of $10.3\sqrt{f'_c}$ gives the most sensible values. If the worst two results are omitted, then the modulus of rupture value of $12\sqrt{f'_c}$ also gives acceptable results.

6. ULTIMATE CAPACITY TEST SETUP

6.1 Introduction

This chapter presents information on the setup for the ultimate bending capacity tests that were part of the outdoor exposure, durability and bond studies. Instrumentation is discussed in Section 6.2 and the test setup described in Section 6.3. The test procedure is outlined in Section 6.4.

6.2 Instrumentation

6.2.1 Concrete Gages

To monitor the concrete strain, four electrical resistance gages model PL-60-1Lfrom Texas Measurements were attached to the top surface of each one of the specimens. RP-2, which is a two component (main agent and hardener) polyester adhesive manufactured by Tokyo Kenkyujo Co. Ltd., Tokyo, Japan, was used to attach the gages to the concrete.

The concrete gages were placed at the quarter points and at 75 mm on either side of the centerline as can be seen in Figure 22.

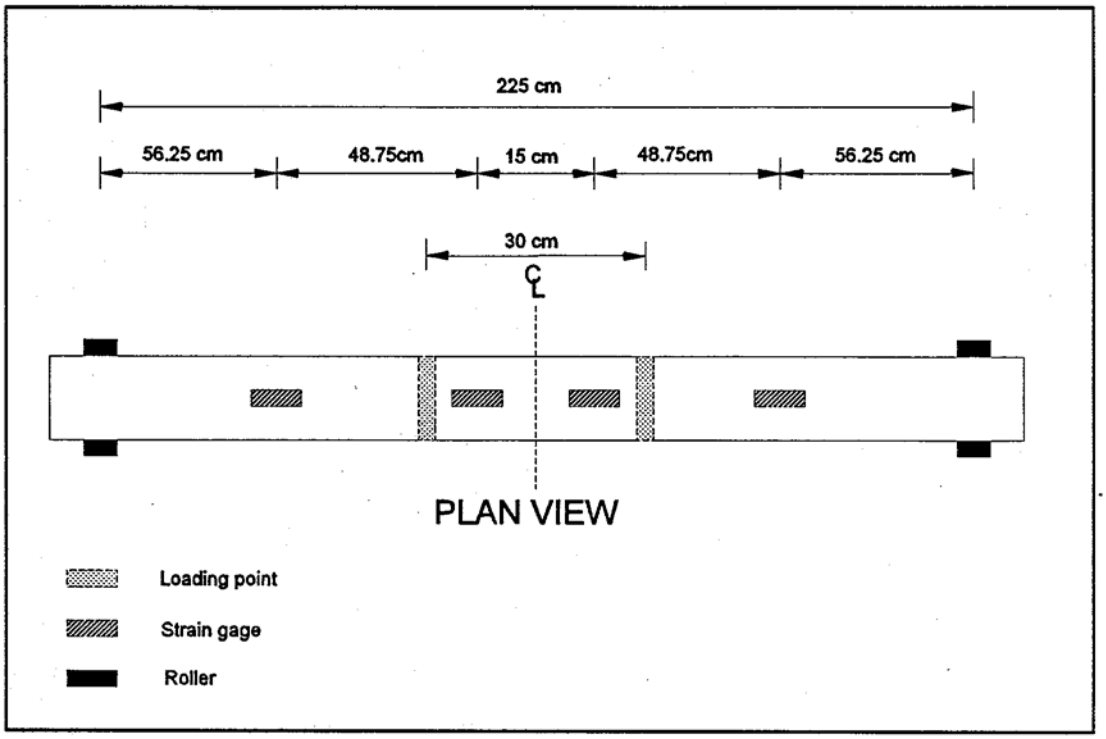

Figure 22. Location of Concrete Gages

Prior to installation of these surface strain gages, their location was smoothened and wiped using gauze moistened with acetone. The adhesive was then mixed in the recommended proportion (98:2) and applied to the back of each gage and to the ground surface. The gage was then carefully set in place and covered with a Teflon sheet provided by the manufacturer to help remove any air bubbles. Duct tape was used to cover and apply pressure to the gage. A voltmeter was then used to verify an expected reading of 120 mΩ.

6.2.2 Linear Variable Differential Transducer (LVDT)

Three LVDTs, model CDP-50 from Texas Measurements with a maximum stroke of 50 mm, were placed under the beams at the quarter points and midspan to measure the vertical deflection due to the applied load. Figure 23 shows the location of the LVDTs.

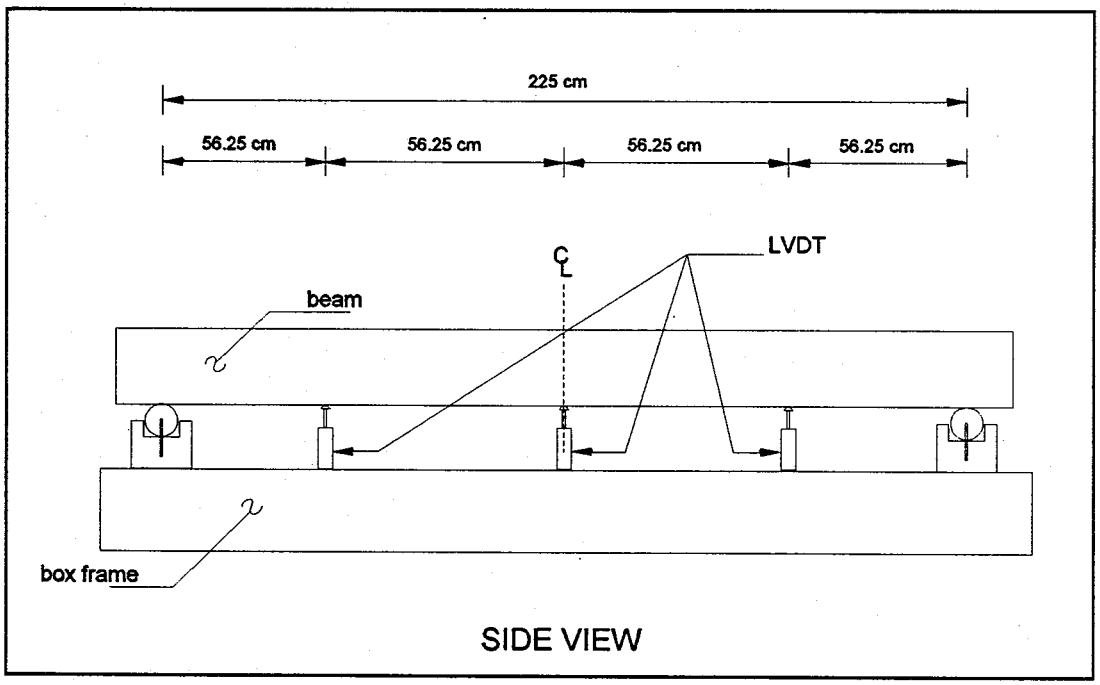

Figure 23. Position of LVDTs

6.2.3 Load Cells

The applied load and reactions were monitored by two different types of load cells. The applied load was measured with a load cell rated at a capacity of 22.2 kN. The

reactions were measured with two load cells rated at a capacity of 222 kN each.

6.2.4 Data Acquisition System

Data recording from concrete strain gages, LVDTs and load cell was fully automated using a SYSTEM 4000 data acquisition system. This system includes the Data Acquisition Control Unit (DACU), an IBM personal computer and printer. The DACU contained five strain gage scanners capable of scanning 100 strain gage based transducers and two universal scanners capable of scanning twenty LVDT channels. The software accompanying the system allowed the continuous monitoring of the concrete strain, deflections, applied load and reactions by displaying the scanned channels on the computer's monitor. This software also allowed the recording of the data in a floppy disk and its printout. Platel l shows the SYSTEM 400 data acquisition system.

6.3 Test Setup

The ultimate bending capacity tests were performed in the Structures Laboratory at the University of South Florida, Tampa, Florida.

The specimens were simply supported on rollers that were anchored to a steel box frame made of two I sections welded together. These rollers, fabricated by the USF machine shop, allowed rotational movement at both ends but could restrain horizontal translation at either end. The steel box frame was also simply supported on the two load

cells that were located directly under the rollers so as to transmit the vertical load without deformation.

An Enerpac hydraulic jack was used to apply the load. This jack was loaded against a reaction frame and the load was transmitted through a swivel head assembly to which a 150 mm x 150 mm x 9.5 mm square steel hollow section was directly bolted.

Two special roller type attachments were screwed to the hollow section so as to distribute the load from the hydraulic jack to two points on the specimen located 300 mm. apart from each other and centered with respect to the supports. This two point load subjected the center portion of the specimen to pure bending. Plates 12 and 13 show the actual test setup and the two point load assembly.

6.4 Test Procedure

Prior to each series of tests, the load cells were calibrated using a digital load cell so as to verify the validity of the readings in the SYSTEM 4000. After placing the beam on the steel box frame, the LVDTs were calibrated against a cubic piece of aluminum of known dimensions. After this calibration, the concrete strain, deflection and load readings were zeroed.

The static load was applied in 900 N increments up to the cracking load. Above this value, the increments were smaller and readings were recorded depending on the individual response of the specimens. The beams were loaded to failure and information about failure mode and crack pattern was recorded.

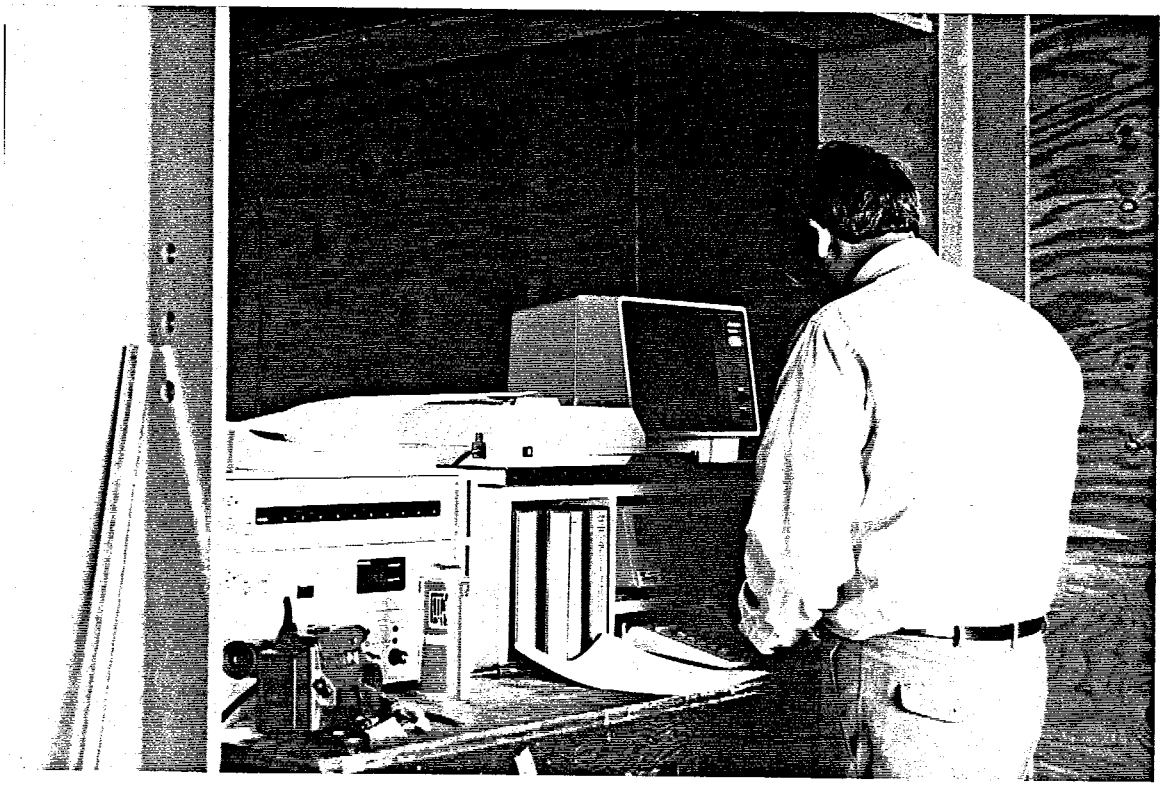

Plate 11. SYSTEM 4000 Data Acquisition System

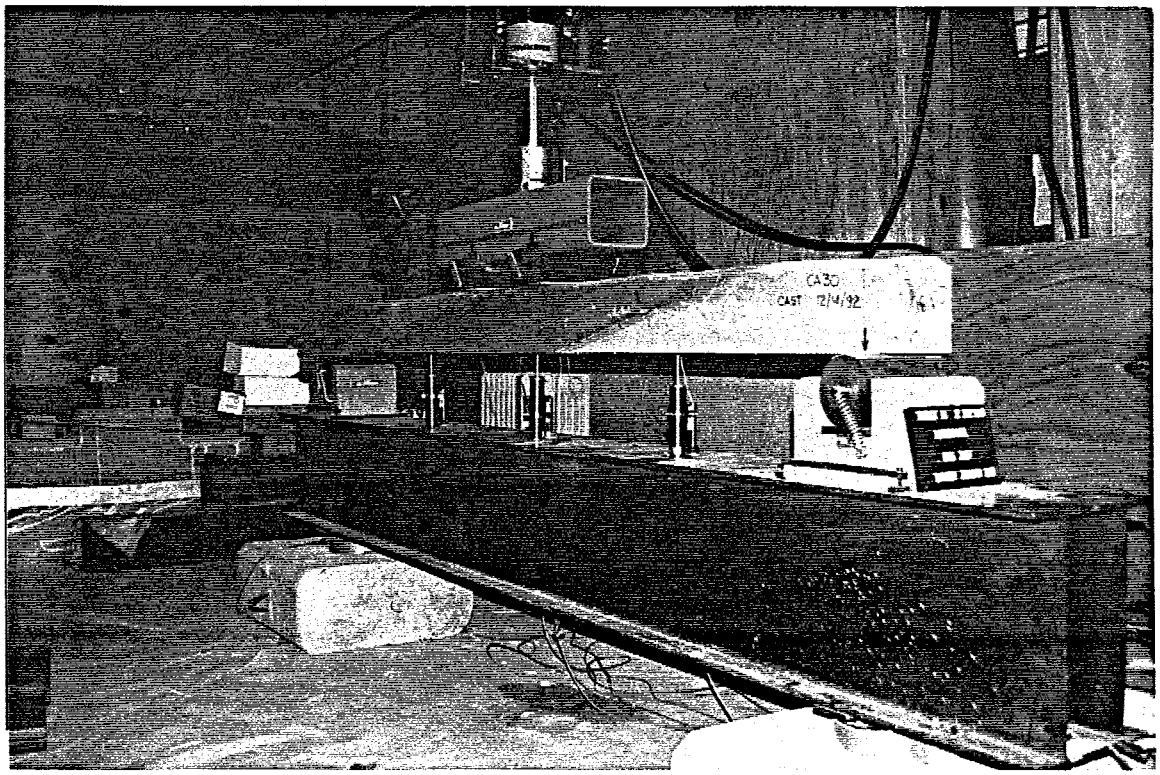

Plate 12. Test Setup

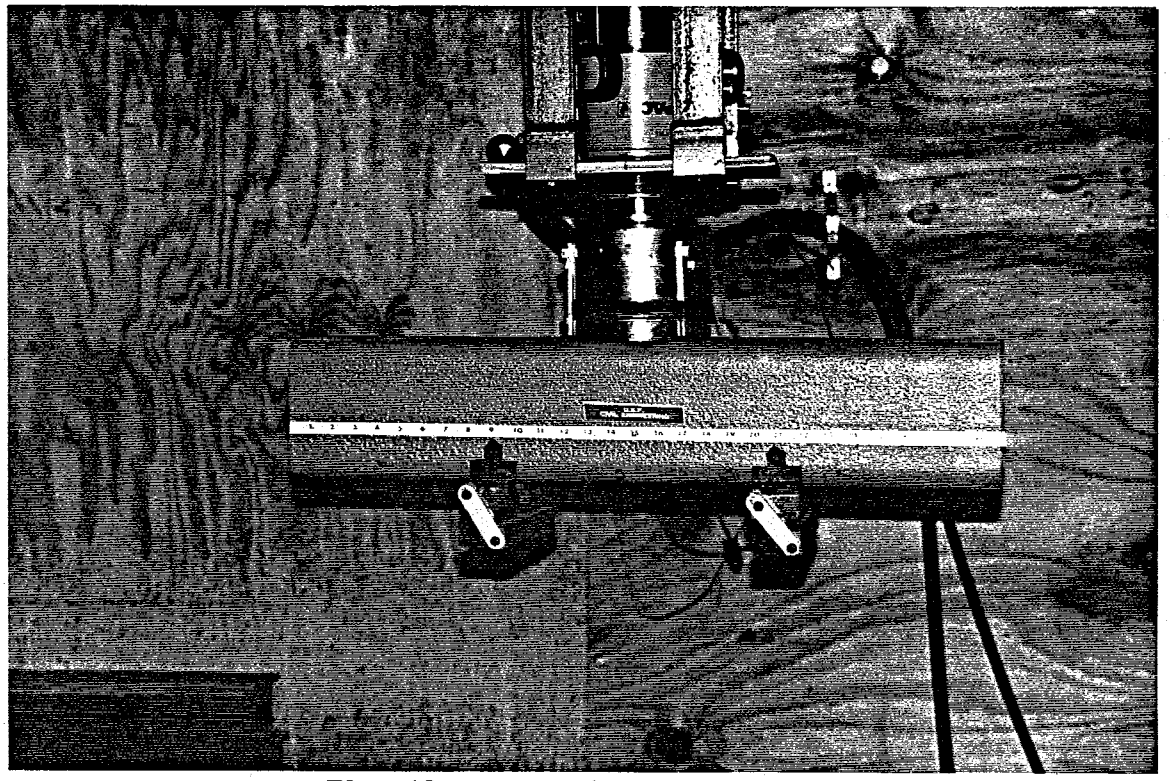

Plate 13. Two Point Load Assembly

7. OUTDOOR EXPOSURE STUDY

7.1 Introduction

This chapter presents interim results from the outdoor exposure study. A total of four series of tests were planned. Of these, three have been completed to date.

The test program is described in Section 7.2. Ambient temperature conditions for these tests are addressed in Section 7.3. Section 7.4 summarizes the test results. A discussion of the results is presented in Section 7.5.

7.2 Experimental Program

Of the thirty three beams cast, twenty two were set aside for the durability (Chapter 8) and bond (Chapter 9) studies. Nine others were set aside for the outdoor exposure where they were exposed to the elements. Of these nine beams, one (CA 20) was damaged during removal from the prestressing bed.

Details of the dimensions, number of pre-cracks and eccentricity of these beams are summarized in Table 13.

Table 13. Selection of Beams for Outdoor Exposure Study

Beam #	Width (mm)	Depth (mm)	# of cracks	Pre-cracking load (kN)	Series # (# of mos)
CA2	114	147	5	10.1	1 (2 mos)
CA 3	114	156	4	13.4	
CA 12	113	151	3	12.2	
CA 13	113	154	2	12.4	1 (2 mos)
CA 14	109	152	3	11.6	2 (20 mos)
CA 15	113	152	3	11.5	2 (20 mos)
CA 18	113	156	3	12.6	
CA 20	114	152	-	-	3 (26 mos)
CA 25	116	152	4	10.5	1 (2 mos)

A total of four series of tests were planned. In general, the timing of the tests coincided with the on-going exposure tests. Since the first and last series provided the most important results, three beams were set aside for each of these tests. The three remaining beams were tested in the intermediate series.

The first series of tests (involving three beams) were concluded between February 12-19 1993, almost two months after casting the beams and just before the commencement of the durability study. The beams were selected on the basis of their cross-sectional dimension. From these measurements, three beams with nominal dimensions closest to the design dimension (see Figure 1) were selected as controls. The results for these control beams are used as a base line for assessing the deterioration in both the durability and bond studies.

The second series of tests were conducted after twenty months. Because this was near the half way point for the study, two beams were tested. An additional specimen was

tested after twenty six months only to provide a measure of the deterioration in the bond and durability specimens that were tested at the same time.

Ultimate capacity tests were conducted on all the beams using the setup described in Chapter 6. In all the three series, the concrete strength was established by testing standard cylinders.

7.3 Temperature Data

The beams tested were exposed to outdoor conditions for the whole duration of twenty six months. To provide an index of exposure conditions, information on Tampa's weather as reported in the Tampa Tribune was used.

Because temperature is a key variable, the daily maximum and minimum temperature ranges were plotted for each monthly period since December 14 1992. Since the other studies involved exposure to salt water, the water temperature of the Gulf of Mexico was also included.

Figure 24 - 27 show the temperature variation graphs for the months of February 1994, May 1994, August 1994 and December 1994. Remaining plots covering the period from December 14 1992 to March 31 1995 are included in Sukumar 1995.

In addition to the daily maximum and minimum temperature variations, Figures 24 - 27 also provide information on the monthly maximum, minimum and average temperature ranges. This information is relevant in view of the mismatch in expansion coefficients between CFRP and concrete.

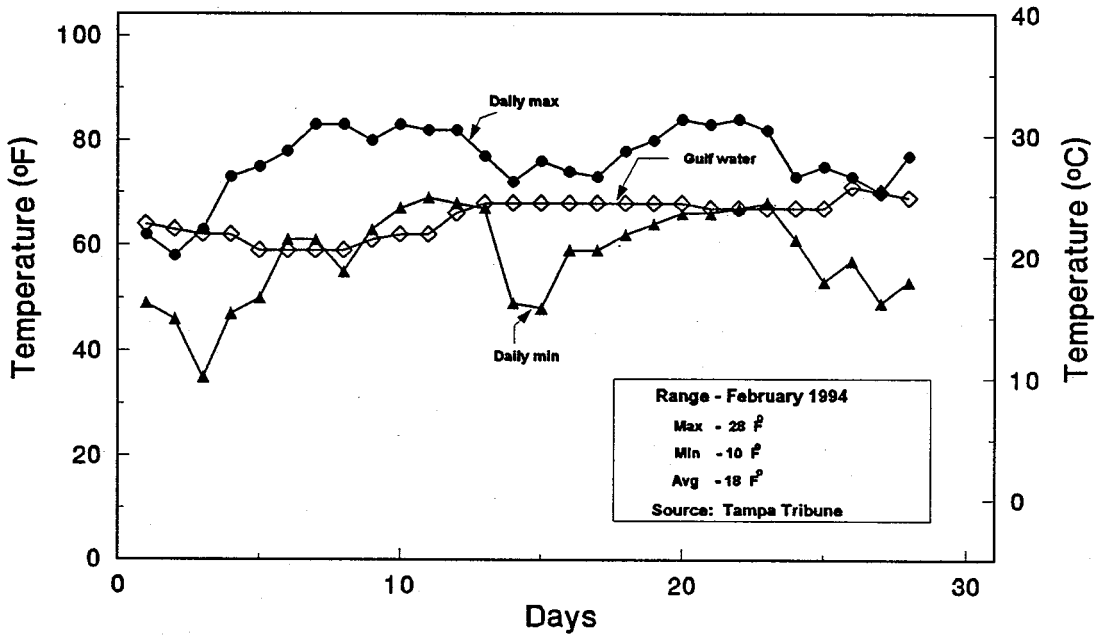

Figure 24. Temperature Variation from Tampa Tribune - February 1994

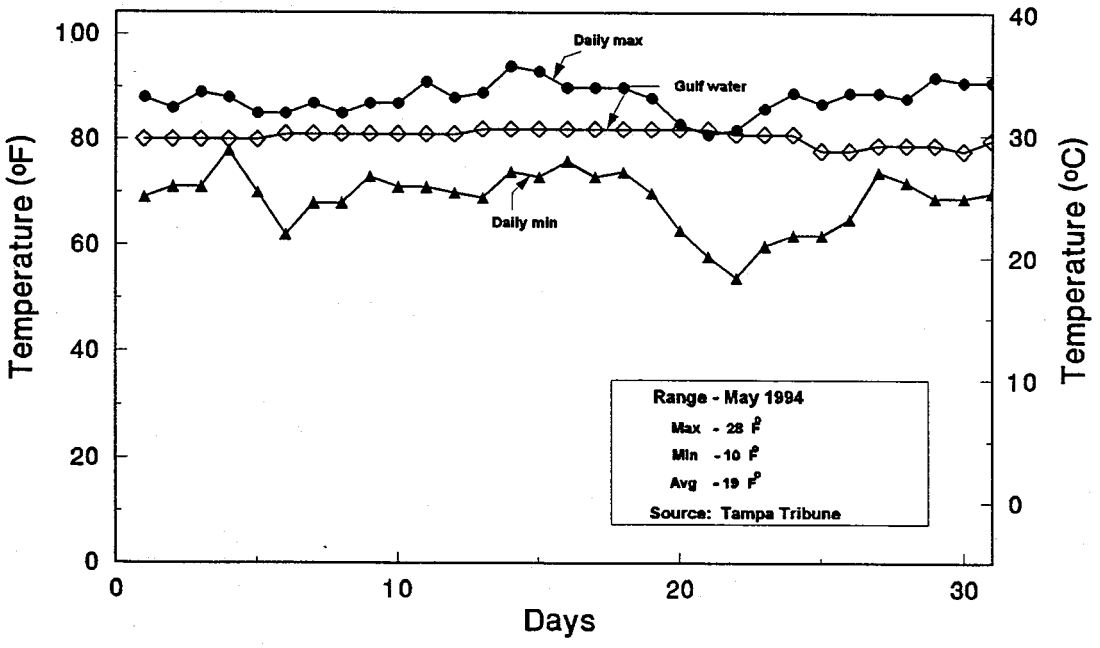

Figure 25. Temperature Variation from Tampa Tribune - May 1994

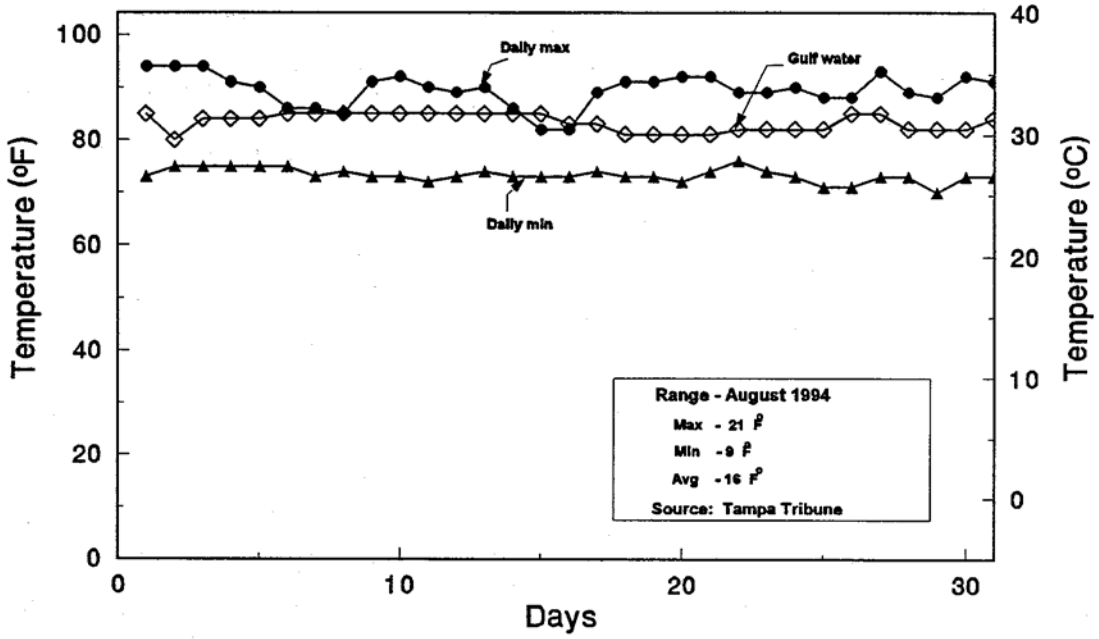

Figure 26. Temperature Variation from Tampa Tribune - August 1994

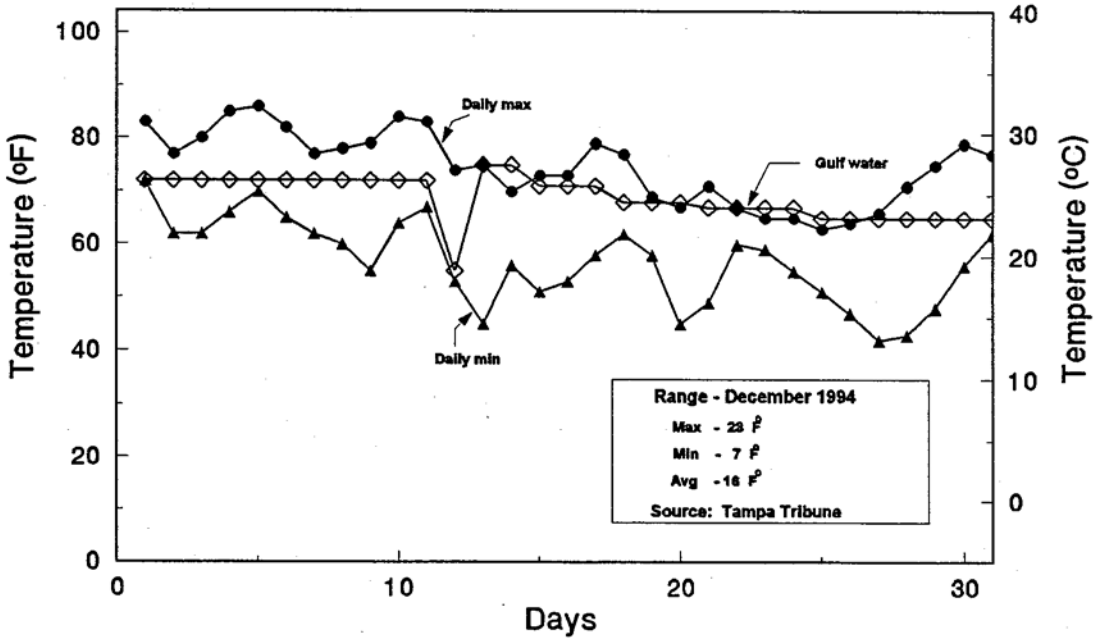

Figure 27. Temperature Variation from Tampa Tribune - December 1994

7.4 Test Results

A summary of the results for all the beams tested is provided in Table 14. This contains information on the cracking loads, failure loads, maximum deflections, ' um concrete strains and concrete strength.

7.4.1 Loads

The outdoor exposure beams tested after two months had a failure load in the range of 20-22 kN, with an average value of 21.1 kN (see Table 14). All three beams filed in flexure in the constant moment region, i.e. between the load points. The failure ode was in accordance with the design (see Section 3.2). Plate 14 shows the failure of control specimen CA 13.

After twenty months the failure load for the outdoor exposure beams dropped by 5.2% relative to the two month value, but the failure mode was still flexure. The average failure load was 20.1 kN.

The failure load dropped to 18.8 kN after twenty six months. This reduction in load was probably due to a pre-existing hairline crack near the top of the beam tested along which it failed.

Table 14. Summary of the Test Results - Outdoor Exposure Beams

Test	Date tested	Beam #	P_{cr} (kN)		P_{ult} (kN)		Max. Conc Strain($\mu\epsilon$)	Max: Defln (mm)		f'_c (MPa)	Mode of failure
			Test	Avg	Test	Avg		Test	Avg		
2 months	2/13/93	CA 2	9.5		20.5		1484	25.4			Flexure
	2/12/93	CA 13	11.5	10.7	21.0	21.1	2093	25.4	25.7	62.8	Flexure-shear
	2/19/93	CA 25	11.0		21.7		1852	26.4			Flexure
20 months	8/26/94	CA 14	11.5	11.0	20.4	20.1	1974	23.8	25.3	76.1	Flexure
	8/26/94	CA 15	10.6		19.9		2541	26.9			Flexure-bond
26 months	3/04/95	CA 20	8.9	8.9	18.8	18.8	1163	23.4	23.4	76.1	Flexure

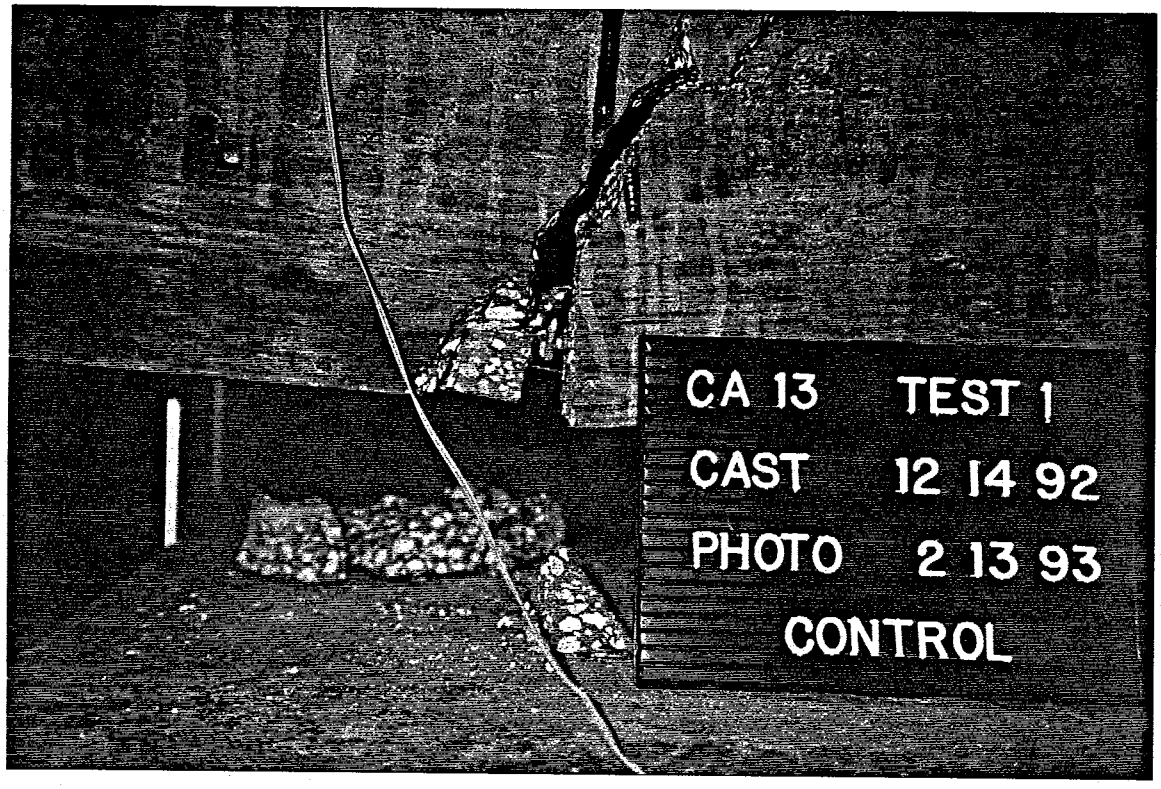

Plate 14. Flexure Failure of the Control Beam

7.4.2 Deflections

The maximum mid-span deflection in the beams tested after two months averaged 25.7 mm. After twenty months, the deflections did not show much change and averaged about 25.3 mm. The beam tested after twenty six months deflected 23.4 mm, which was approximately 90% of the deflections in the previous tests. However, as this failed along a pre-existing hairline crack, the results suggest that outdoor exposure does not lead to any reduction in the ultimate strain capacity of the CFRP rod.

Load-deflection curves for all eight beams tested are shown in Figures 28-30. A comparative plot of selected beams (CA 25, CA 15 and CA 20) from each series

respectively is shown in Figure 31.

Because of an increase in concrete strength over the period of the testing, the last beam CA 20 tested could be expected to display the greatest stiffness in the elastic range. This however is not the case since this beam had a hairline crack as stated earlier.

7.4.3 Crack Patterns

The failed beams were re-assembled after the completion of the tests to assess their crack pattern. This helped in identifying any underlying trends in the failure mode.

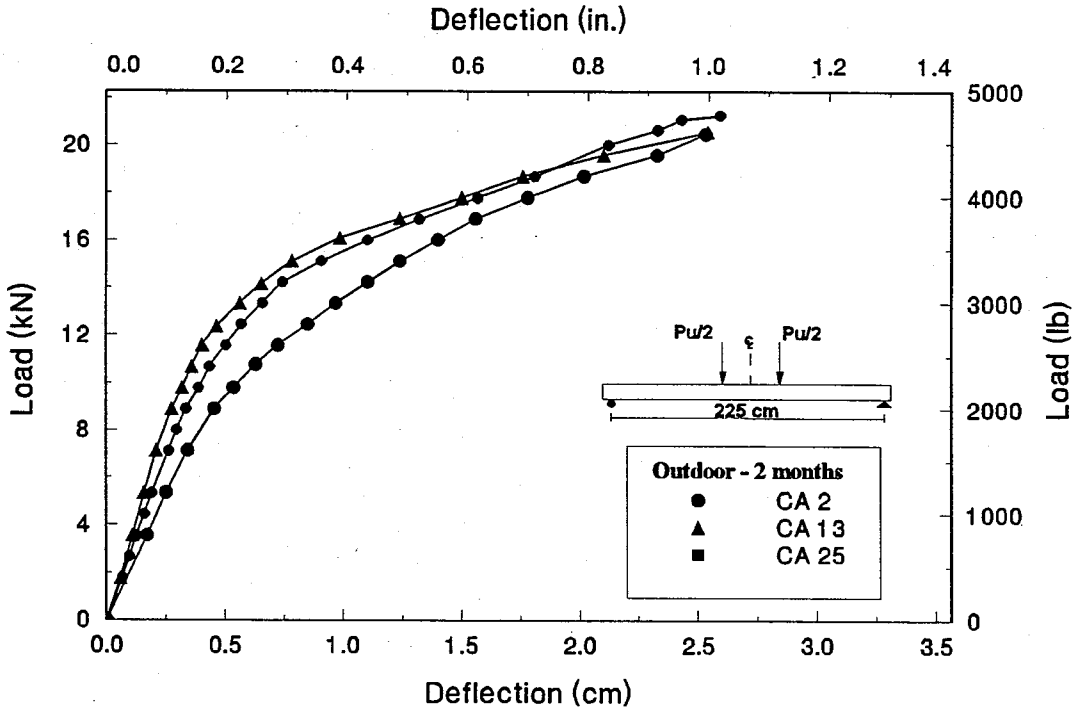

Figure 28. Load-Deflection for Outdoor Exposure Beams - 2 Months

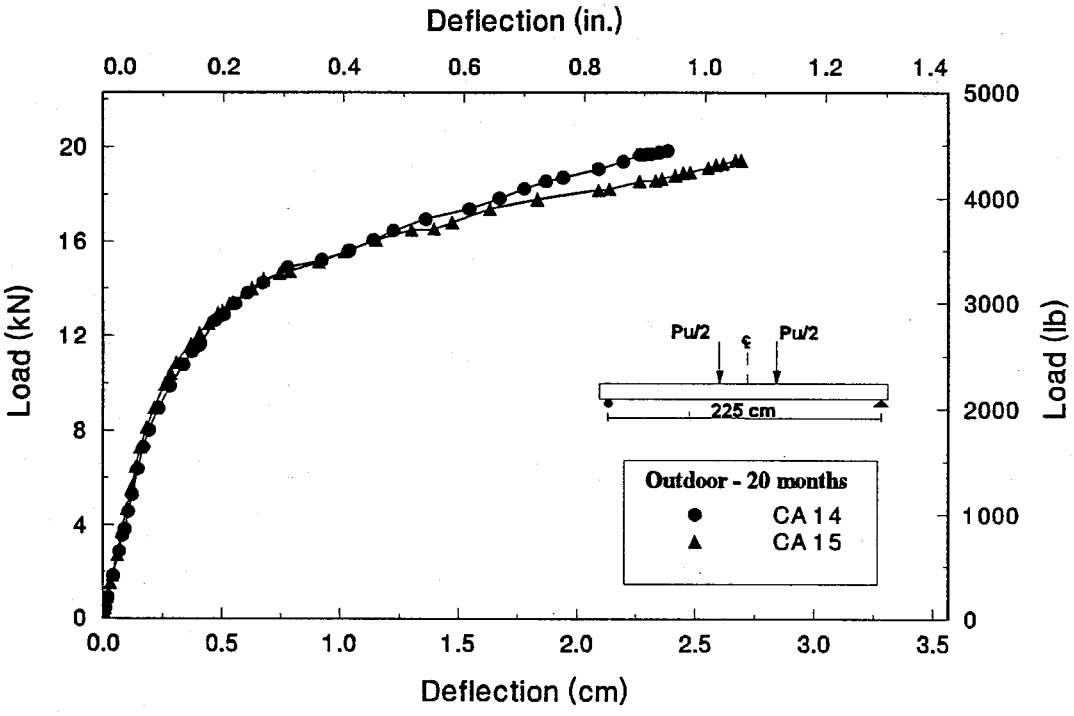

Figure 29. Load-Deflection for Outdoor Exposure Beams - 20 Months

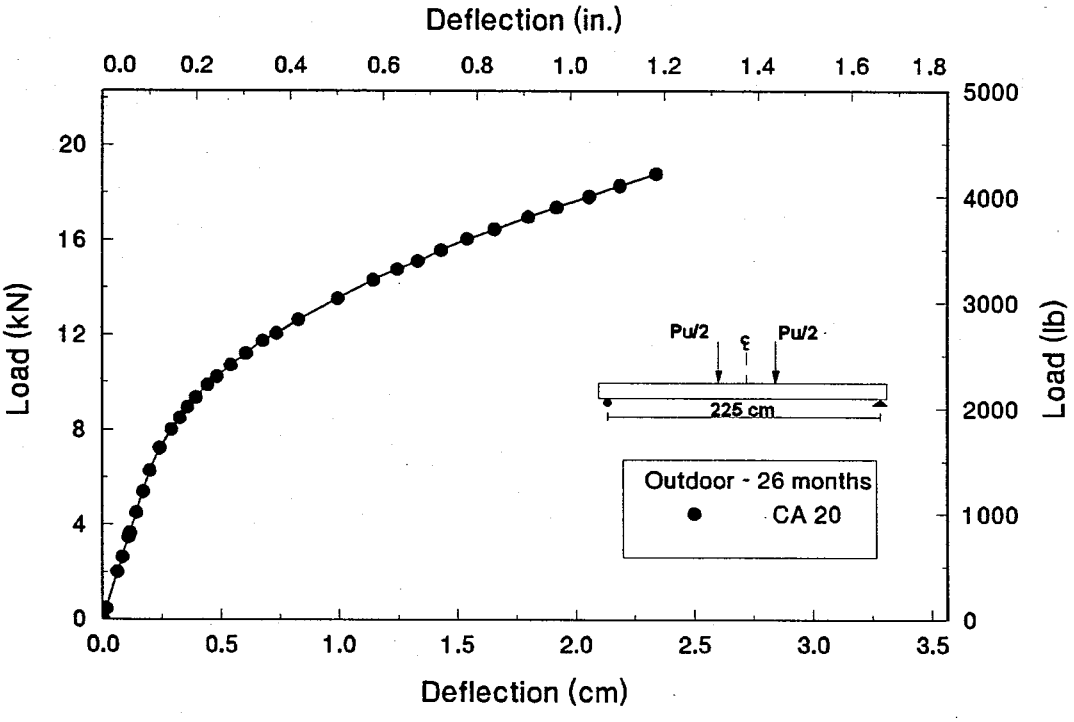

Figure 30. Load-Deflection for Outdoor Exposure Beam - 26 Months

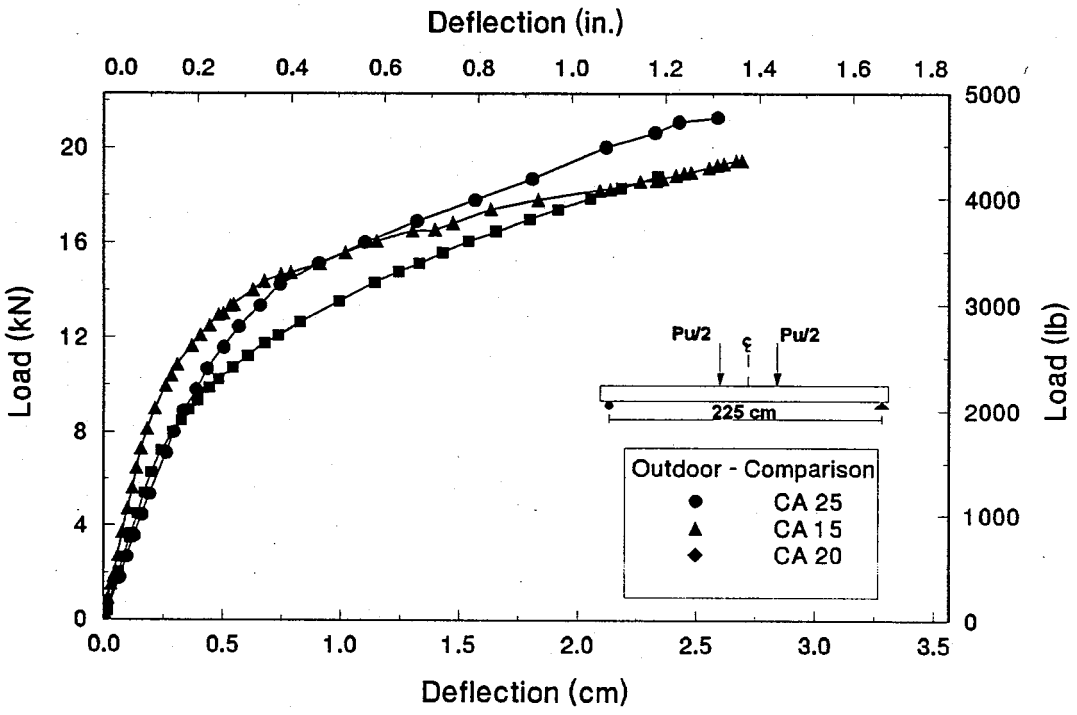

Figure 31. Load-Deflection for Outdoor Exposure Beams - Comparison of Series

A schematic summary of all bond cracks in the outdoor exposure beams is presented in Figure 32. These represent the maximum bond crack observed in any beam of that series tested. Inspection of Figure 32 indicates the bond cracks developed only after an exposure period of twenty months.

Plates 15 - 20 are photographs of the re-assembled crack patterns for beams CA 2, CA 13, CA 25 (two months), CA 14, CA 15 (twenty months) and CA 20 (twenty six months).

Beam CA 2 failed in flexure at the loading point close to the dead end. It also had a bond crack in the loaded region along with a few more flexural cracks. Beam CA 13 failed in flexure shear with a small section of bond cracks. Beam CA 25 failed purely in

flexure. In general, all three outdoor exposure beams tested after two months failed in flexure.

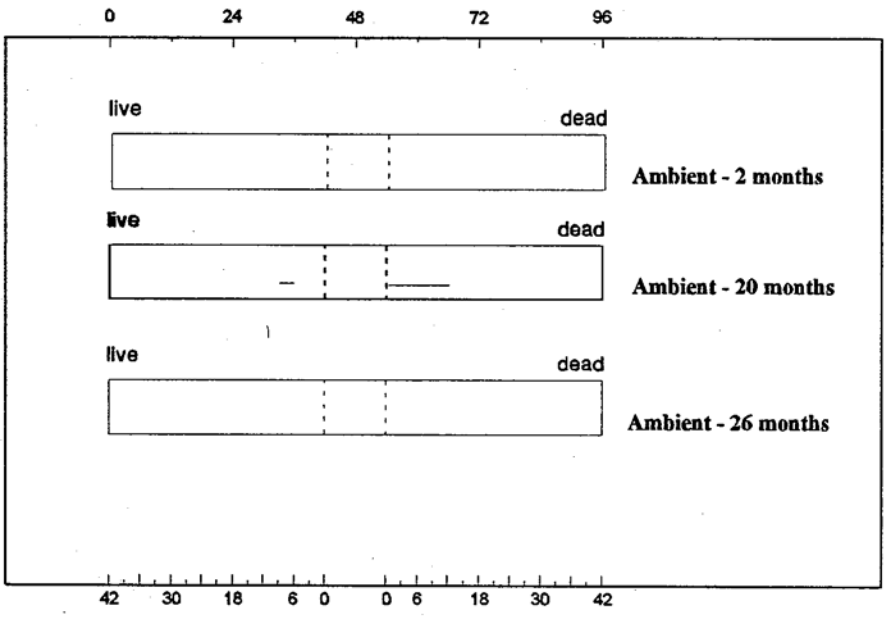

Figure 32. Summary of Bond Cracks in Outdoor Exposure Beams

Of the two beams tested after twenty months, beam CA 14 failed in flexure with no signs of any bond cracks. Although beam CA 15 failed in flexure, there was a significant amount of bond cracking towards the dead end.

The beam tested after twenty six months, CA 20, failed in flexure and showed no bond cracks. This beam had a pre-existing crack and failure occurred at the same crack, 1.07 m from the live end. Since only one beam was tested no underlying trend was discernible.

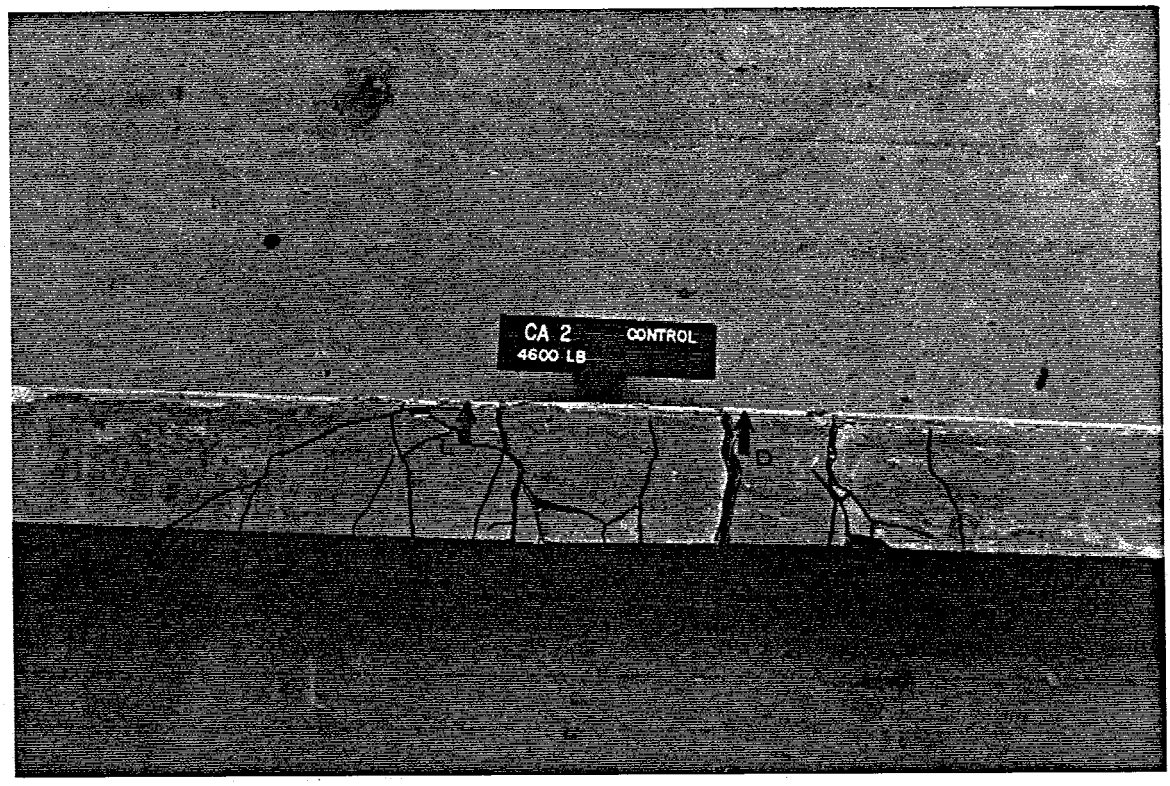

Plate 15. Crack Pattern for CA 2 - 2 Months

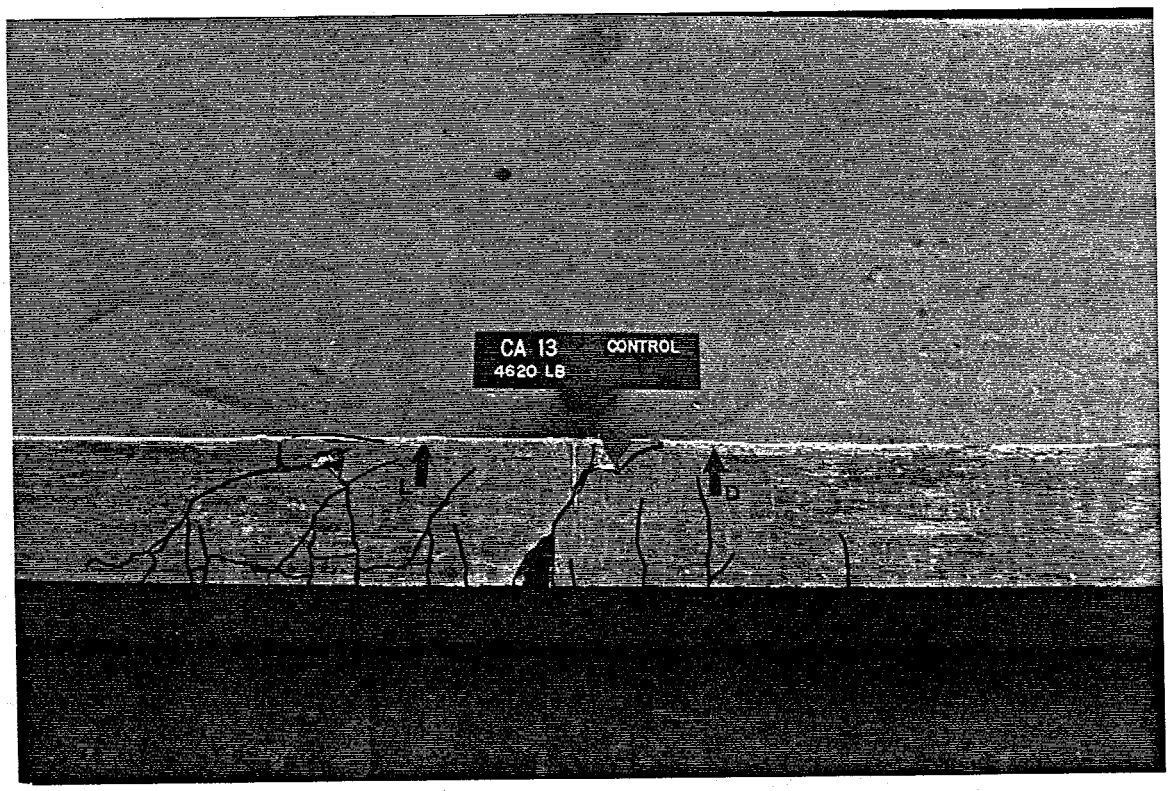

Plate 16. Crack Pattern for CA 13 - 2 Months

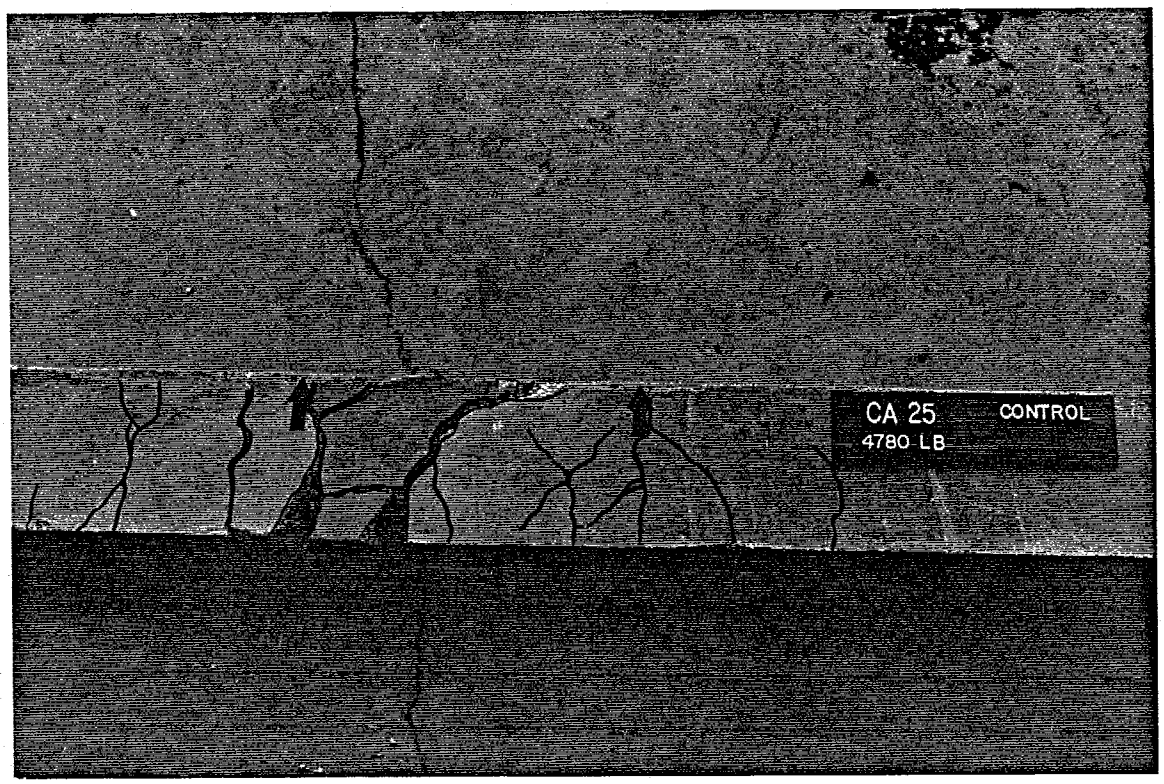

Plate 17. Crack Pattern for CA 25 - 2 Months

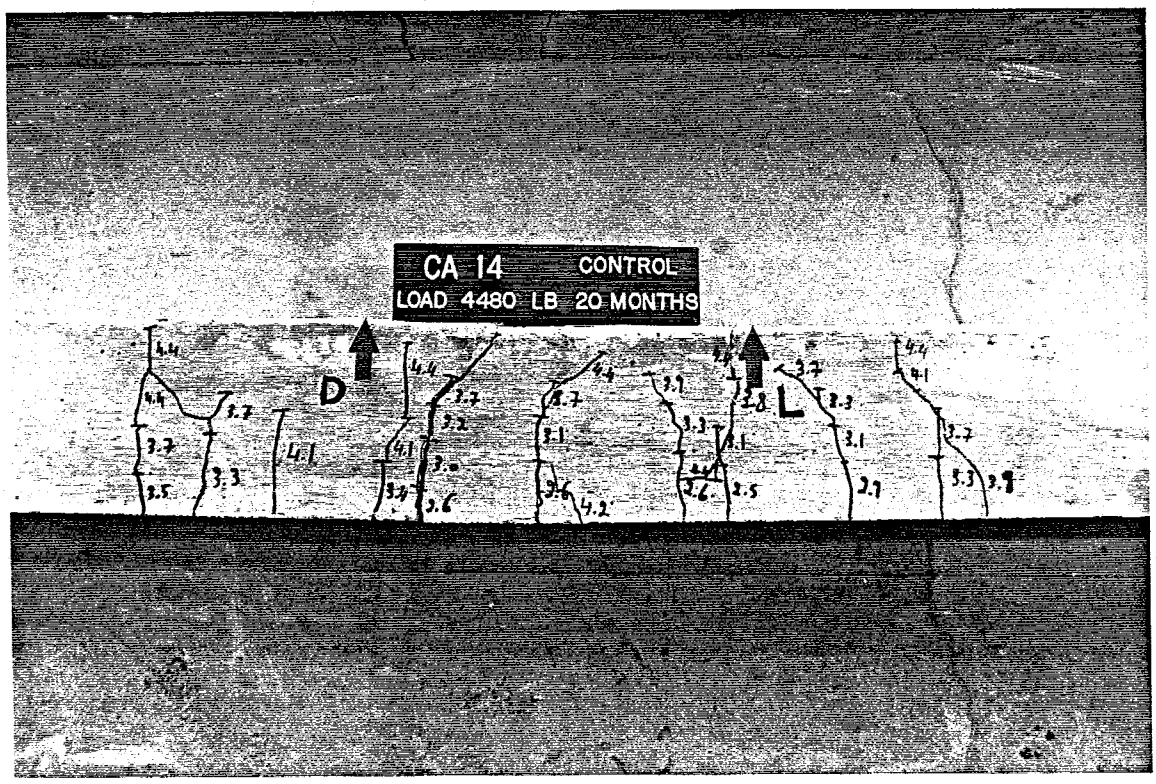

Plate 18. Crack Pattern of CA 14 - 20 Months

Plate 19. Crack Pattern of CA 15 - 20 Months

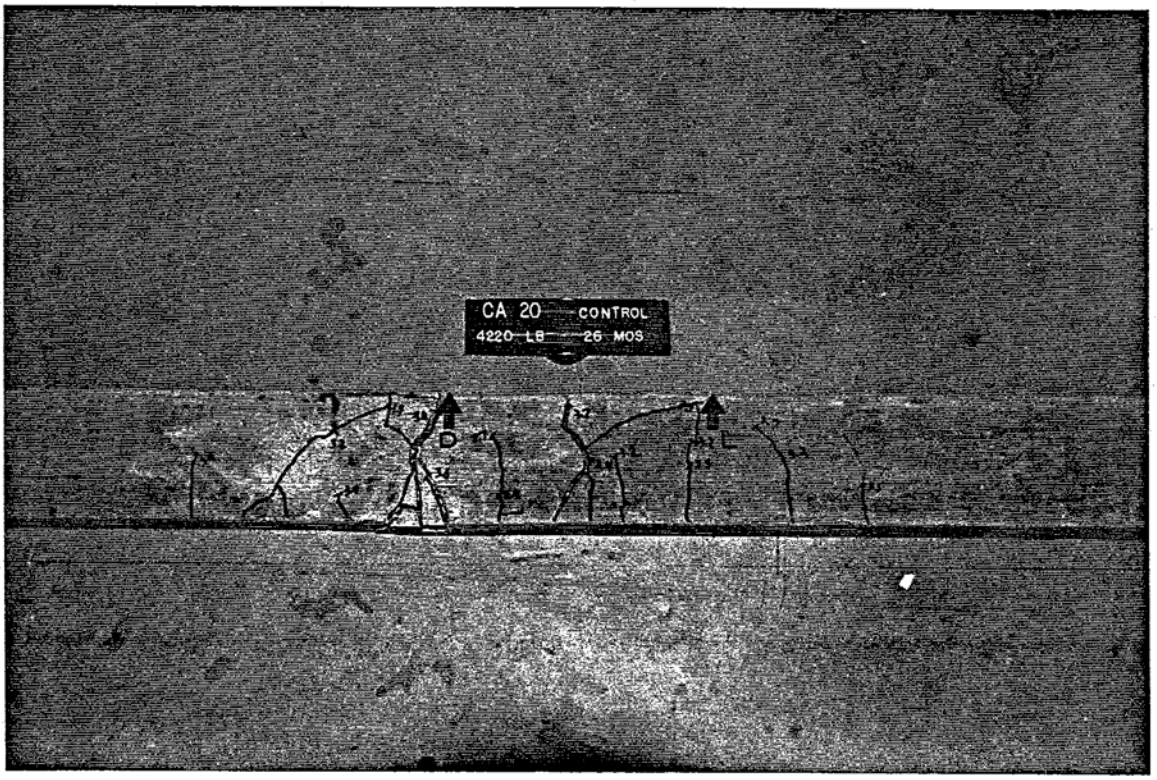

Plate 20. Crack Pattern of CA 20 - 26 Months

7.5 Discussion

In order to assess the change in ultimate capacity for the specimens tested, the effect of the increase in the compressive strength of concrete with time had to be taken into account. Since increased concrete strength leads to a slight increase in the lever arm that increases ultimate capacity, the failure loads obtained from the testing had to be appropriately reduced for a proper comparison to be made.

To determine the "reduced" failure load, the ultimate capacity for the tested beams was re-calculated on the basis of the concrete strength of the control beams, i.e. f'c = 62.8 MPa. This value was then used as the basis of all comparisons.

The reduced failure loads normalized with respect to P_{uo} (the average failure load of the control beams) are plotted against time of exposure in Figure 33. Only results for the first two series are included since the beam tested in the third series was defective.

Inspection of Figure 33 shows that the ultimate load reduced by 6.2% over 20 months. It would, however, be premature to draw any definite conclusions at this time. This must await the conclusion of the final series of tests.

To allow comparison of deflections under the same load, the lowest failure load from all the tests was additionally used. This was 94% of the average failure load for the control beams, P_{uo}. The maximum deflections, Δmax, were normalized with respect to the deflection Amax. corresponding to this load. Inspection of Figure 34 shows that the maximum deflection increased by 9.88% after twenty months, possibly because of long term prestress losses.

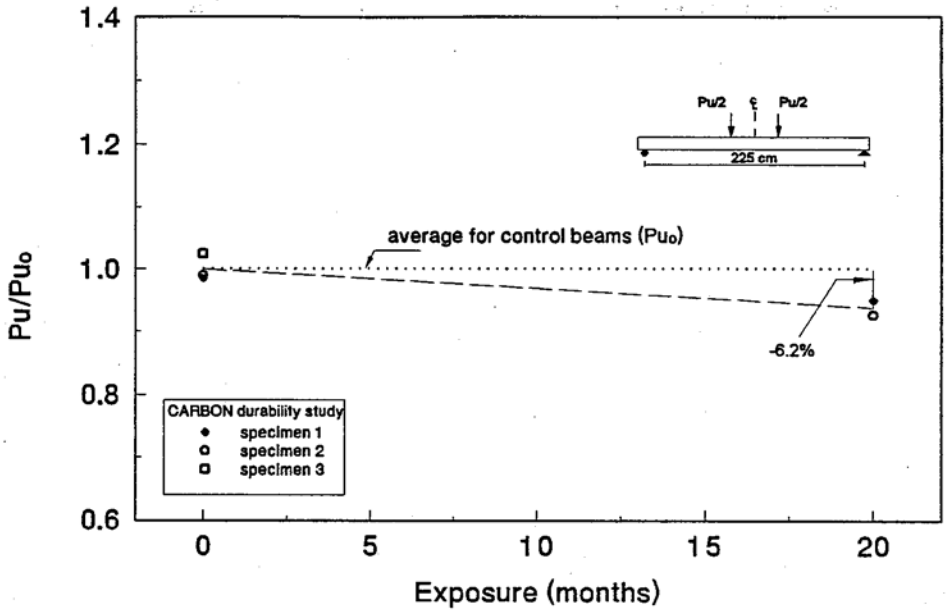

Figure 33. Reduction in Ultimate Load Due to Exposure

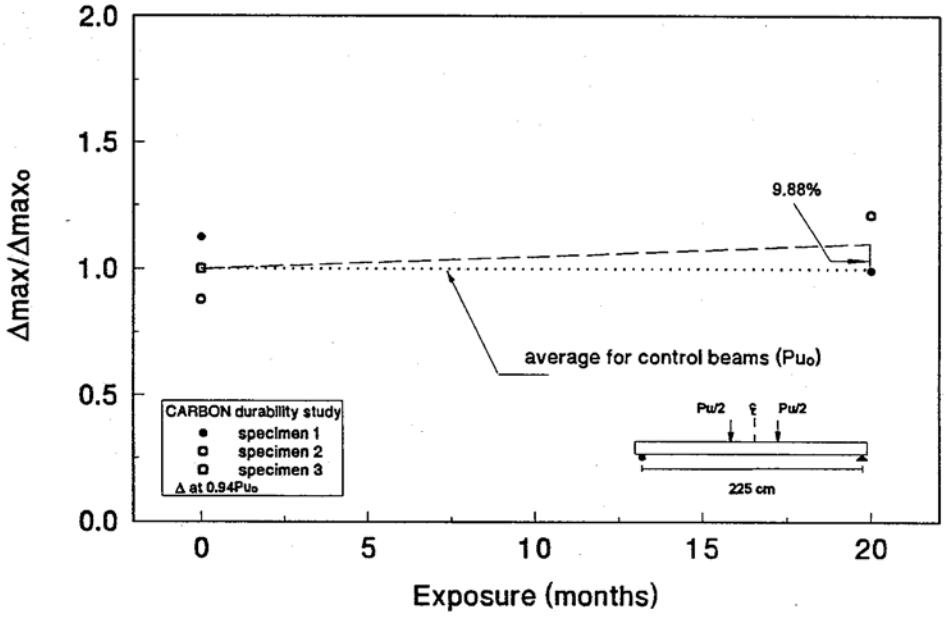

Figure 34. Reduction in Deflection Due to Exposure

8. DURABILITY STUDY

8.1 Introduction

This chapter presents interim results from the durability study that attempted to assess the combined effect of salt water and tidal cycling on the long term performance of CFRP pretensioned elements. The scope of the study is outlined together with a summary and discussion of the results obtained to date.

Of the ten specimens selected for this study, eight have been tested over a period of 24 months. The two remaining are scheduled for testing during 1995. The baseline for comparison was set by the results of the three control beams (see Chapter 7).

The experimental program and the test set-up are described in Sections 8.2 and 8.3. The test procedure is presented in Section 8.4. The results of the ultimate load tests and a discussion of the effect of exposure to a marine environment are summarized in Sections 8.5-8.6.

8.2 Experimental Program

In order to assess durability of the CFRP pretensioned specimens, a set up was designed to simulate marine environment conditions. The beams selected for this study

were subjected to wet and dry cycles (high and low tide periods) by periodically changing the water level inside tanks in which they were placed. Details of water level variation and beam position inside the tank are given in Section 8.3.

To date, four series of ultimate capacity tests have been conducted. Two beams were tested in each series. The series were conducted after 6, 12, 18 and 24 months of exposure. Reduction in ultimate bending capacity was assessed by comparing the test results between exposed and unexposed specimens.

8.3 Experimental Setup

Ten CFRP pretensioned specimens were selected for this study and were placed inside a fiberglass tank containing 15 % sodium chloride solution. This sodium chloride concentration was selected to be the same as that used earlier, Sen *et al* 1993a, and was prepared by diluting White Crystal Kiln Dried Coarse Solar Salt for Water Softening, manufactured by Morton White Crystal, with tap water. Figure 35 shows the variation in salt concentration in the tank over 24 months.

To simulate tide change conditions, water was pumped from the tank containing the CFRP specimens into a tank containing AFRP specimens that were also part of the overall study, Sen *et al* 1995. A plumbing system was designed and set up to carry out the tide changing operation once a week. During low tide periods, the water level was lowered to 150 mm and during high tide periods it was raised to 375 mm. Figure 36 shows a schematic of the plumbing system.

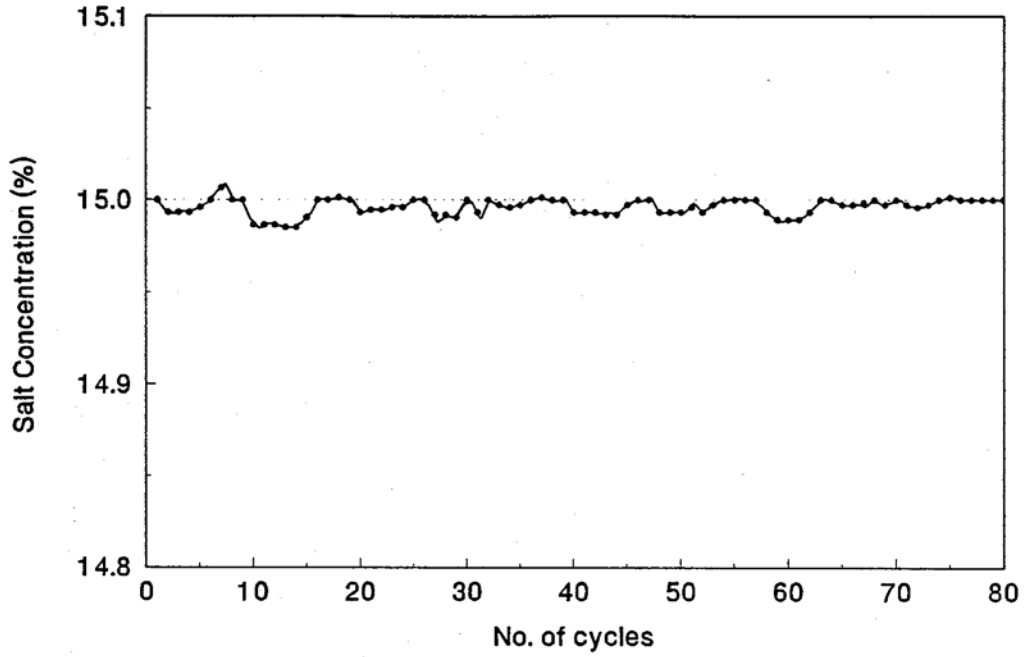

Figure 35. Salt Concentration Over 24 Months

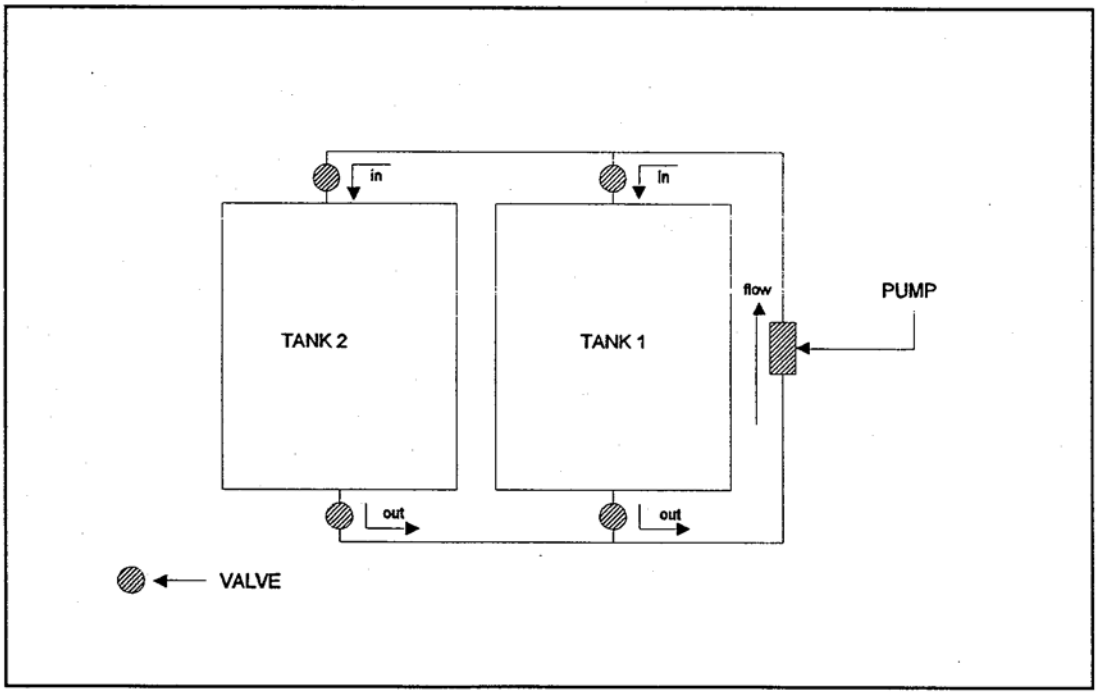

Figure 36. Schematic of Plumbing System

Since the specimens were placed in an inclined position inside the tanks, the water level variation clearly defines three zones. The top zone, which was always exposed to air and the bottom zone, which was always submerged were referred to as the "dry zone" and the "wet zone" respectively. The middle zone, which was always exposed to water level variations was referred to as the "splash zone". Figure 37 shows the beam position inside the tanks as well as the dry, splash and wet zones.

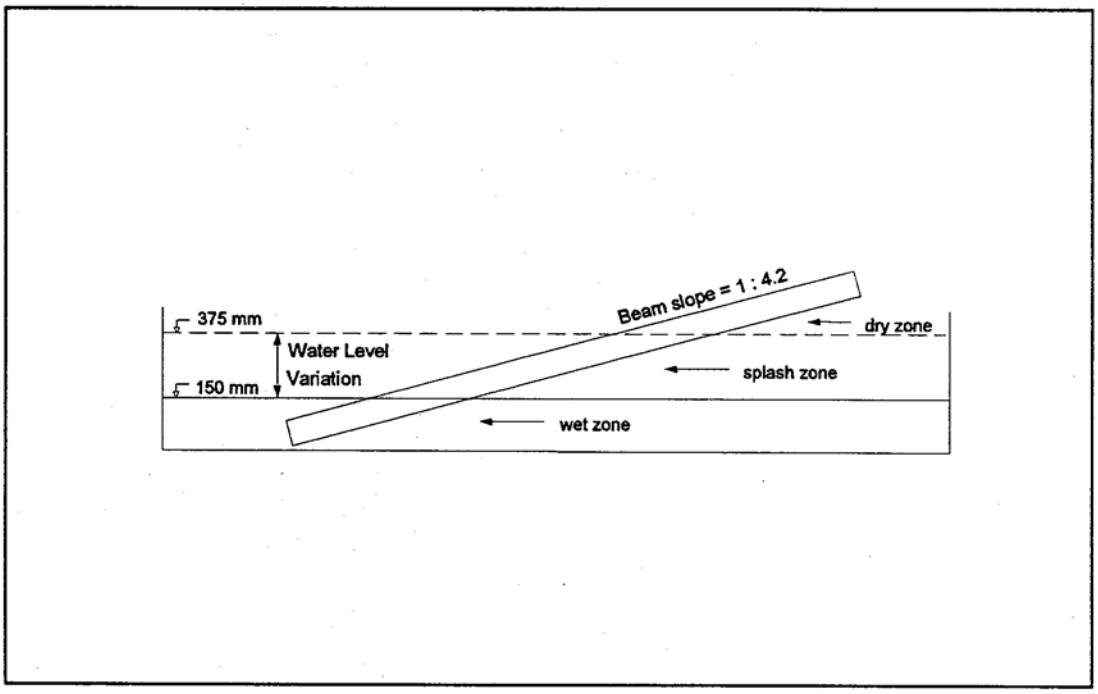

Figure 37. Beam Position in Tank

In order to utilize the actual compressive strength of the concrete in the interpretation of results, twelve standard cylinders that were poured at fabrication, were subjected to the same conditions. Two cylinders were tested after each series of ultimate bending capacity tests.

After placing the beams inside the tank, a crane system was designed to facilitate the inspection and removal of the specimens prior to testing.

8.4 Test Procedure

The specimens to be tested were selected largely on the basis of their pre-cracking response. Table 15 gives the dimensions, pre-cracking load and the number of cracks at pre-cracking for all the beams in the tank. Out of the ten beams in the tank, the beam with the most cracks (6) and the one with the most representative number of cracks (4) were left to be tested in the end.

The beams selected for each test were checked for cracks at the ends, sides, top and bottom before they were removed from the tank. They were removed from the tank and carefully transported back to the Structure Laboratory where all the testing was carried out.

The beams were allowed to dry for at least twenty four hours. Strain gages were then attached to the concrete surface and the beams prepared for testing. The setup for the ultimate load test is described in Chapter 6.

Table 15. Selection of Beams for Testing Based on Pre-Cracking Results

Beam #	Width (mm)	Depth (mm)	# of cracks	Pre-cracking load (kN)	Series # (# of mos)
CA 5	114.0	149.0	5	11.8	3 (18 mos)
CA 7	112.7	150.8	4	11.7	1 (6 mos)
CA 11	109.5	150.8	4	12.5	2 (12 mos)
CA 19	112.7	154.0	4	12.5	3 (18 mos)
CA 24	114.3	154.0	4	9.8	4 (24mos)
CA 26	112.7	157.2	3	12.7	1 (6 mos)
CA 27	115.9	152.4	4	11.4	
CA 28	112.7	157.2	6	10.2	
CA 30	114.3	157.2	3	11.9	2 (12 mos)
CA 32	114.3	152.4	5	10.1	4 (24 mos)

8.5 Test Results

8.5.1 Loads

Table 16 provides a summary of all tests results for the eight beams tested to date. This includes the cracking loads, failure loads, maximum concrete strains, maximum deflections, mode of failure and the concrete strengths.

The ultimate loads in the first three series of tests ranged from 20 - 22 kN. However, in the fourth series tested after twenty four months it dropped to 17 - 20 kN.

Table 16. Summary of Test Results - Durability Study

Test Series	Date Tested	Beam #	P_{cr} (kN)		P_{ult} (kN)		Max. Conc Strain ($\mu\epsilon$)	Max: Defln (mm)		f'_c (MPa)	Mode of failure
			Test	Avg	Test	Avg		Test	Avg		
6 months	8/26/93	CA 7	12.5	12.9	20.2	20.6	1874	22.6	21.4	70.3	Flexure-shear
	8/26/93	CA 26	13.2		20.9		1777	20.1			Flexure
12 months	2/22/94	CA 11	13.3	13.7	20.9	21.4	1880	23.6	26.3	68.4	Flexure-bond
	2/22/94	CA 30	14.1		21.9		1762	29.0			Flexure-bond
18 months	8/24/94	CA 5	11.1	11.5	20.0	20.4	2112	25.4	23.9	65.9	Flexure-shear
	8/24/94	CA 19	11.9		20.7		1944	22.3			Flexure
24 months	2/19/95	CA 32	9.35	10.7	17.6	18.5	1842	21.1	21.4	66.4	Flexure-bond
	2/19/95	CA 24	12.1		19.4		1701	21.6			Flexure

The average failure load was 20.6 kN for the six month test and increased to 21.4 kN in the twelve month test. After the twelve month test, the ultimate load dropped initially to 20.4 kN (18 month) and then to 18.5 kN after 24 months. This is due in part to changes in concrete strength over the twenty four month period as shown in Figure 38.

8.5.2 Deflections

The average deflections for the six months, twelve months, eighteen months and twenty four months test were 21.4 mm, 26.3 mm, 23.9 mm and 21.4 mm, respectively. Though the deflection increased for the twelve and eighteen month tests, it dropped during the twenty four months test.

Figures 39 - 42 show the load vs. deflection curves for the four series of tests. The similarities in the response of all the beams tested is evident from these graphs.

8.5.3 Crack Patterns

The beams were re-assembled after testing to verify and analyze the failure mode. Though none of the beams failed in bond, some had visible bond cracks.

Figure 43 shows the maximum bond cracks, among all the beams, from the four series of tests. Plates 21 - 28 show the crack patterns for all the beams tested so far.

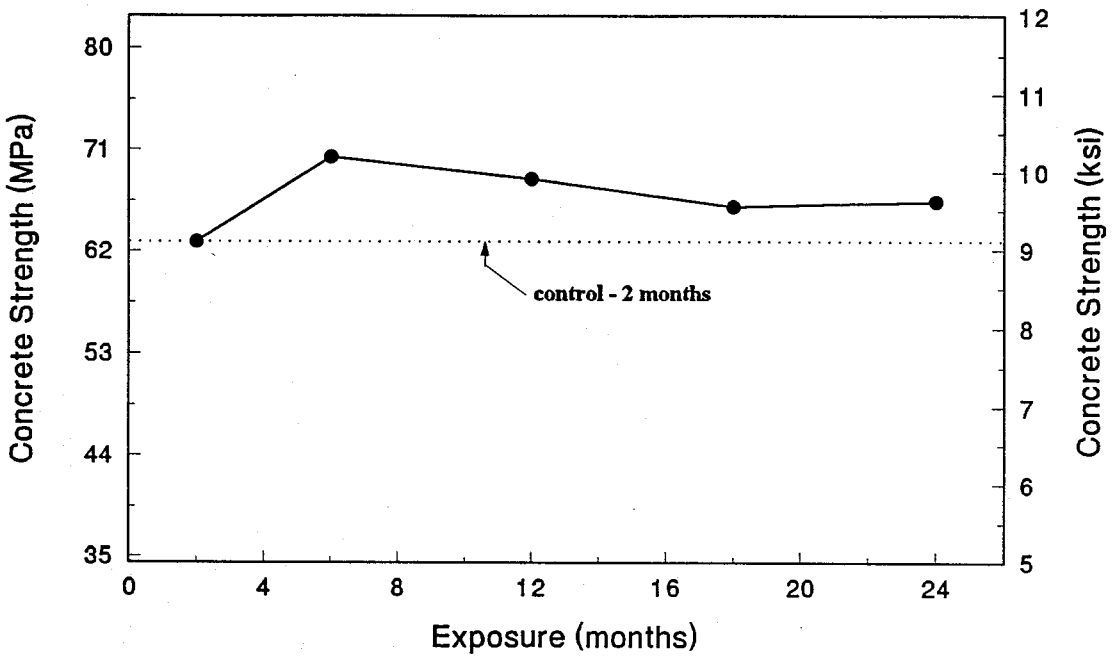

Figure 38. Variation of Concrete Strength with Exposure

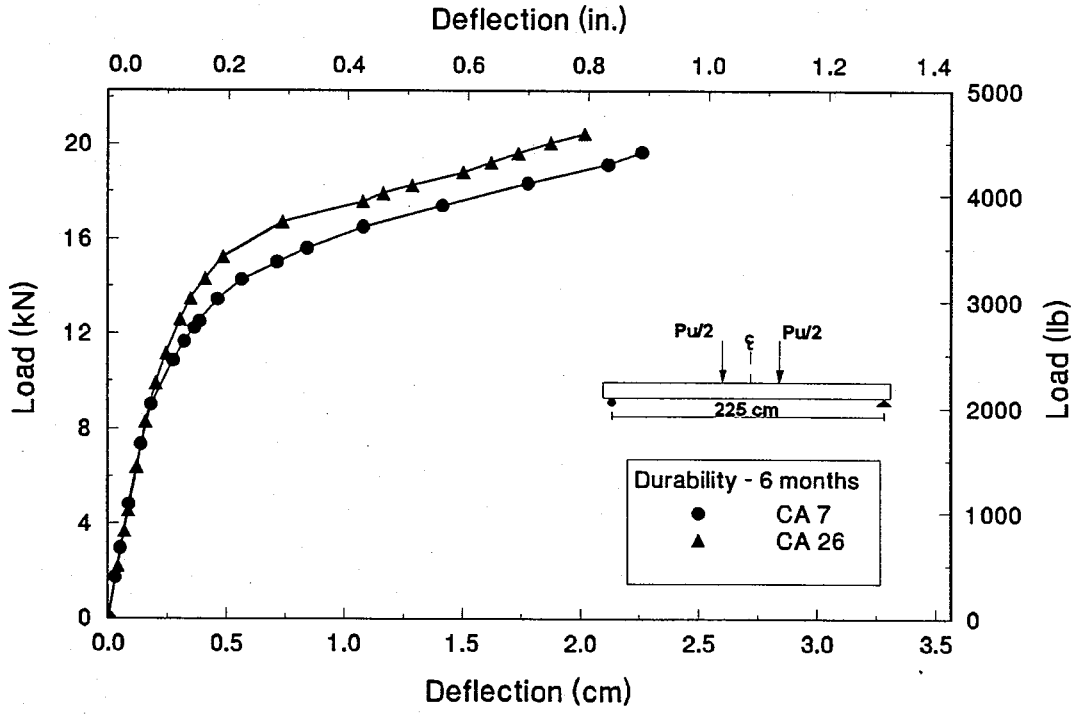

Figure 39. Load-Deflection for Carbon Beams - Comparison of 6 Months

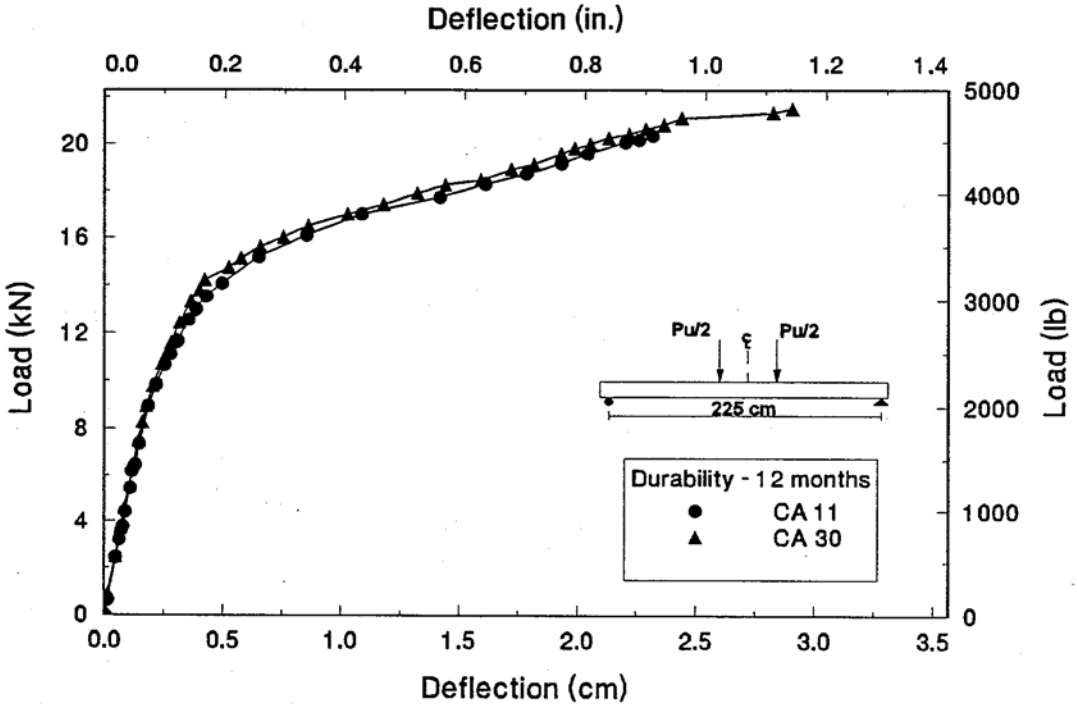

Figure 40. Load-Deflection for Carbon Beams - Comparison of 12 Months

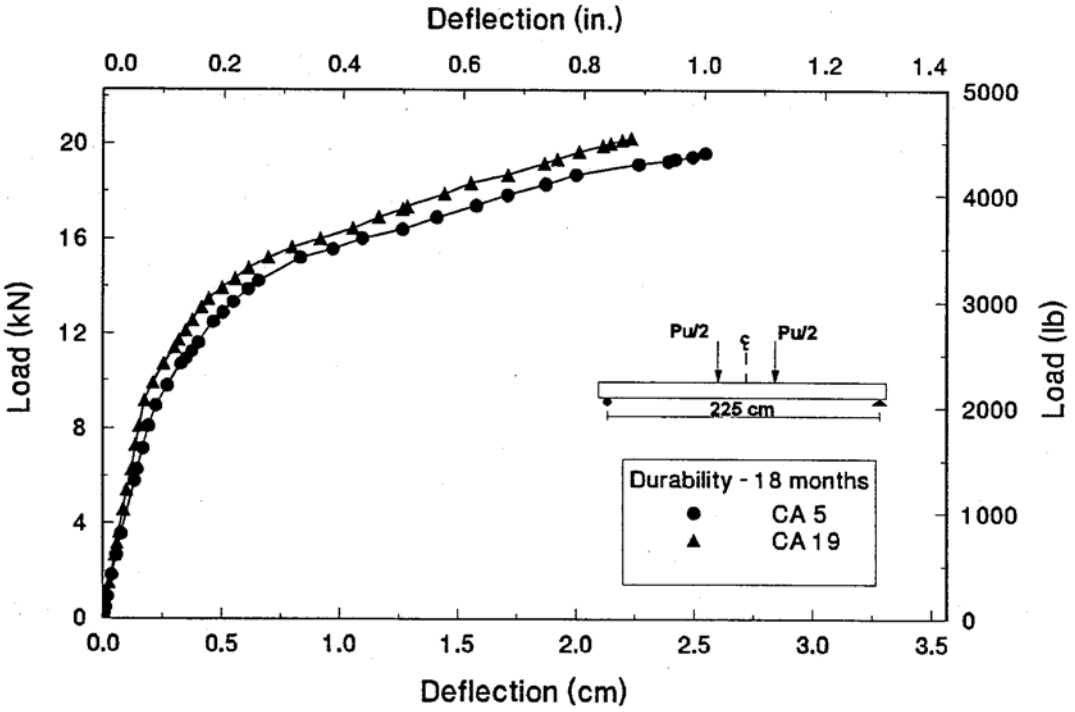

Figure 41. Load-Deflection for Carbon Beams - Comparison of 18 Months

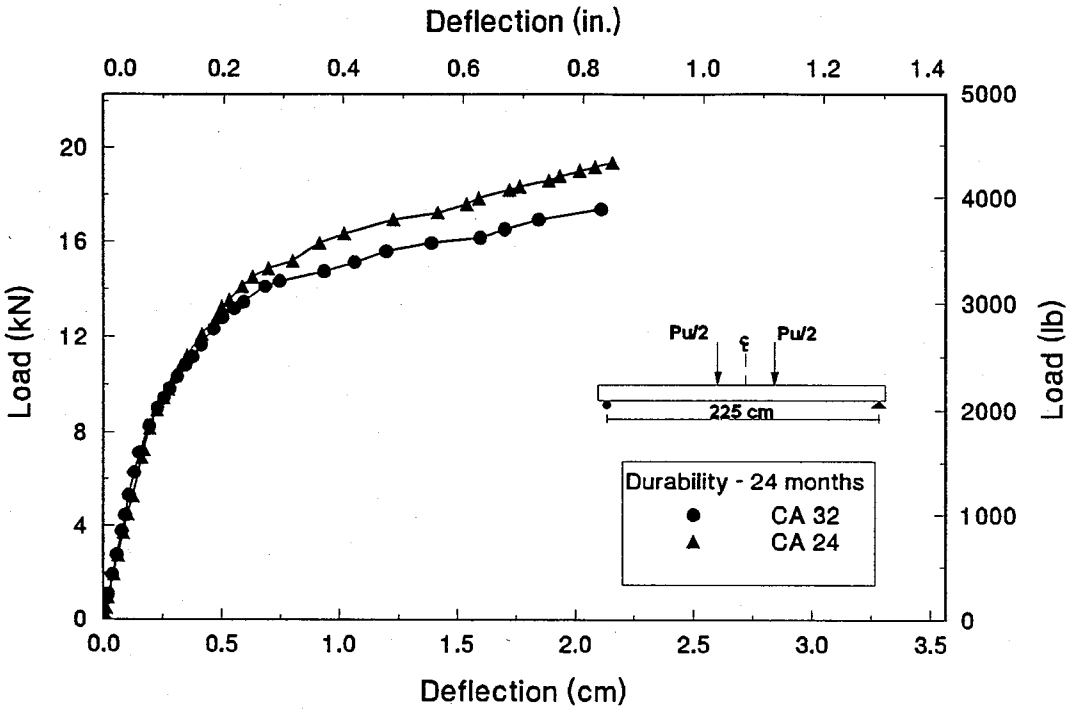

Figure 42. Load -Deflection for Carbon Beams - Comparison of 24 Months

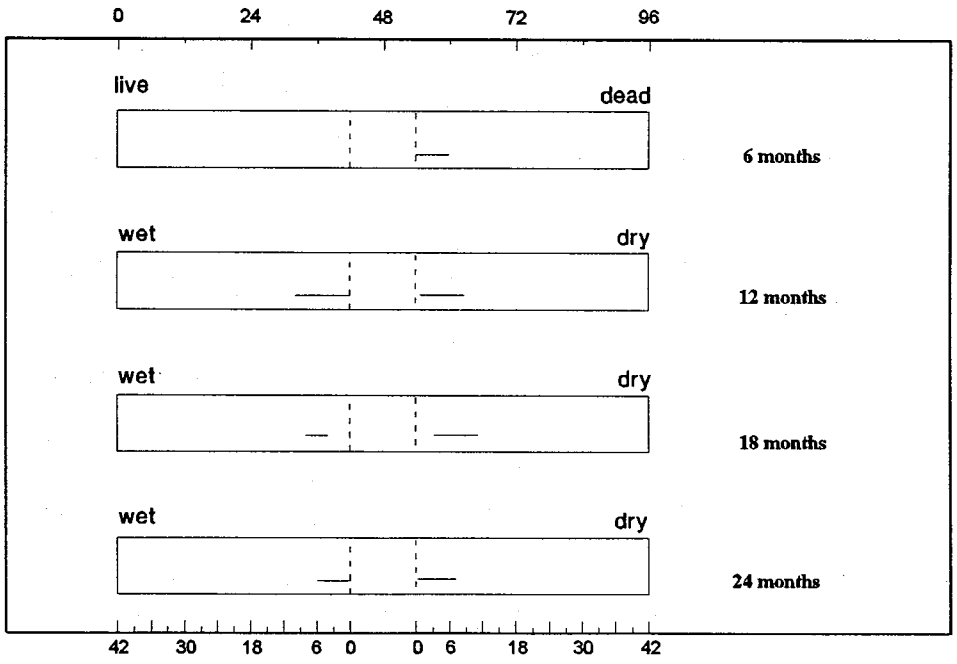

Figure 43. Maximum Crack Length for the Durability Study Beams

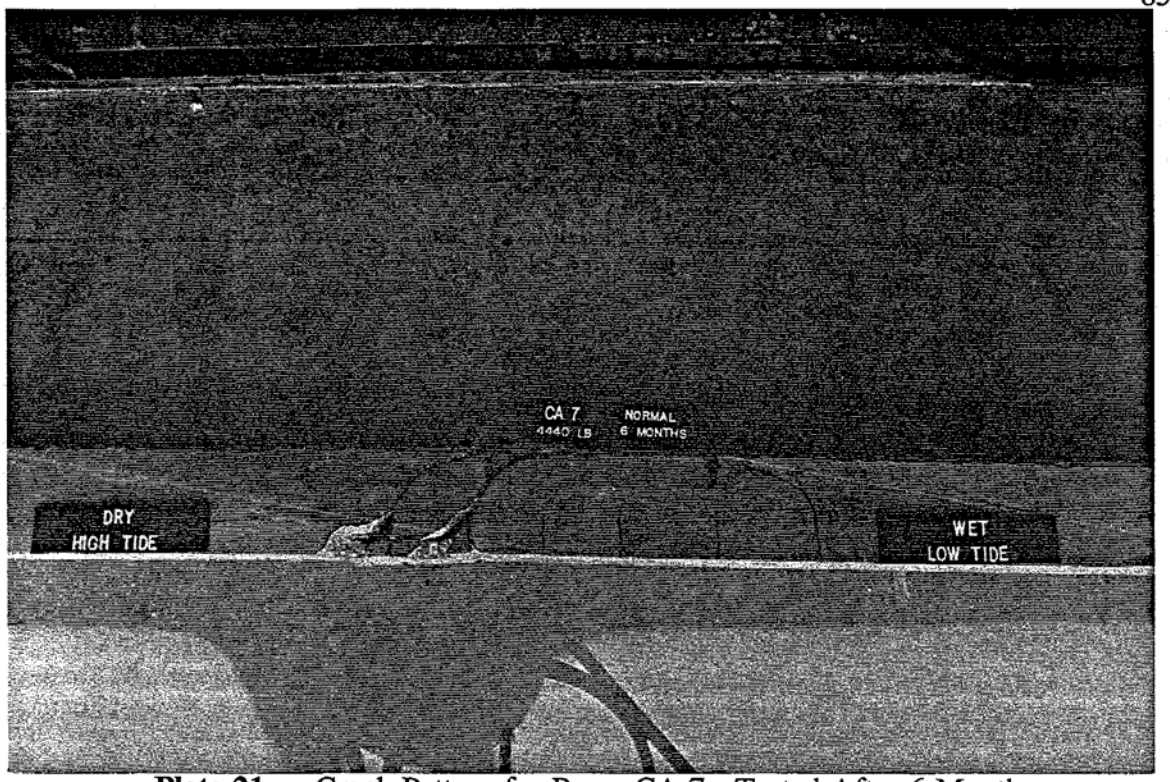

Plate 21. Crack Pattern for Beam CA 7 - Tested After 6 Months

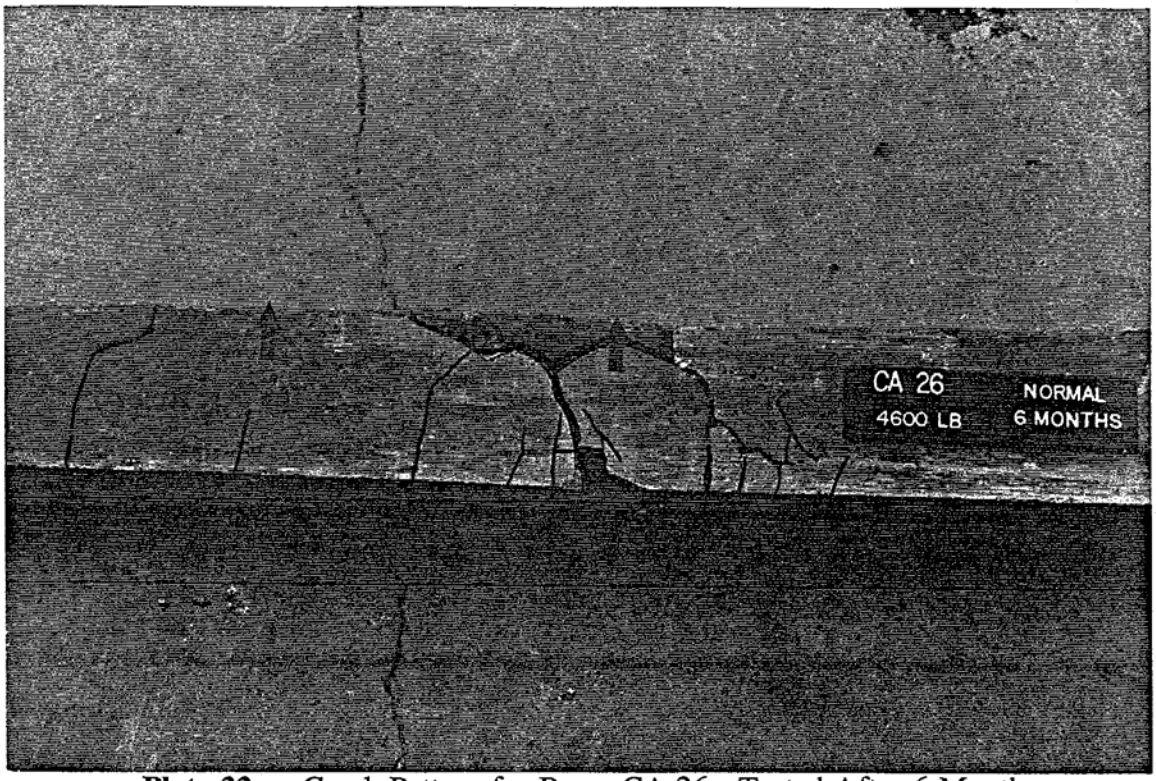

Plate 22. Crack Pattern for Beam CA 26 - Tested After 6 Months

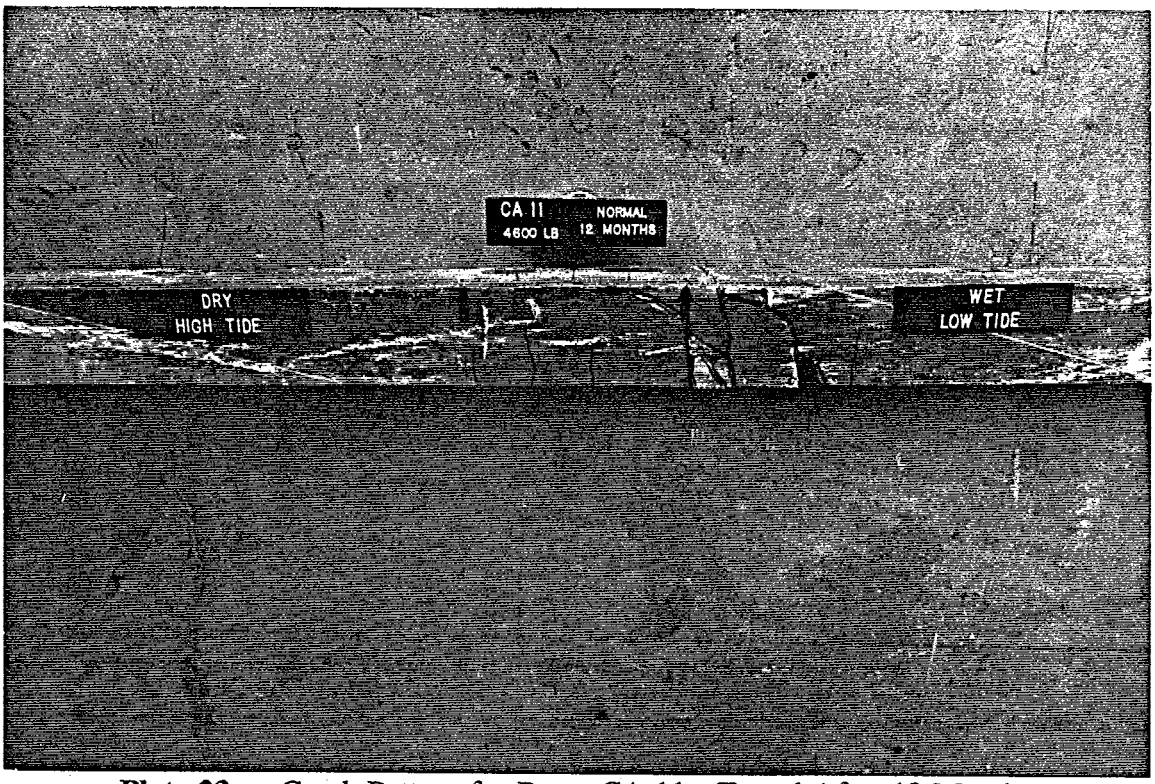

Plate 23. Crack Pattern for Beam CA 11 - Tested After 12 Months

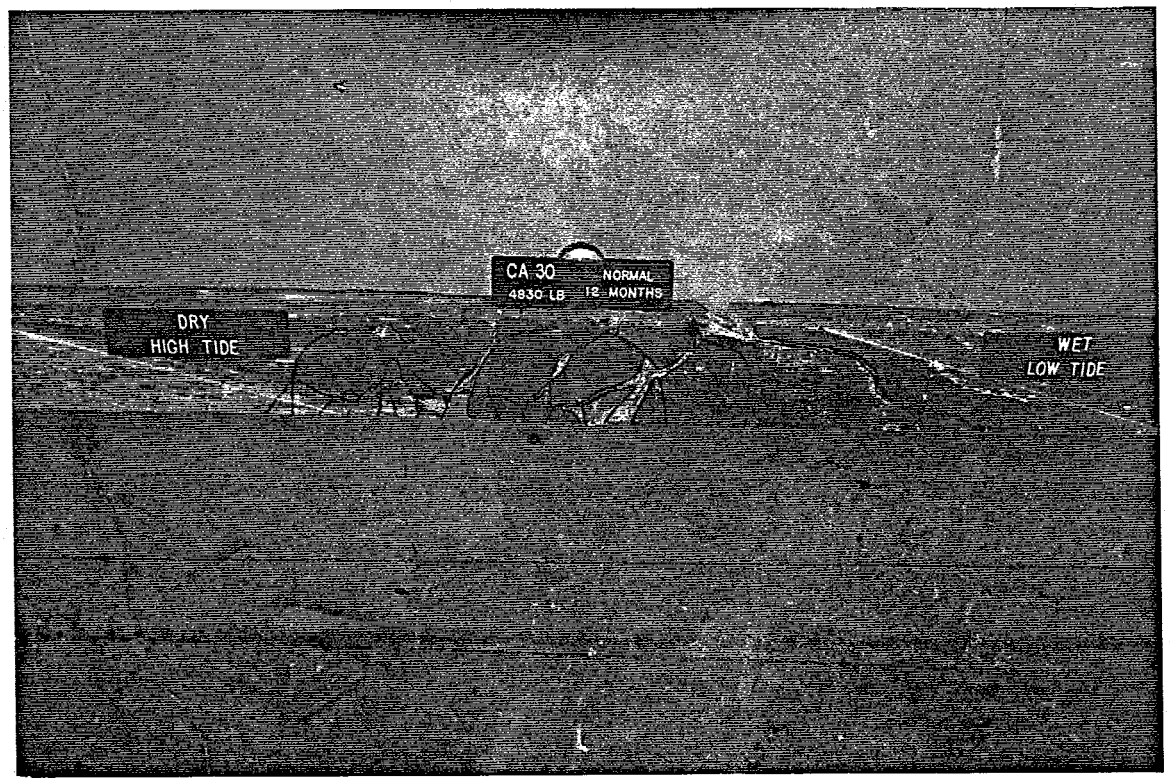

Plate 24. Crack Pattern for Beam CA 30 - Tested After 12 Months

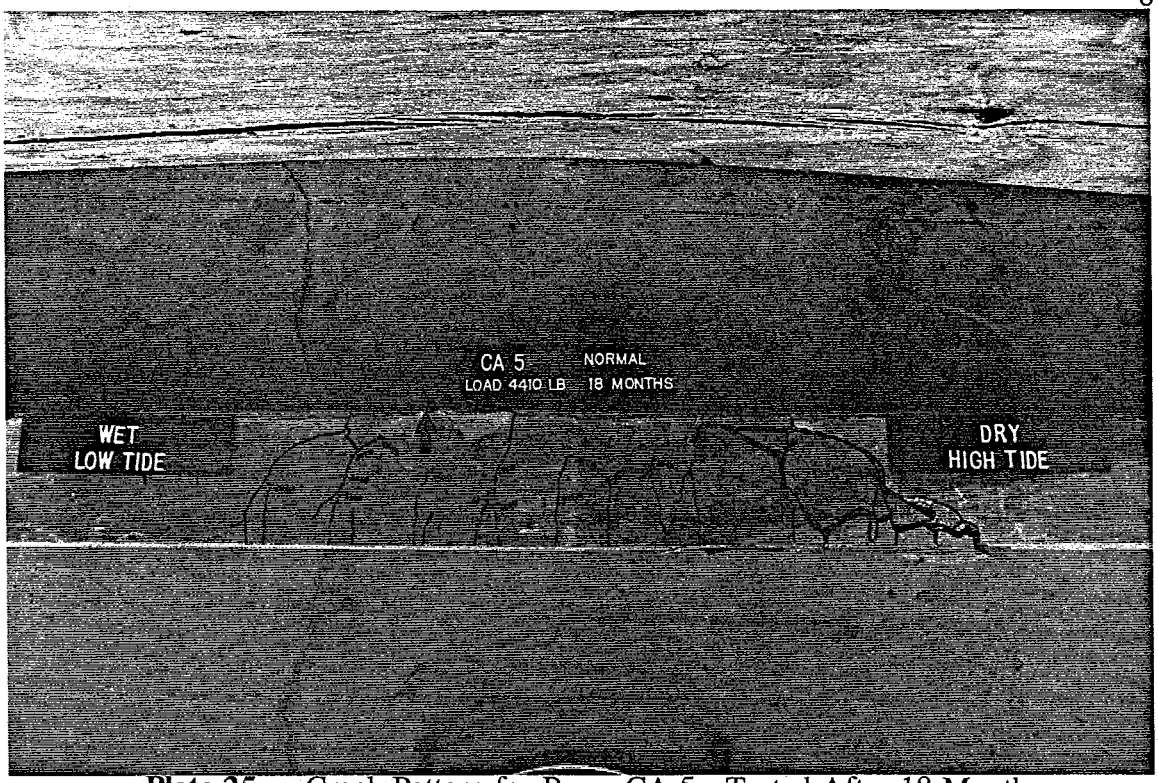

Plate 25. Crack Pattern for Beam CA 5 - Tested After 18 Months

Plate 26. Crack Pattern for Beam CA 19 - Tested After 18 Months

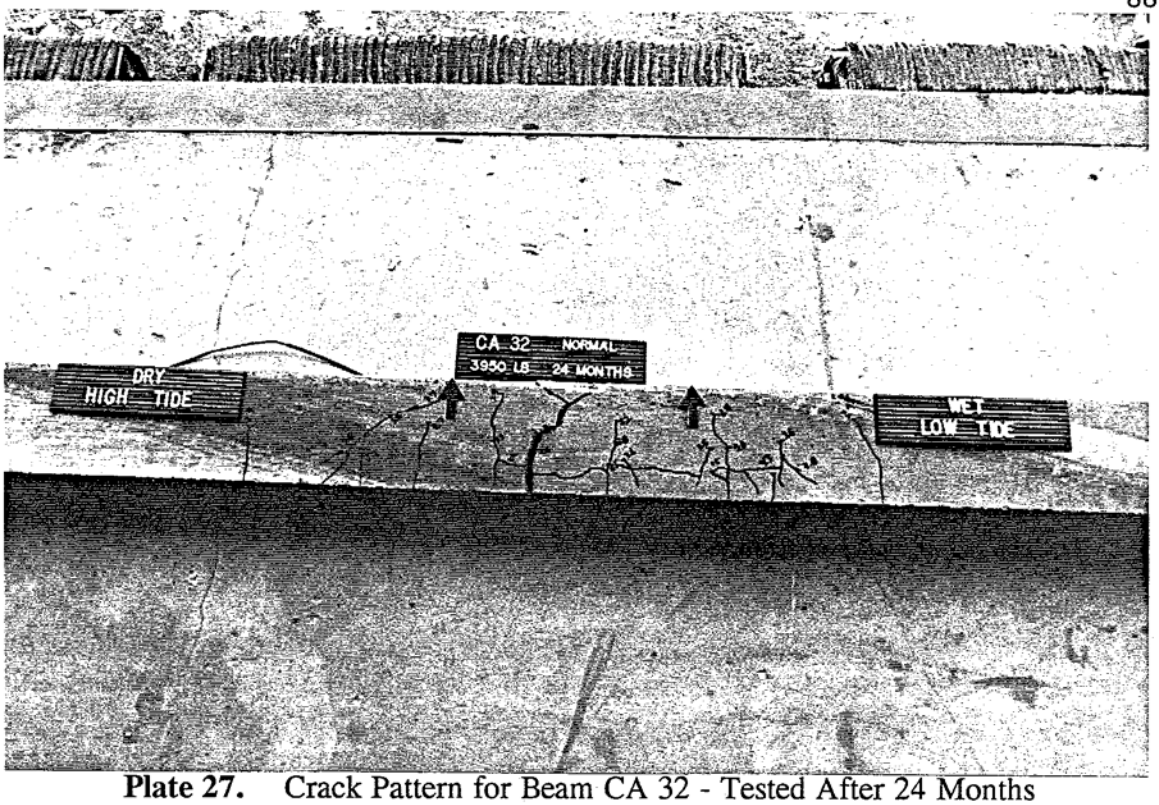

Plate 27. Crack Pattern for Beam CA 32 - Tested After 24 Months

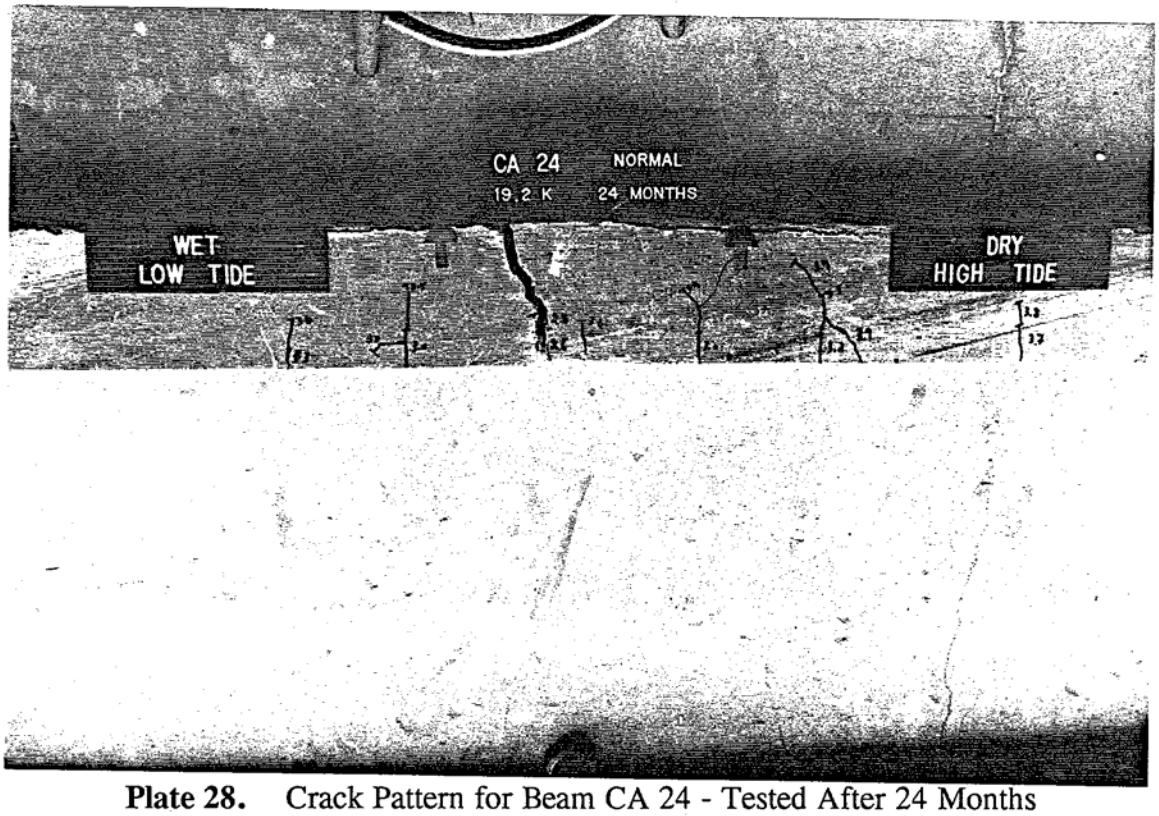

Plate 28. Crack Pattern for Beam CA 24 - Tested After 24 Months

8.6 Discussion

In order to assess the loss of strength due to exposure, the effect of changes in concrete strength had to be factored out as explained in Section 7.5.

Figure 44 plots the variation in ultimate strength normalized with respect to that of the average ultimate load of the control beams tested after 2 months, P_{uo} (see Chapter 7) against exposure.

Inspection of Figure 44 shows minimal reductions in ultimate capacity over the first 12 months of exposure. However, in subsequent tests, reductions of 4 % and 11.35 % were observed after exposure of 18 and 24 months respectively.

A similar analysis was conducted to determine the changes in ultimate deflection. As before, the maximum deflection was normalized with respect to the lowest load - 84 of the control beams so that the relative deflections under the same load could be compared.

Figure 45 plots the variation of the normalized deflection with respect to exposure. Inspection of this figure shows that proportionately smaller deflections were observed during the first 18 months. In the last test, deflections were larger.

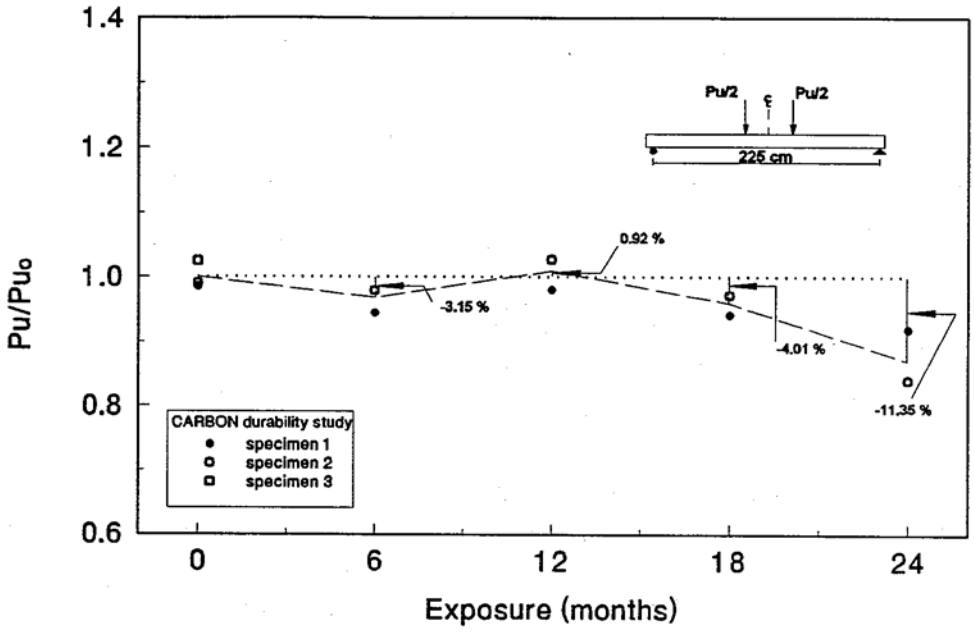

Figure 44. Reduction in Ultimate Load Due to Exposure

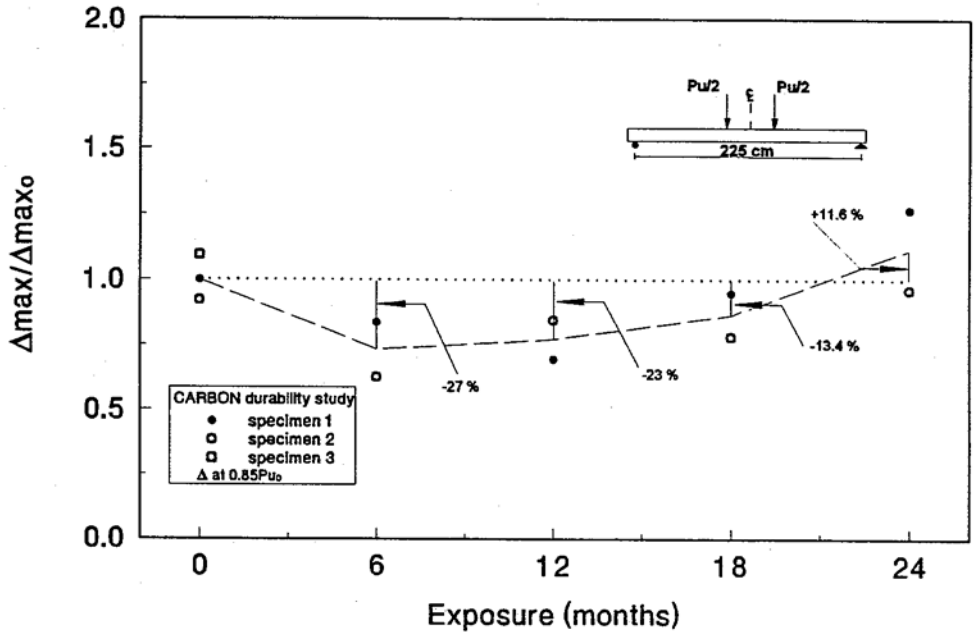

Figure 45. Reduction in Deflection Due to Exposure

9. BOND STUDY

9.1 Introduction

This chapter presents interim results from the ongoing bond study to investigate the effect of mis-match in expansion coefficients between CFRP and concrete. Twelve beams were used in this study and five series of tests planned; four have already been completed. The fifth series will be delayed as much as possible to allow the maximum time of exposure.

A description of the test program is presented in Section 9.2. The set-up used for thermal cycling is described in Section 9.3. The test procedure is outlined in Section 9.4. The test results are summarized in Section 9.5. Section 9.6 presents a discussion of the results.

9.2 Experimental Program

Since the thermal expansion coefficent for CFRP is about three times larger than that of concrete, CFRP pretensioned beams were subjected to thermal cycling to accelerate the degradation in bond.

The CFRP pretensioned beams were exposed to wet/dry cycles and thermal cycles twice a week. Since the beams were being put through hot/cold cycles along with the wet/dry cycles, a heating system was designed to heat and maintain the salt water temperature at 60°C. This heating system is described in Section 9.3.

Since the temperature range beams were subjected varied with the ambient temperature, the interval between tests was not kept the same. The tests carried out in summer were conducted after 1,000 hours and 10,000 hours exposure. In winter, tests were conducted after 6,500 hours and 15,500 hours. In each case, this followed a spell of severe cold weather by Florida standards so that the temperature range the CFRP pretensioned beams were subjected was maximized.

A total of nine beams have been tested in four series to date. Three beams were tested in the first series conducted after 1,000 hours of exposure. In the subsequent three series, two beams were tested after 6500 hours, 10,000 hours and 15,500 hours. The difference in capacity between the exposed and unexposed control beams (Chapter 7) provided a measure of the deterioration in the strength of the beams.

9.3 Experimental Set Up

9.3.1 Tank Set Up

The test set-up was identical to that described in Section 8.3.1 excepting that the salt concentration was 5 % and the beams were kept upright with the CFRP material

nearest to the water surface. The variation of salt concentration with time is shown in Figure 46.

Tides were simulated by raising and lowering the water level inside the tanks. The plumbing system was similar to the one used for the durability study, Figure 36. For each tide change water was pumped from the tank at a higher tide to the tank at a lower tide. Low tide was maintained by keeping 150 mm of water in the tank and high tide by maintaining it at 375 mm. The tide change caused a "splash zone" in the beams. The "splash zone" was in the mid region of the beam as seen in Figure 47. The tank at high tide (tank-1) was then heated to 60°C and maintained at that temperature till the next tide change, while the tank at low tide (tank-2) was allowed to cool. During tide change tank-1 was brought to low tide and allowed to cool while tank-2 was brought to high tide and heated.

The salt water in the tanks was heated using commercial water heaters. Figure 48 shows a schematic diagram of the heating system. When the tank was being heated, it was kept covered using styrofoam panels so that the temperature could be maintained at 60°C. The tank was connected to a thermostat which helped maintain the temperature at 60°C. Every time the temperature dropped 2°C below the required temperature, the heater would start circulating hot water and vice versa when the temperature rose 2°C above.

Twelve cylinders, which were poured the same time as the beams, were also placed in the tank to obtain the strength of concrete under the same conditions as the beam. One cylinder was tested for every beam tested.

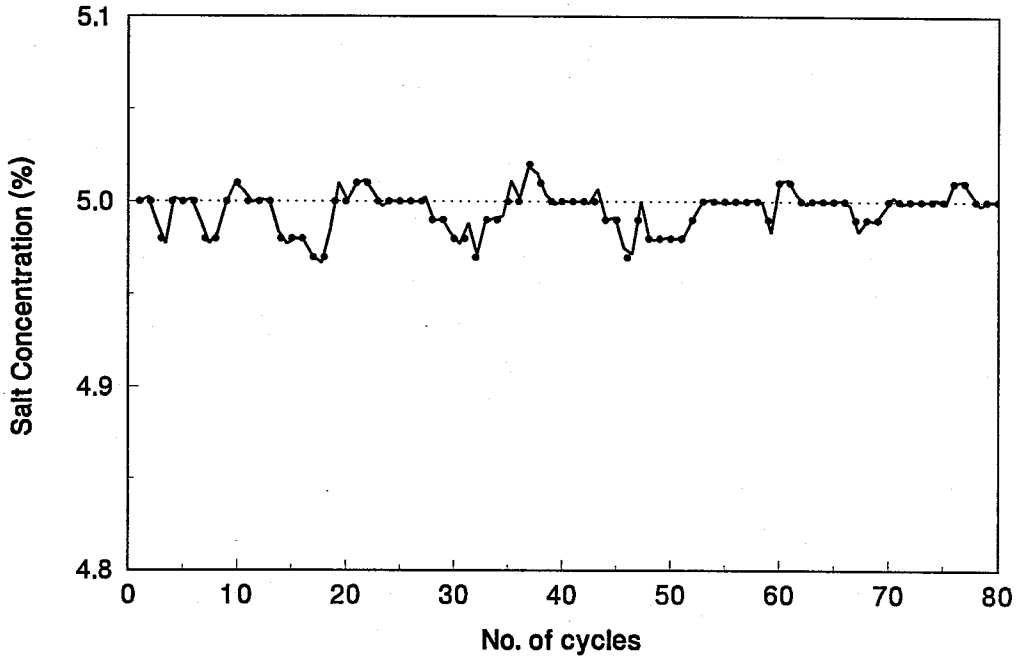

Figure 46. Salt Concentration in the Tank

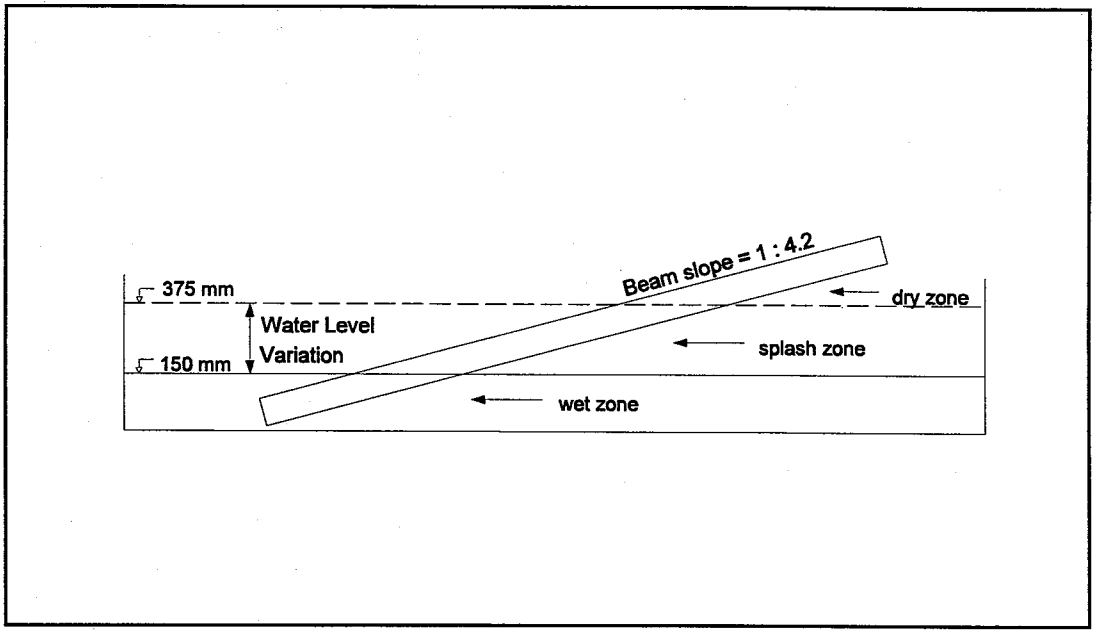

Figure 47. Position of Beam in the Tank

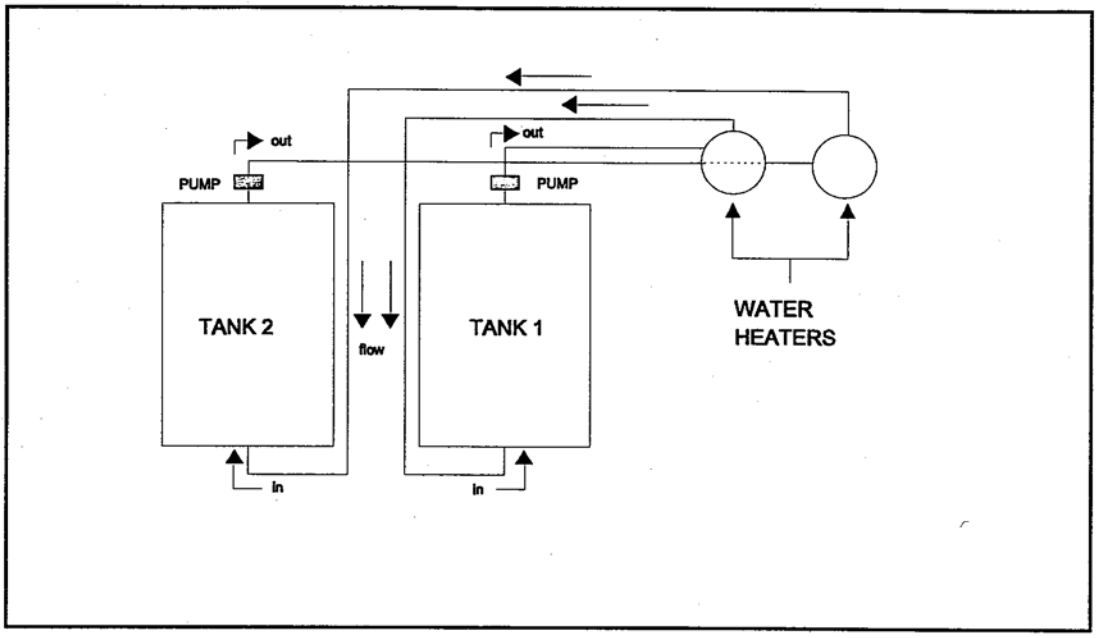

Figure 48. Schematic Diagram of the Heating System

9.3.2 Temperature Monitoring System

Since the bond study revolved mainly around the heating and cooling of the beams, it was crucial to monitor the temperature and humidity inside the tanks. The computer system used to monitor these parameters was the same as the system used in the durability study, Section 9.3.2. Thermocouple and humidity meters were placed inside the tank to record the temperature and humidity. These were hooked up to the computer so that data could be continuously recorded if needed.

9.3.2.1 Temperature Data

The temperature and humidity measurmentes inside the tanks was recorded automatically every fifteen minutes so that the amount of data recorded was manageable. Unfortunately, during summer months, the computer system was sometimes knocked out due to severe weather even though the heat cycle was unaffected.

Figures 49 - 52 show some typical graphs of the temperature variation with time. The temperature range is indicated in the plots in some cases. The remaining plots until March 31, 1995 are included in Sukumar 1995.

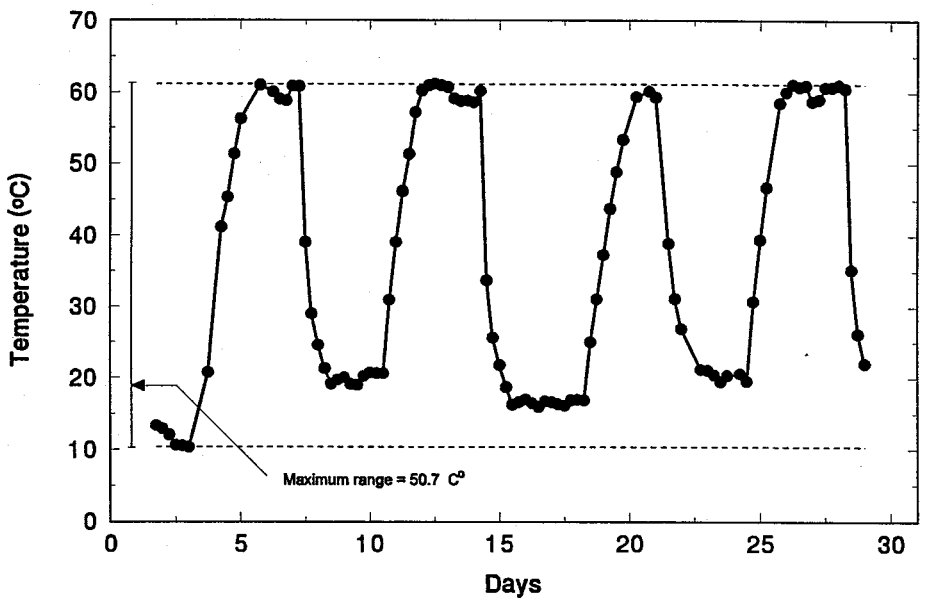

Figure 49. Temperature Cycle for February 1994

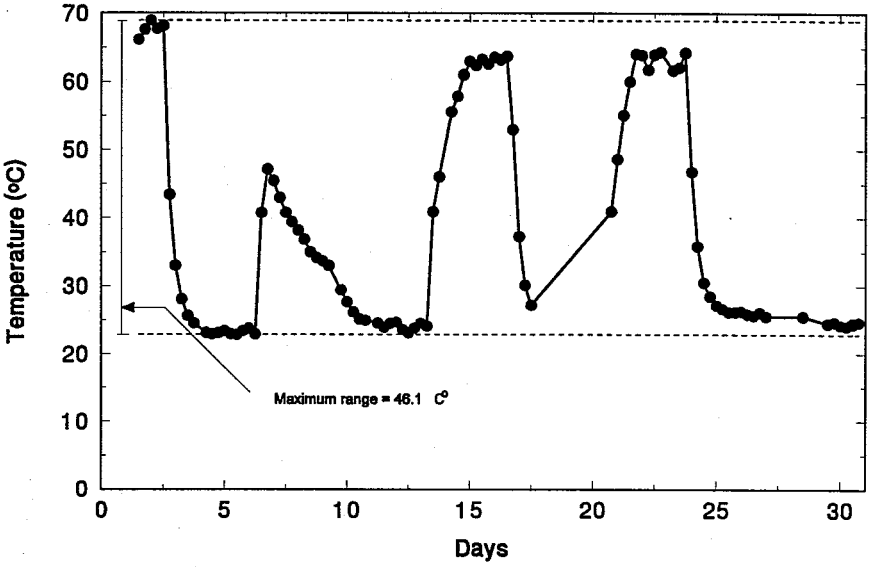

Figure 50. Temperature Cycle for June 1994

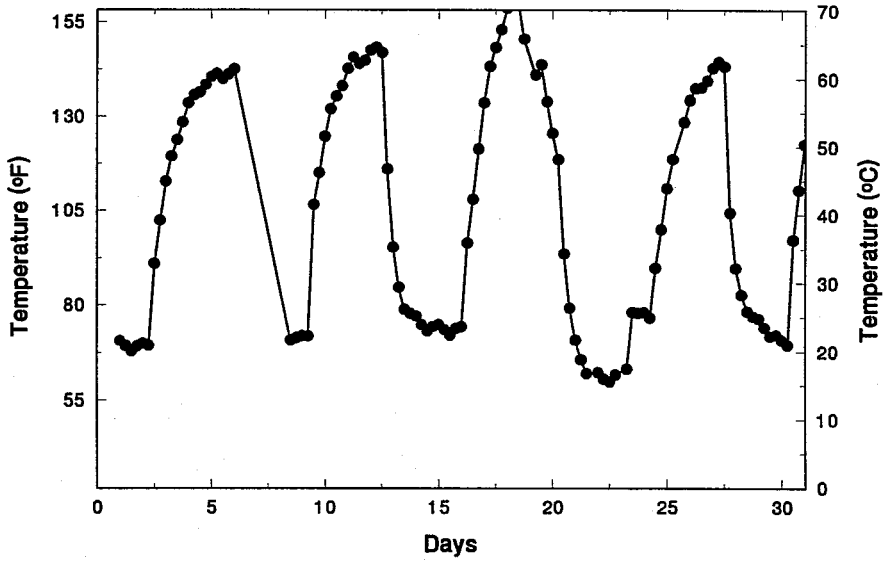

Figure 51. Temperature Cycle for May 1994

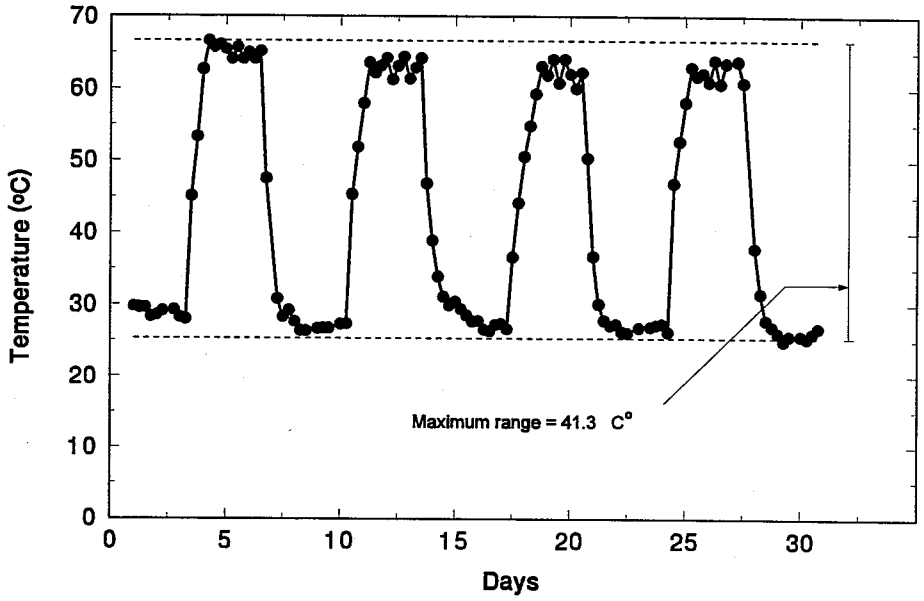

Figure 52. Temperature Cycle for September 1994

9.4 Test Procedure

The removal of specimens for testing was based entirely on their pre-cracking response since no external cracks were detected.

Table 17 summarizes the beam dimensions, pre-cracking load and the number of cracks during pre-cracking for all the beams in the study. The three beams remaining have 3, 4 and 5 cracks that are representative of the numbers of cracks in specimens tested throughout the study. These beams will be tested as late as possible to provide maximum period of exposure.

Table 17. Selection of Bond Study Beams Based on Pre-Cracking Results

Beam #	Width (mm)	Depth (mm)	# of cracks	Pre-cracking load (kN)	Series # (# of hr)
CA 4	114.3	147.7	4	10.2	1 (1000 hr)
CA 6	114.3	150.8	5	11.6	1 (1000 hr)
CA 8	112.7	152.4	4	13.2	3 (10,000 hr)
CA 9	112.7	154.0	4	12.5	2 (6500 hr)
CA 16	112.7	157.2	5	9.9	2 (6500 hr)
CA 17	112.7	154.0	4	11.6	4 (15,500 hr)
CA 21	113.2	154.0	5	11.7	4 (15,500 hr)
CA 22	112.7	152.4	3	11.6	1 (1000 hr)
CA 23	111.1	149.2	5	9.6	
CA 29	114.3	152.4	3	12.2	3 (10,000 hr)
CA 31	114.3	152.4	3	11.6	
CA 33	114.3	152.4	4	11.4	

The beams selected for each test were checked for cracks at the ends, sides, top and bottom before they were removed from the tank. The beams were then removed from the tank using a crane system and allowed to dry.

Once the beam surfaces were dry, they were instrumented and tested, as explained in Chapter 6.

9.5 Test Results

The results presented cover an exposure period of approximately 22 months. In each series, cylinders subjected to the same conditions were also tested.

9.5.1 Loads

Table 18 gives the cracking loads, failure loads, maximum concrete strains, maximum deflections, mode of failure and the concrete strengths of the nine beams tested for the bond study.

The ultimate loads in all the four series of tests ranged from 20 - 22 kN. The average failure loads were 20.9 kN, 20.6 kN, 21.5 kN and 20.2 kN for the 1,000 hours, 6,500 hours, 10,000 hours and 15,500 hours, respectively. Thus, there was not much variation in the failure load for all the four series

There was some reduction in concrete strength due to exposure in salt water, similar to that encountered in the durability test (see Table 16). Figure 53 shows the variation of concrete strength over the twenty two month period of testing.

The average cracking load fluctuated between 9.7 kN and 11.5 kN for the four series of tests. This was lower than the original pre-cracking load presumably due to long term prestress losses.

9.5.2 Deflections

The average deflections for the 1,000 hours, 6,500 hours, 10,000 hours and 15,500 hours were 29.6 mm, 27.9 mm, 27.3 mm and 27.9 mm, respectively. The deflection reduced by 5.7% after the 1,000 hours test. Figures 54 - 57 show the load vs. deflection curves for the four series of tests.

Table 18. Summary of Test Results - Bond Study

Test Series	Date Tested	Beam #	P_{cr} (kN)		P_{ult} (kN)		Max. Conc Strain ($\mu\epsilon$)	Max: Defln (mm)		f'_c (MPa)	Mode of failure
			Test	Avg	Test	Avg		Test	Avg		
1,000 hr	7/20/93	CA 4	9.88		20.9		2,077	27.5			Flexure
	7/20/93	CA 6	9.43	9.95	20.7	20.9	2,274	32.4	29.6	67.9	Flexure-bond
	7/20/93	CA 22	10.54		20.9		1,903	29.0			Flexure-bond
6,500 hr	3/1/94	CA 9	11.57	11.5	21.0	20.6	2,169	24.9	27.9	64.6	Flexure-bond
	3/1/94	CA 16	11.35		20.2		2,503	30.9			Flexure-bond
10,000 hr	7/22/94	CA 8	9.88	10.9	21.6	21.5	1,608	27.5	27.3	64.2	Flexure
	7/22/94	CA 29	11.97		21.5		2,418	27.1			Flexure-bond
15,500 hr	3/2/95	CA 17	9.83	9.72	20.1	20.2	2,340	25.7	27.9	65.0	Flexure
	3/2/95	CA 21	9.61		20.2		2,489	30.1			Flexure

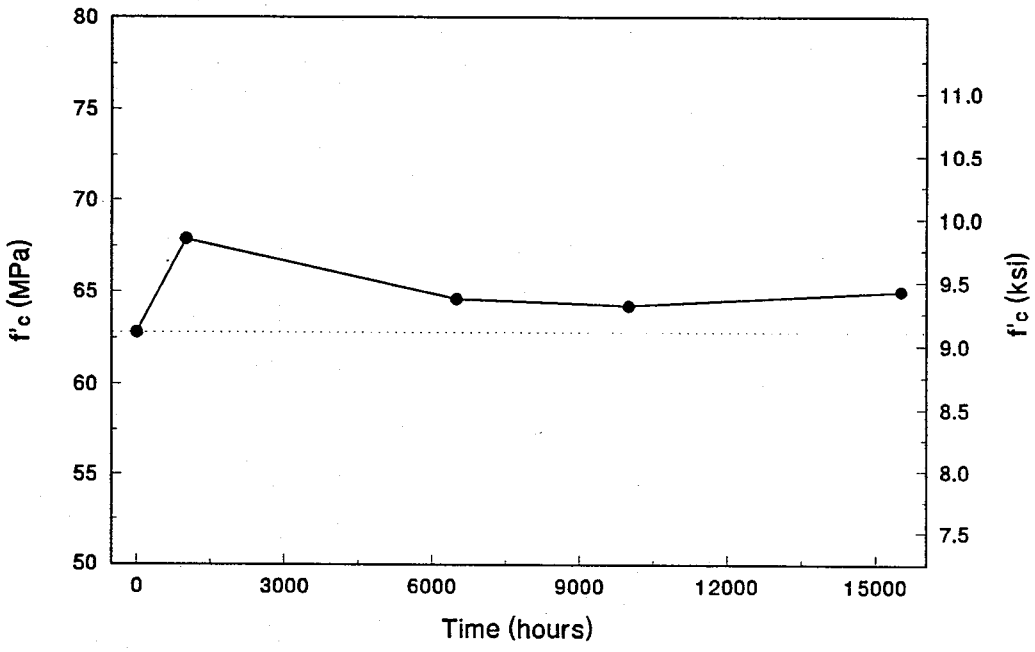

Figure 53. Variation of Concrete Strength with Time

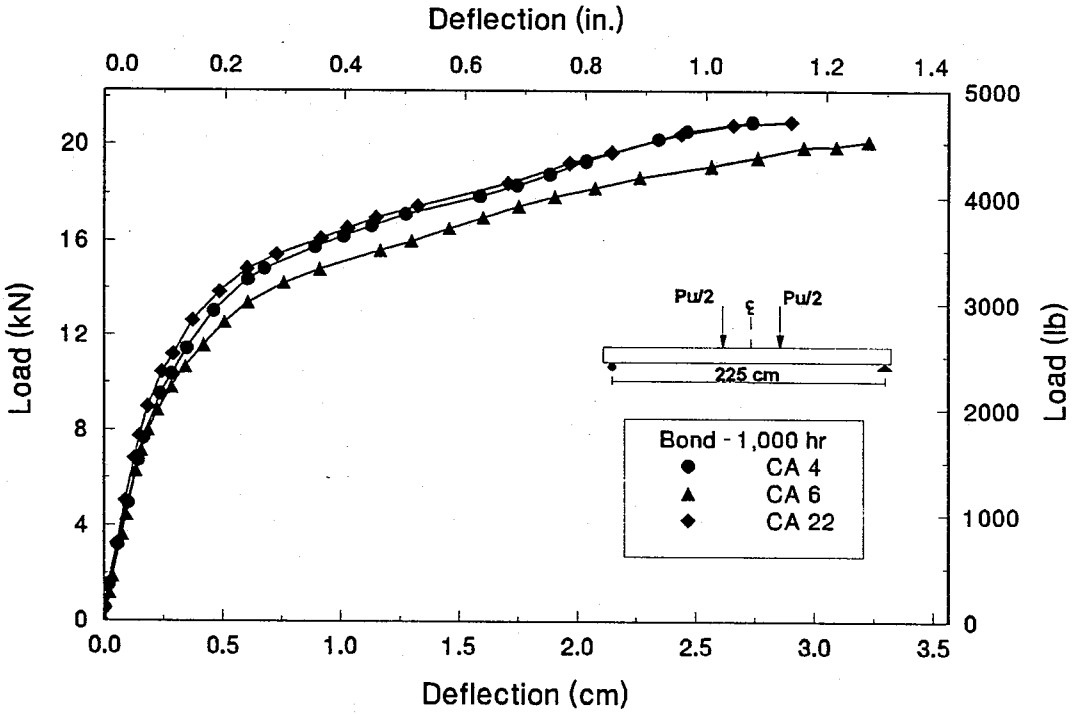

Figure 54. Load-Deflection for Carbon Beams - Comparison of 1,000 Hour Tests

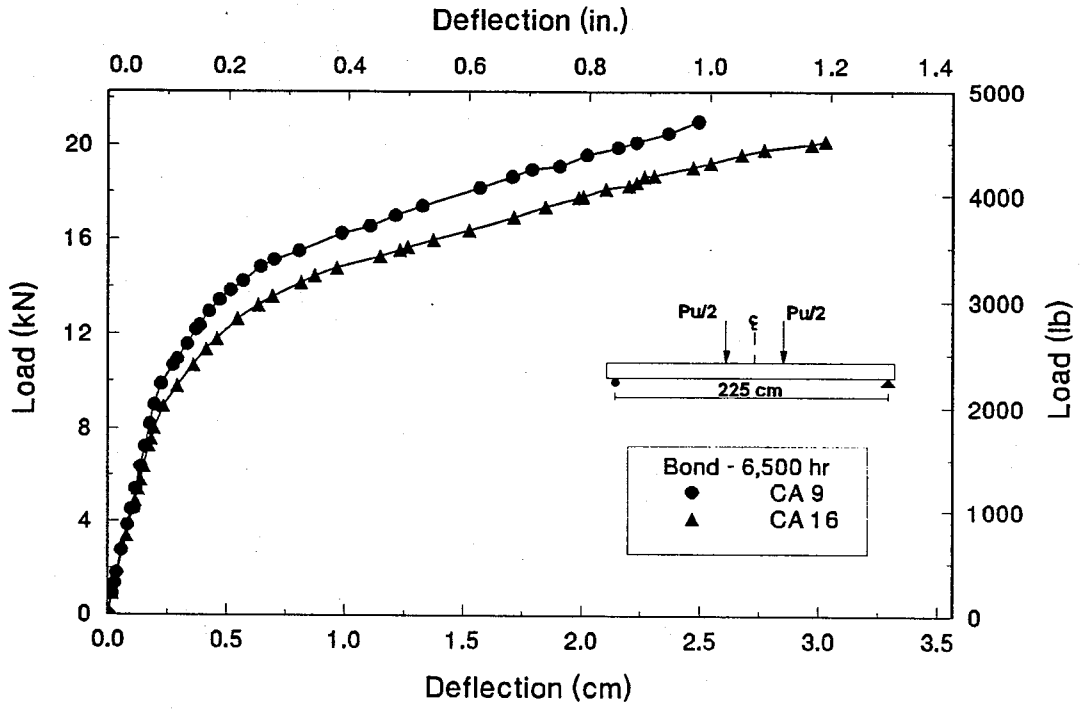

Figure 55. Load-Deflection for Carbon Beams - Comparison of 6,500 Hour Tests

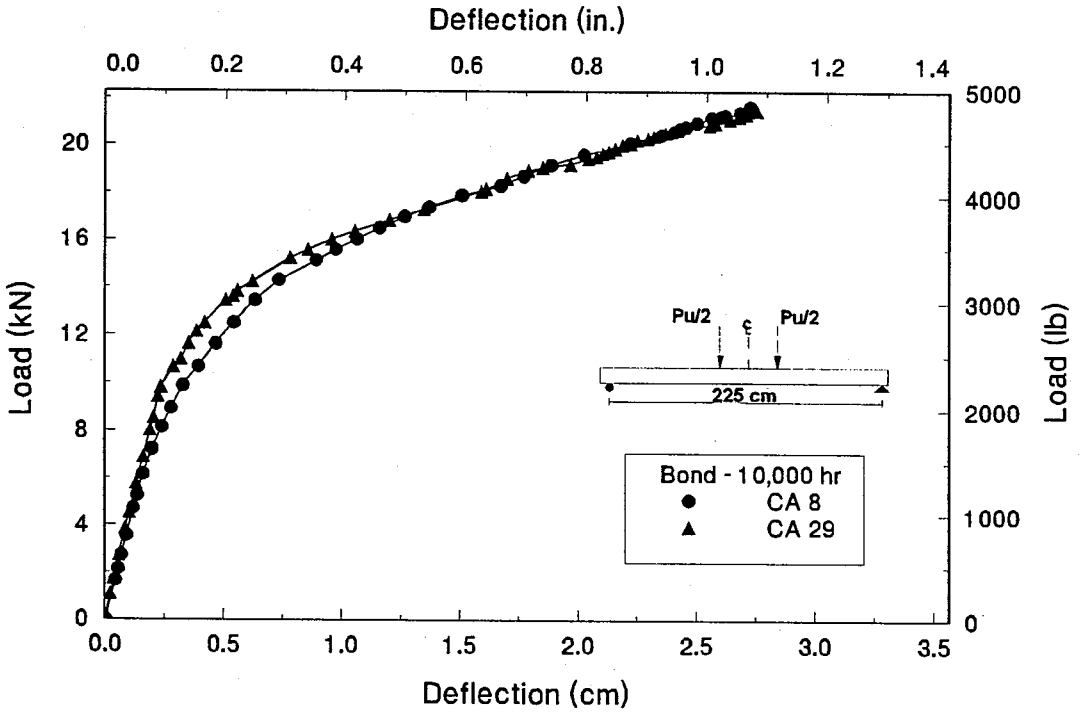

Figure 56. Load-Deflection for Carbon Beams - Comparison of 10,000 Hour Tests

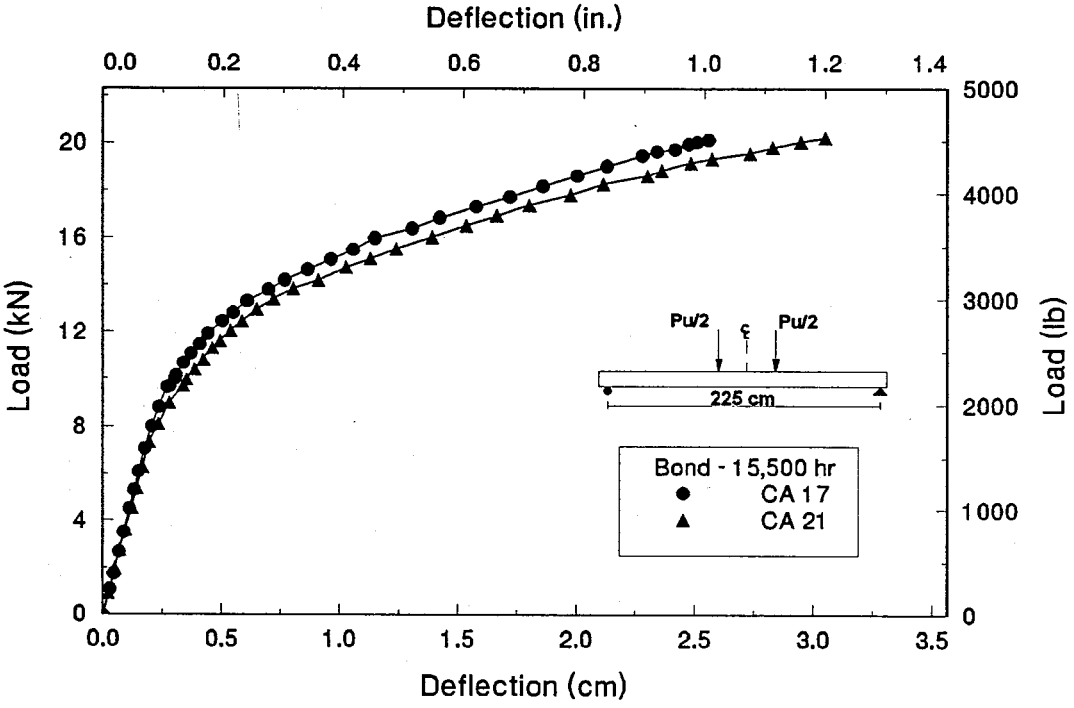

Figure 57. Load-Deflection for Carbon Beams - Comparison of 15,500 Hour Tests

9.5.3 Crack Patterns

9.5.4

As before the crack patterns of the beams were determined by reassembling the beams after testing. Reassembling the beams made the identification of failure patterns simpler. Bond cracks were present in all the beams, though the beams did not necessarily fail in bond.

Figure 58 shows the maximum. bond cracks among all the beams from the four series of tests. Plates 29 - 37 show the re-assembled crack pattern for all the beams tested.

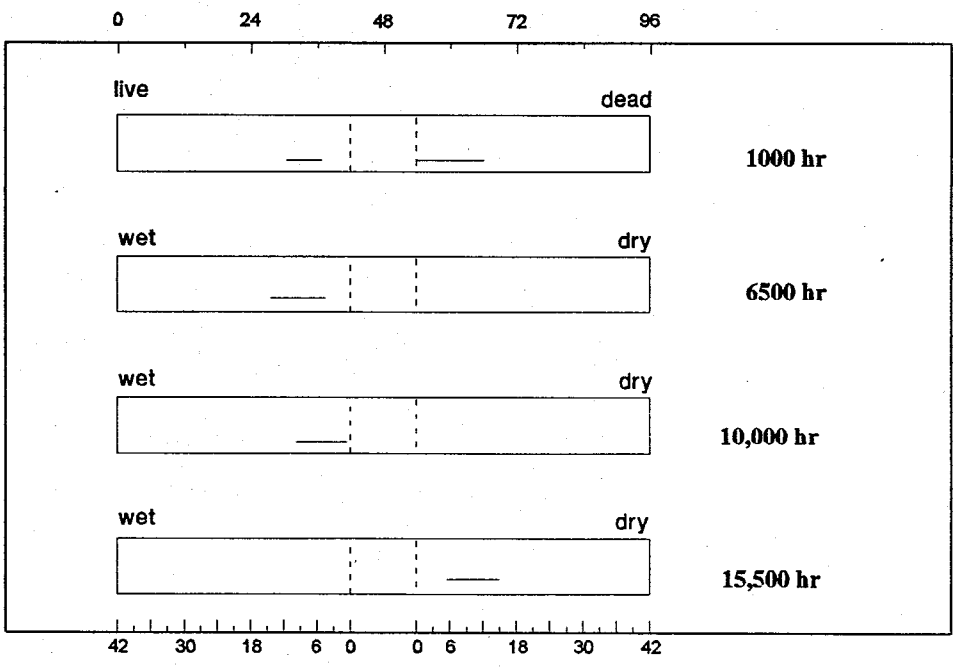

Figure 58. Maximum Bond Cracks - Bond Study

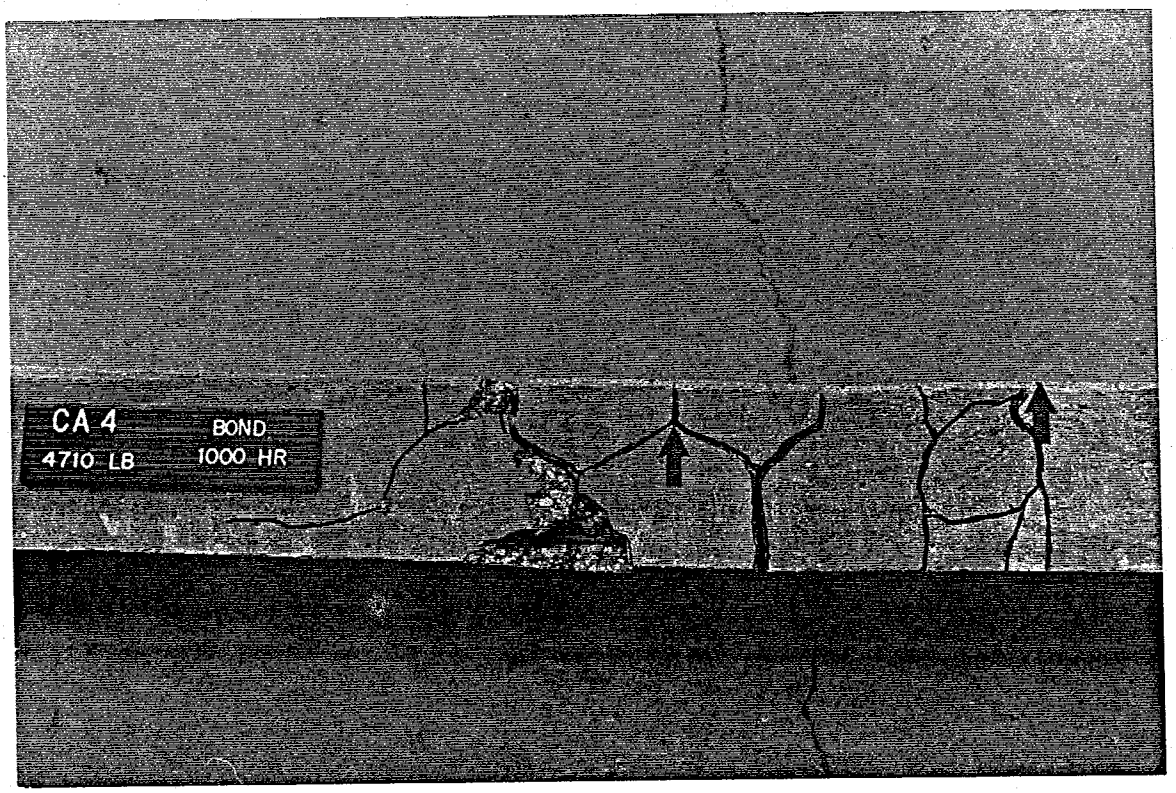

Plate 29. Crack Pattern for Beam CA 4 - Tested After 1,000 Hours

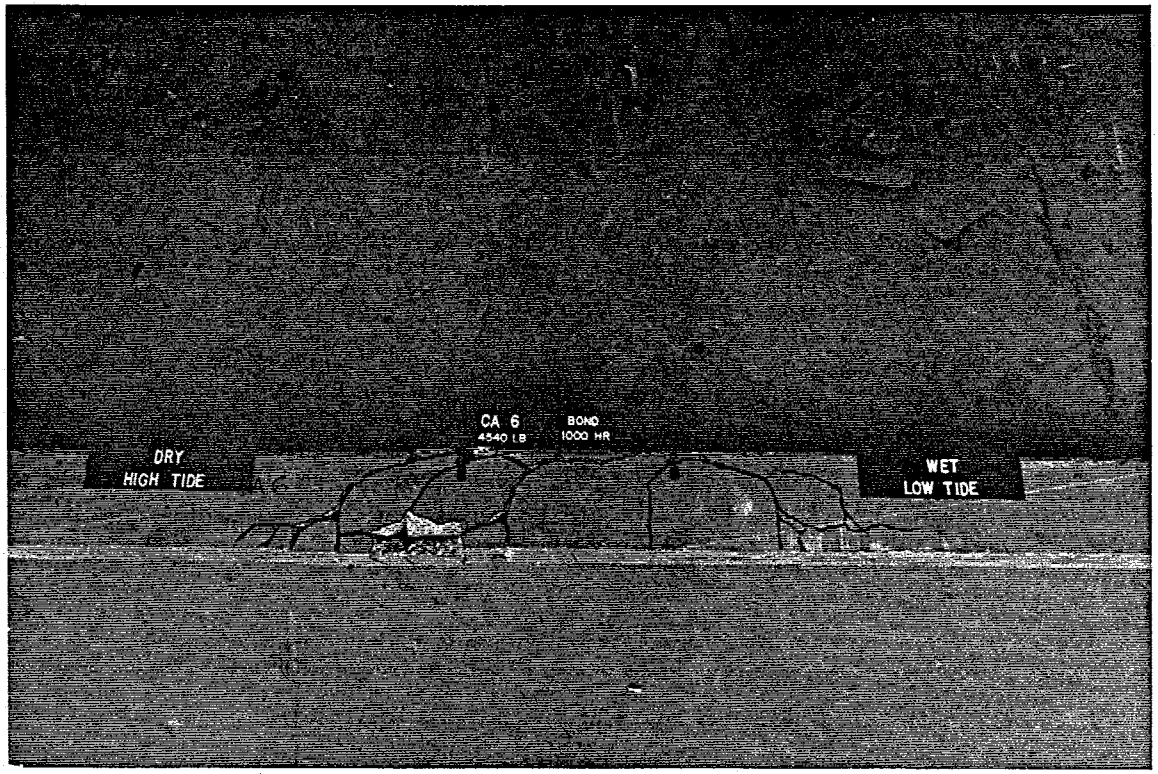

Plate 30. Crack Pattern for Beam CA 6 - Tested After 1,000 Hours

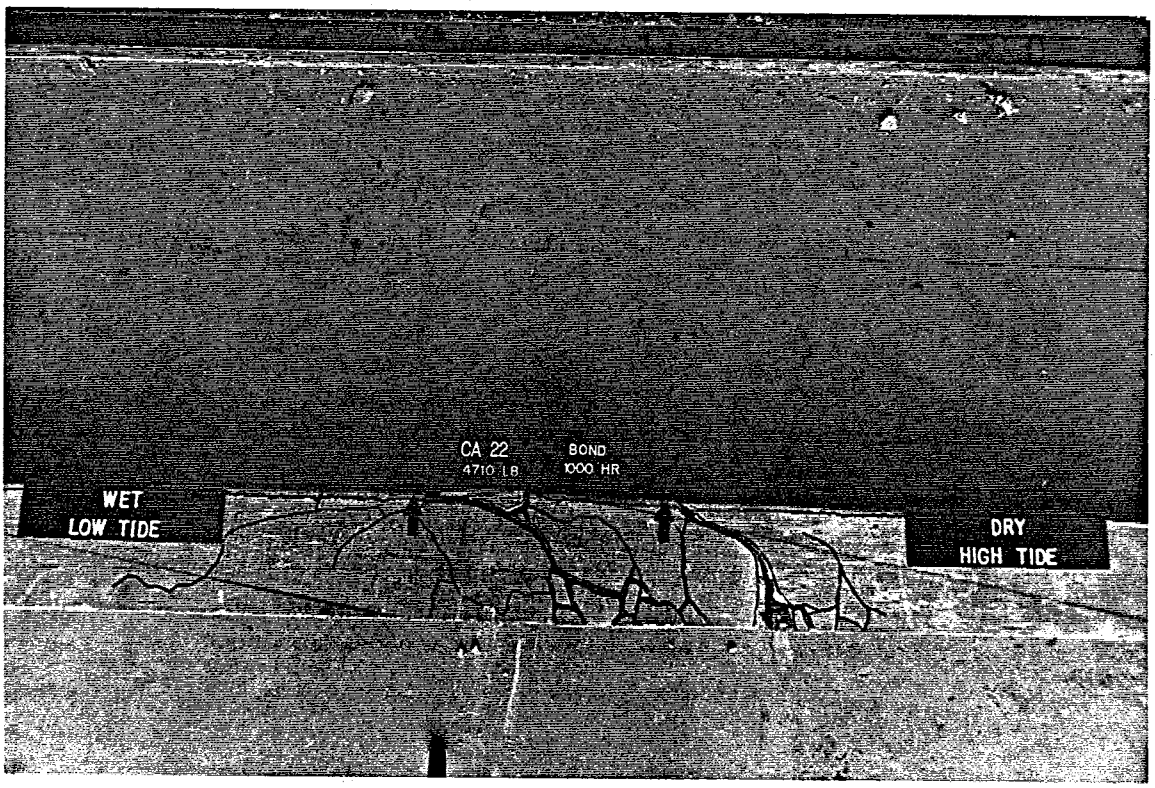

Plate 31. Crack Pattern for Beam CA 22 - Tested After 1,000 Hours

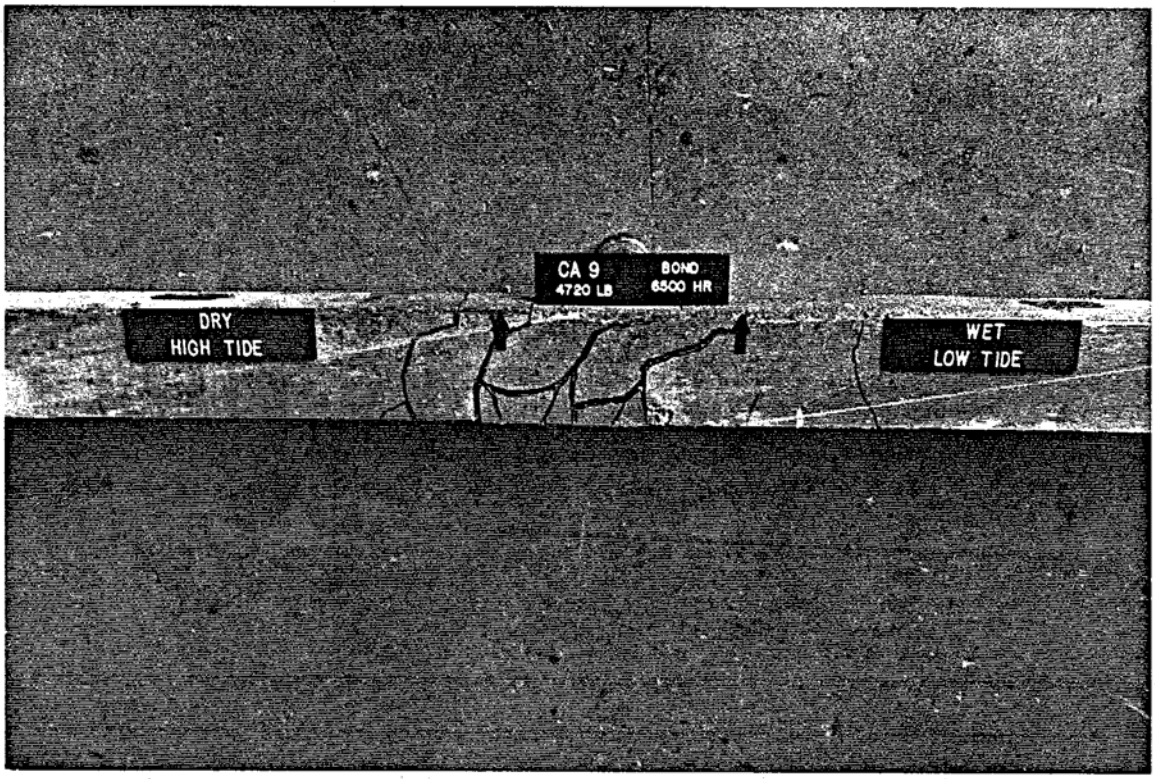

Plate 32. Crack Pattern for Beam CA 9 - Tested After 6,500 Hours

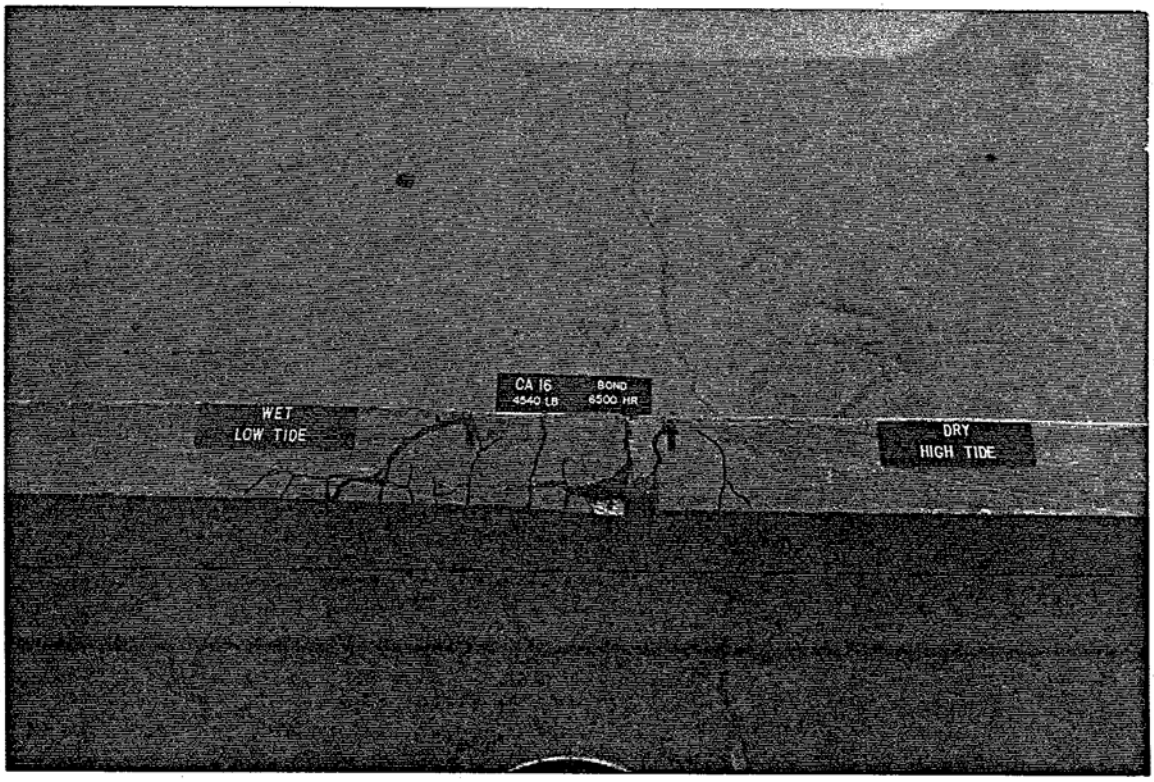

Plate 33. Crack Pattern for Beam CA 16 - Tested After 6,500 Hours

Plate 34. Crack Pattern for Beam CA 8 - Tested After 10,000 Hours

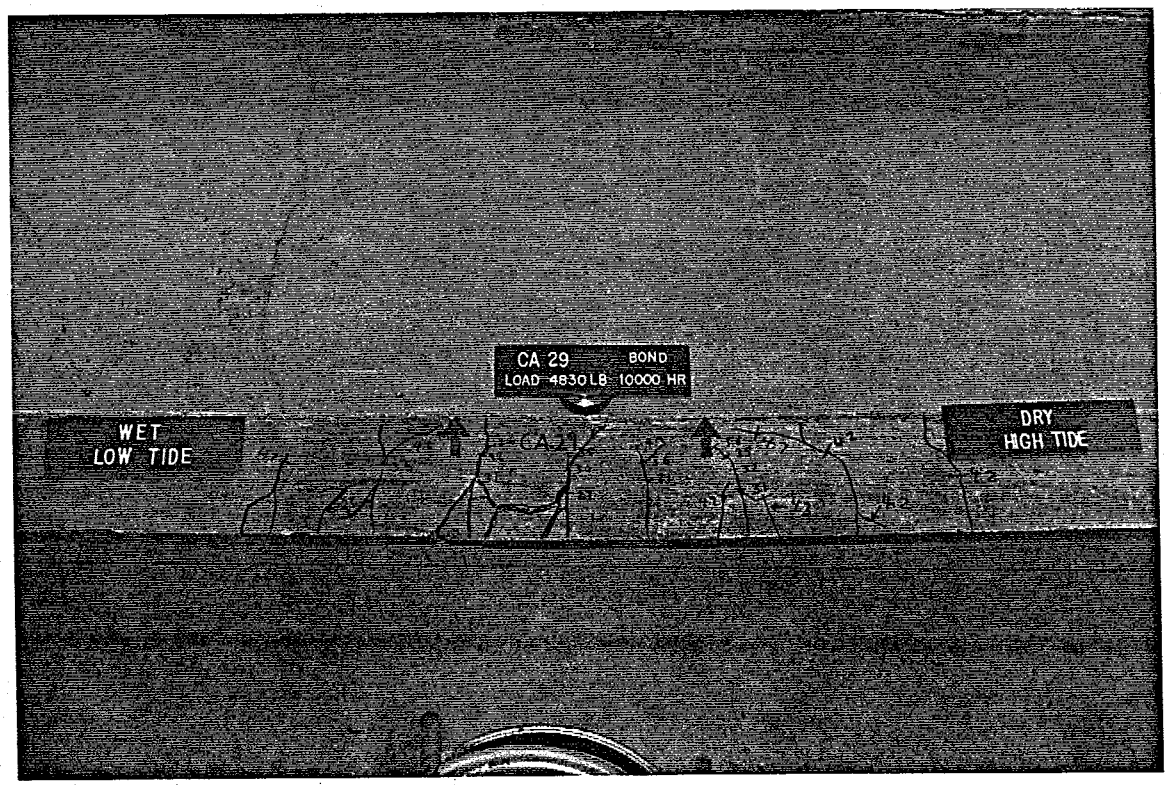

Plate 35. Crack Pattern for Beam CA 29 - Tested After 10,000 Hours

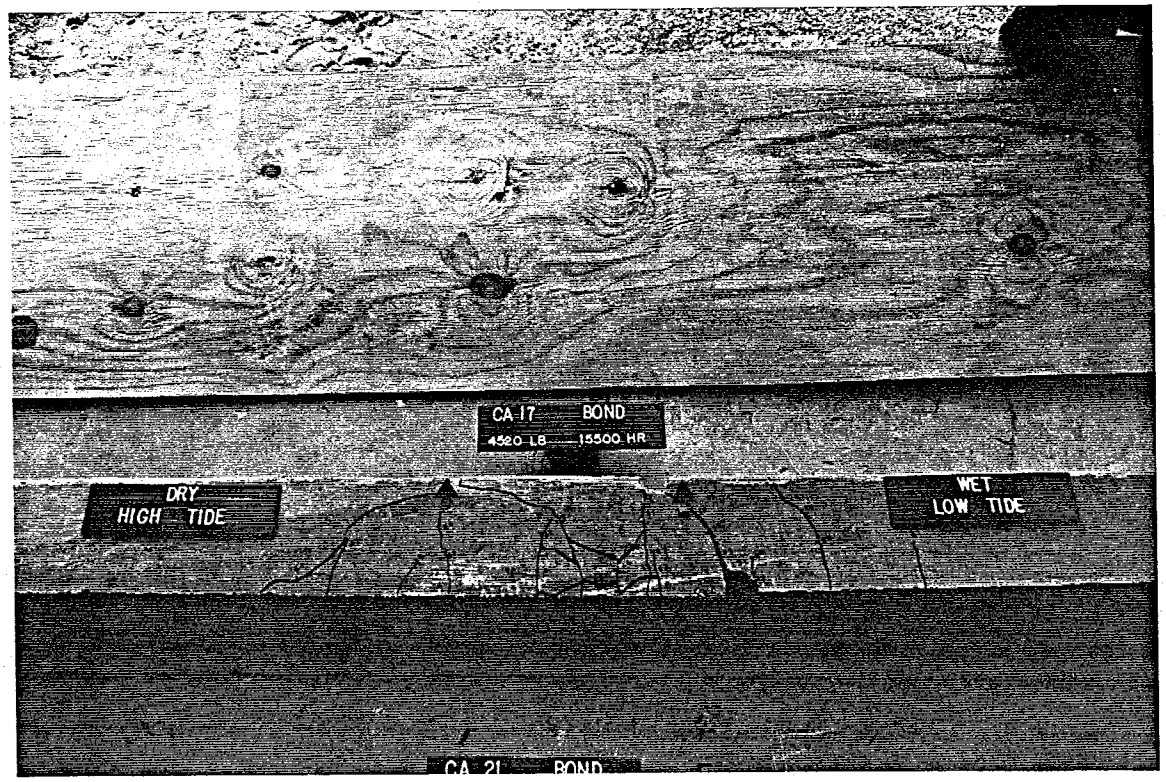

Plate 36. Crack Pattern for Beam CA 17 - Tested After 15,500 Hours

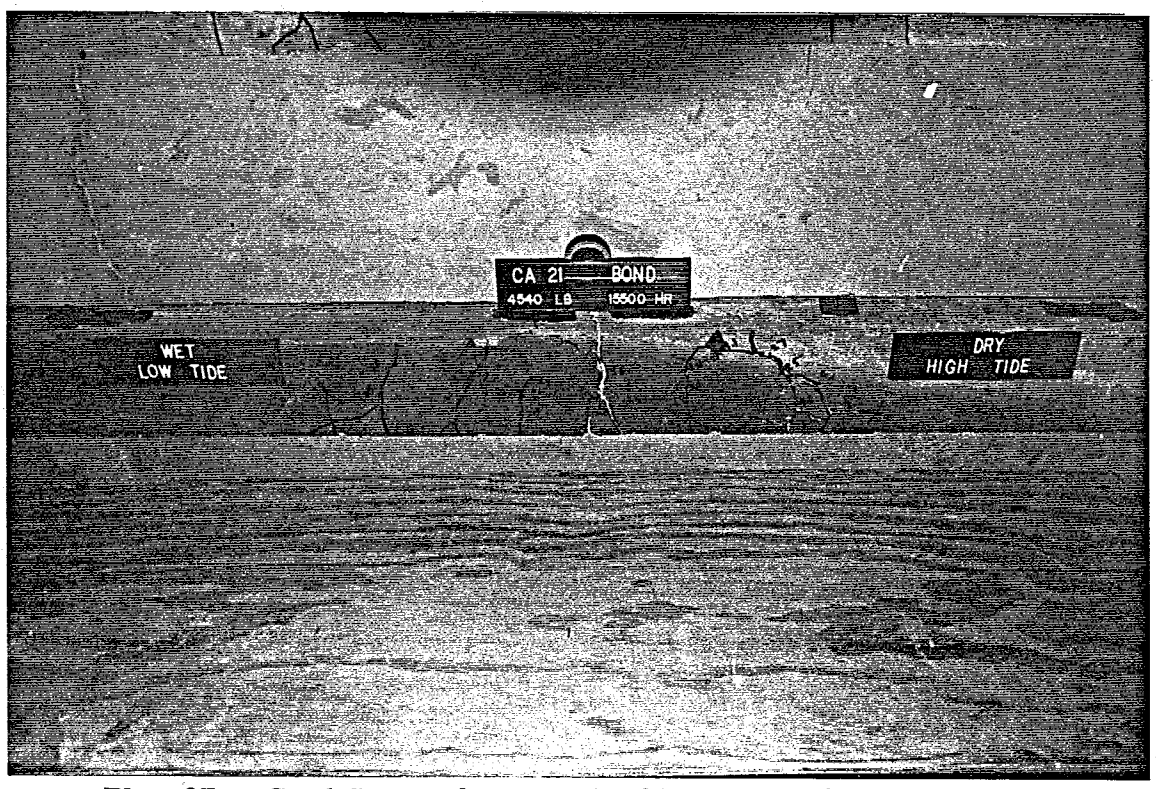

Plate 37. Crack Pattern for Beam CA 21 - Tested After 15,500 Hours

9.6 Discussion

To assess the loss of strength in the beams due to exposure, an analysis similar to the one conducted in the durability study was performed. The reduction in the ultimate load in the beams was calculated as a ratio of the average failure load of the control beams, which were the two month outdoor exposure test results, Chapter 7. As can be seen from Figure 59, the average failure load did not vary much for the 1,000 hours and 6,500 hours test. There was an increase in the ultimate load for the 10,000 hour test and a reduction of 3.2% for the 15,500 hours test. Thus, the ultimate load did not show any trends for the whole period of exposure to thermal cycling.

A similar analysis was conducted to determine the loss in deflection of the beams at failure, due to exposure. This analysis was also similar to that described in Section 7.5. The lowest failure load from all the four series of tests, which was 97 % of the failure load of the control beams, was selected for the comparison. The deflections were then expressed as a ratio of the average deflection of the control beams.

Figure 60, gives the plot of the ratio of deflection versus the exposure time. There was no reduction in deflection for the 1,000 hours and 6,500 test. The reduction was only 5.4 % for the 10,000 hours test and there was an increase in deflection by 15.7% for the 15,500 hours test. This shows that there no reduction in strain capacity of the CFRP rods with exposure.

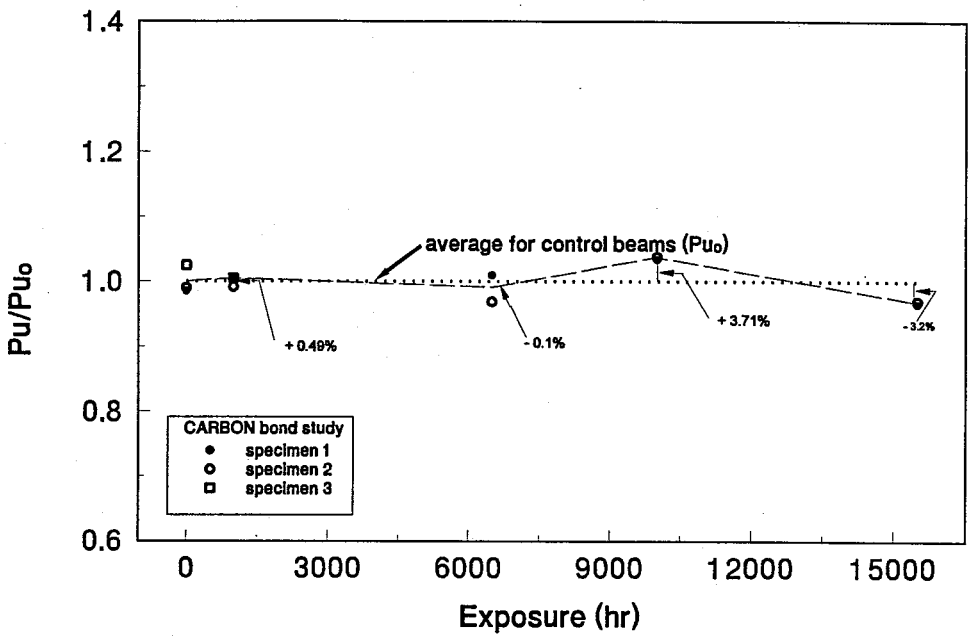

Figure 59. Reduction in Ultimate Load Due to Exposure - Bond Study

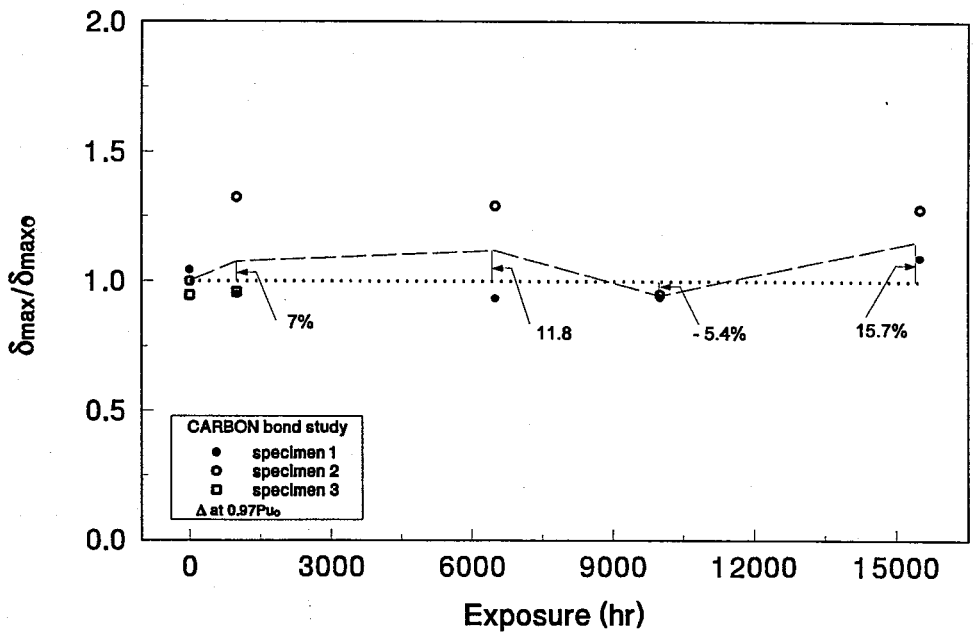

e 60. Reduction in Deflection Due to Exposure - Bond Study

10. CONCLUSIONS

10.1 Introduction

The object of this study was to investigate the durability of CFRP pretensioned piles in a marine environment. As such, three major investigations were initiated in which durability was assessed for outdoor exposure, in concrete subjected to wet/dry cycles and under a combination of tidal and thermal cycling. The only short term study conducted was a field investigation of transfer length.

10.2 Short Term Study .

1. The theoretical transfer length of CFRP pretensioned beams was approximately 31 diameters or 18 cm. This is smaller than the 50 diameter used for steel.
2. Transfer length measurements in outdoor sites using drop-in forms may yield different answers than anticipated form theoretical considerations. In this study, the most probable cause of discrepancy was identified as frictional forces caused by bending due to the eccentricity of the prestress force about the weak axis.
3. Existing facilities for prestressing steel can be readily adapted for CFRP.

10.3 Long Term Study

1. The outdoor study showed some reduction in ultimate strength with the duration of exposure. There was a 6.2% reduction in strength between the beams tested at two months and those tested at twenty months. The bond was unaffected nor was there evidence of a reduction of strain capacity in the CFRP rod.
2. There was a 11.35% loss in strength after 24 months in the CFRP pretensioned beams used in the durability study. However, there was no deterioration in bond or evidence of increased brittleness.
3. There no was reduction in ultimate strength in the bond study specimens after 15,500 hours of exposure, although there was some evidence of bond cracking in the failed beams. This suggests that the effect of mis-match in thermal expansion coefficients between concrete and CFRP may be unimportant.

As the investigation is still on-going, the conclusions presented are ***necessarily preliminary*** and are subject to change pending the outcome of the outstanding tests.

REFERENCES

American Association of State Highway and Transportation Officials (1994), *Standard Specifications for Highway Bridges,* 15th Edition, Washington, D.C. ACI 318-89 (1992), *Building Code and Commentary,* American Concrete Institute, Detroit, MI.

Carrasquillo, R.L, Nilson, A.H. and Slate F. O. (1981), "Properties of High Strength Concrete Subject to Short-Term Loads," ACI *Journal,* May-June, pp 171178.

Dolan, C.W. (1990), "Development in Non-Metallic Prestressing Tendons," PCI *Journal, Vol.* 35, No. 5, September-October, pp. 80-88.

Gerritse, A. (1993), Private communication with R. S en dated May 30.

Iyer, S.L. and Sen, R. (1991), *Advanced Composite Materials in Civil Engineering Structures,* ASCE, New York, NY.

MacGregor, J.G. (1992), *Reinforced Concrete: Mechanics & Design,* Prentice-Hall, NJ, Second Edition.

Mehta, P.K. and Monteiro, P. (1993), *Concrete: Structure, Properties and Materials,* Prentice-Hall, NJ, Second Edition.

Nilson, A.H. (1987), *Design of Prestressed Concrete,* John Wiley & Sons, Second Edition.

Rosas, J. (1995), "Studies in Durability of AFRP Pretensioned Piles." Master's Thesis submitted to Department of Civil Engineering & Mechanics, University of South Florida, Tampa, FL, May.

Rostasy, F. S. (1989), "New Prestressing Materials," *Congress Report,* FIP'88-IXth Congress, Jerusalem, Israel, September, pp. 148-159.

Sen, R., Issa, M. and Mariscal, D.(1992), "Feasibility of Fiberglass Pretensioned Piles in a Marine Environment," August, *Report CEM/ST/92/1,* Florida Department of Transportation.

Sen, R., Mariscal, D. and Shahawy, M. (1993a), "Durability of Fiberglass Pretensioned Beams," ACI *Structural Journal, Vol* 90, No. 5, September-October, pp. 525-533.

Sen, R., Mariscal, D. and Shahawy, M. (1993b), "Investigation of S-2 Glass/Epoxy Strands in Concrete." ACI *Special Publication 138, International Symposium on FRP Reinforcement for Concrete Structures* (Ed. A. Nanni & C. Dolan), pp. 15-34.

Sen, R., Issa, M., Wadsack, P. and Shahawy, M. (1993c), "Driving Stresses in Fiberglass Pretensioned Piles," ACI *Structural Journal, Vol* 90, No 6, NovemberDecember, pp. 666-674.

Sen, R., Spillett, K. and Shahawy, M. (1994), "Fabrication of aramid and carbon fiber pretensioned beams," *Concrete International, Vol 16,* No *6, pp.* 45-47.

Sen, R. and Shahawy, M. (1994), "Accelerated Durability Testing of FRPs used in Highway Construction." *Nenv Experimental Techniques for Evaluating Concrete Material and Structural Pel formance, ACI SP-143* (Ed. D. Stevens & M. Issa), pp. 297-314.

Sen, R., Rosas, J. and Sukumar, S. (1995), "Durability of AFRP Pretensioned Piles in a Marine Environment. " *Interim Filial Report Vol 1* submitted to Florida and US Department of Transportation, August.

Shah, S.P and Ahmad, S.H (1985), "Structural Properties of High Strength Concrete and its Implications for Precast Prestressed Concrete," PCI *Journal,* Nov-Dec, pp 92-118.

Sukumar, S. (1995), "Studies in Durability of CFRP Pretensioned Piles,". MSCE Thesis submitted to Department of Civil Engineering & Mechanics, University of South Florida, Tampa, FL, May.